The Messenger

No. 144 – June 2011

Astronomy in Brazil
Science impact of HAWK-I
Mid-infrared imaging of evolved stars
The Carina dwarf spheroidal galaxy

Brazil's Route to ESO Membership

Albert Bruch[1]

[1] Laboratório Nacional de Astrofísica – LNA, Itajubá, Brazil

On 29 December 2010, in a ceremony held at the Ministry of Science and Technology in Brazil´s capital, Brasília, the then Minister, Sergio Machado Rezende and the ESO Director General Tim de Zeeuw signed the accession agreement by which, pending ratification by the Brazilian Congress, Brazil becomes the 15th ESO Member State and the first non-European member. An overview of the historical background, the current state of astronomy in Brazil, and the motivation that made Brazil apply to become an ESO Member State is presented.

Figure 1. A contemporary engraving by Zacharias Wagener of a building in 17th century Recife that may have hosted the first astronomical observatory in the Americas.

History

The signature of the accession agreement to ESO (see de Zeeuw, 2011) is the latest highlight in Brazilian astronomy's very long and distinguished history, which goes back much further than most non-Brazilian astronomers are aware. Long before Brazil was established as a state, at a time when various European powers still disputed dominion over its vast expanses, Brazil hosted the first astronomical observatory, not just in the Americas, but also in the southern hemisphere. In 1639 the German naturalist and astronomer Georg Marcgrave founded an observatory in Recife (Prazeres, 2004), which was then the capital of a Dutch colony. The probable appearance of this observatory is shown in Figure 1. Should we consider this as the first "European Southern Observatory"?

However, troubled times and warfare between the countries disputing hegemony over the rich Brazilian colonies impeded the long-term survival of these initial astronomical activities and astronomy only took firm root in Brazilian soil after the country became an independent empire in 1822. On 15 October 1827, the Emperor Dom Pedro I established the institution that has now evolved into the Observatório Nacional (ON) in Rio de Janeiro (Videira, 2007), and is shown in Figure 2. It was originally meant to provide essential services to the newly founded state such as time-keeping, and fundamental scientific research in astronomy only gradually became part of its activities. Arguably the observatory's most notable scientific achievement was the organisation of the expedition to observe the solar eclipse of 1919 in Sobral, Ceará, which contributed decisively to the first observational proof for Einstein´s theory of general relativity.

Astronomy began to establish itself in other Brazilian institutions in the late 19th century and this progressed, primarily in the universities, and most notably in São Paulo and in Porto Alegre, at a rather modest pace during much of the 20th century. Astronomy in Brazil has only really taken off during the past three or four decades. The three main factors that have contributed to this substantial and very successful increase are:

MAST

Figure 2. The early home of the Observatory Nacional in Rio de Janeiro, photographed in 1921, which today hosts the Museum of Astronomy and Related Sciences.

1. New funding lines that permitted promising Brazilian students to receive their professional education abroad, mainly in Europe and in the USA.
2 Newly created graduate courses in astronomy, meaning that scientists could be trained in Brazil, taking advantage of the expertise brought back by others who had obtained their degrees in foreign countries.
3. The creation of the Observatório do Pico dos Dias (OPD) and the installation of a medium-sized (at the time) telescope which gave the growing astronomical community access to a competitive observational infrastructure for the first time.

The above-mentioned factors resulted in the dramatic growth of Brazilian astronomy, both in terms of the number of scientists, as well as in scientific output. It quickly became evident that the available instruments were insufficient to satisfy the rapidly growing demand and that there is no really good site for a modern optical observatory in Brazil. So, instead of enlarging the existing facilities at a location that is far from ideal for astronomical observations, and following the modern trend towards the globalisation of science, it was recognised that international collaborations were the right way forward for the further development of astronomy in Brazil.

Infrastructure for astronomical research

So as to make telescopes and instruments with a wide range of apertures, characteristics and capabilities available to Brazilian astronomers, Brazil became a partner in the Gemini Observatory, the SOAR Telescope and finally entered into a Cooperative Agreement with the Canada–France–Hawaii Telescope (CFHT), giving Brazilian astronomers access to a range of facilities besides the Brazilian OPD.

Brazilian observational optical astronomy takes place primarily at the OPD (shown in Figure 3). When the observatory was planned in the 1970s, logistical considerations demanded that the observatory was built within easy reach of the big population centres where most astronomers were located. A site within the triangle formed by the cities of São Paulo, Rio de Janeiro and Belo Horizonte was chosen as a compromise between easy accessibility and good observing conditions. The observatory is operated by the National Astrophysical Laboratory (Laboratório Nacional de Astrofísica [LNA]), based in Itajubá, Minas Gerais, which is a research institute of the Ministry of Science and Technology, and is responsible for providing the optical astronomical infrastructure to the entire scientific community. Today the OPD hosts three telescopes with apertures between 1.6 metres and 0.6 metres, and it is equipped with an instrument suite that is tailored to serve its users well. An effort to upgrade the observatory is underway to keep it competitive, despite the increasing light pollution and the growing number of other facilities that are now open to Brazilian astronomers.


LNA

Figure 3. Aerial view of the OPD, the principal observatory on Brazilian territory, located in the Serra da Mantiqueira in the southern part of the State of Minas Gerais, operating a 1.6-metre telescope (main building) and two 0.6-metre telescopes.

The Gemini Observatory operates two 8-metre-class telescopes on Hawaii (Mauna Kea) and in Chile (Cerro Pachón) on behalf of a consortium of seven countries. Although very well used by Brazilian astronomers, and extremely important for the development of optical astronomy in Brazil, the rather small share of Gemini that Brazil was able to purchase has proved to be a severe limitation. Brazil currently owns 2.5% of Gemini. In 2010 it purchased additional observing time from the United Kingdom, increasing its access to the telescopes by a factor of two and it is anticipated that Brazil will increase its share in Gemini to about 6% after 2012, when the UK leaves the partnership.

With abundant access to rather small telescopes (OPD) and limited access to big telescopes (Gemini), the Brazilian astronomical community felt the need for something in between: a decent amount of time at an intermediate-sized telescope. So Brazil joined forces with three US institutions (NOAO, University of North Carolina and Michigan State University) to build and operate the SOAR Telescope (Southern Astrophysical Research Telescope), located next to Gemini South on Cerro Pachón (see Figure 4). SOAR is a 4.1-metre telescope that is optimised for high image quality. Brazil entered this consortium as the majority shareholder with a stake of about 34%. Brazilian astronomers also have access to the 4-metre Blanco Telescope at CTIO through an agreement with NOAO about the exchange of observing time, which complements the services and instruments offered by SOAR.

The cooperative agreement with the CFHT, which is located on Mauna Kea, Hawaii, is meant to provide access to a

SOAR Inc.

Figure 4. The 4.1-metre SOAR Telescope on Cerro Pachón, Chile.

José-Willams Vilas-Boas

Figure 5. The dome of the Itapeninga Radio Observatory (ROI) in Atibaia, São Paulo.

highly productive wide-field 4-metre-class telescope with competitive instruments in the northern hemisphere. The agreement is limited in time and will be reviewed, with the aim of potentially renewing the contract, in 2012.

Brazilian participation in all these international observatories is managed by the LNA, which thus exercises a key role in optical astronomy in Brazil. Apart from these installations, which are open to the entire astronomical community, some institutions operate their own facilities on a more modest scale, and these either serve a specific scientific purpose or concentrate on education and outreach. The most recent and arguably most important (and certainly the biggest) of these is IMPACTON, a robotic one-metre telescope for observations of near-Earth objects, which is currently being commissioned by the Observatório Nacional, and is located in the interior of Pernambuco State.

Other areas of astronomical research have also benefitted from Brazil's contributions to international projects and collaborations. These include space astronomy (Brazil is a partner in the CoRoT space mission, and it is also engaged in the PLATO mission), high energy astrophysics (through the participation of Brazil in the Auger experiment), and cosmology (Brazilian institutions are members of the International Center for Relativistic Astrophysics Network [ICRA-Net]).

The growing importance of large surveys and the exploitation of data banks for astronomical research has been recognised and has led to the recent creation of the Brazilian Virtual Observatory (BraVO), as the national branch of the International Virtual Observatory Alliance. BraVO unites researchers from various institutions in a coordinated effort to create infrastructure and tools for data-mining and to disseminate the concept of the Virtual Observatory in Brazil. In parallel, the LIneA (Laboratório Interinstitutional de e-Astronomia) collaboration is formed by scientists working at three research institutes of the Ministry of Science and Technology (MCT) to develop the infrastructure and software to store and process large astronomical datasets.

LNA

Figure 6. Mounting the 1300 optical fibres of the SOAR Integral Field Spectrograph at the LNA Optics Laboratory.

Radio astronomy, which was already comparatively well developed before the steep increase in optical astronomy activities began, has not followed the same steeply rising path. Apart from some modest investments in specialised instruments operated by small groups, no major effort has been made to provide access to a competitive infrastructure for the general community. The Itapeninga Radio Observatory (ROI; Figure 5), located in Atibaia, some 50 kilometres from São Paulo, and operated by the Nacional Space Research Institute (Instituto Nacional de Pesquisas Espaciais [INPE]) is the only instrument available to all astronomers. This 18–90 GHz, 14-metre antenna has not had a major upgrade since it was built in 1974. Access to more modern equipment would be very much welcomed by the radio-astronomy community.

Instrumentation

The desire to participate in both scientific research in astronomy and in technological development has led to the implementation of the necessary infrastructure to build astronomical instruments for use at international observatories, such as SOAR. These efforts are concentrated at the LNA and INPE, in collaboration with the universities and other scientific institutions.

While most of the activities in instrument development at INPE are related to fields other than astronomy (e.g., observation of the Earth from space), a group at INPE is currently building MIRAX, a small survey satellite to observe the spectral and temporal behaviour of a large number of transient X-ray sources. Moreover, INPE is collaborating with the LNA and the Instituto de Astronomia, Geofísica e Ciências Atmosféricas (IAG) of the University of São Paulo to develop the Brazilian Tunable Filter Imager (BTFI), which is an innovative camera and integral field spectrograph for the SOAR telescope. Other long-term collaborations between INPE and LNA on instrumentation for the OPD are also ongoing.

In the past, instrumentation development at LNA was rather modest and restricted to immediate OPD needs. But during the past decade much effort has been invested in turning such activities into one of the fundamental pillars of the institute. The LNA has built laboratories and workshops, and provided them with state-of-the-art equipment, with a special emphasis on optical metrology and the handling of optical fibres for astronomy (see Figure 6 as an example). In collaboration with the IAG and other university institutes, the LNA has built SIFS, a 1300-channel integral field spectrograph (currently being commissioned at the SOAR Telescope). It is also constructing the SOAR Telescope Echelle Spectrograph (STELES) and is planning a similar instrument for the OPD. The LNA was a member of the winning team in an international competition for the detailed design study of the Wide Field Multiple Object Spectrograph (WFMOS) for Gemini, where it was responsible for the fibre feed between the telescope and the bench spectrograph (although, unfortunately, through lack of funding the instrument was never built). In a successful attempt to find a place on the international market for astronomical instrumentation, the LNA has also built the fibre feed for the Frodospec spectrograph at the Liverpool Telescope on La Palma.

Independent efforts in instrument development are ongoing at the Observatório Nacional, which, in collaboration with the IAG, is building a camera for the J-PAS (Javalambre Physics of the accelerating Universe Astrophysical Survey) project in Spain. Facilities for instrumentation development are also being installed at the Federal University of Rio Grande do Norte in Natal.

Size of the Brazilian astronomical community

According to a census (updated in 2010), there are 341 fully trained and active astronomers (i.e. with a PhD) in Brazil (up from no more than a handful some 40 years ago). This workforce is complemented by 313 postgraduate (Master's and PhD) students. Thus, more than 650 scientists are active in astronomical research. While there is a concentration of astronomers in a few universities and federal research institutes, the number of groups in other places is rapidly increasing as a result of the policy of the federal government to strengthen science and higher education in less well-developed parts of the country. In consequence, astronomy is being pursued today in 46 institutions (… and counting), which are widely spread across Brazil. While many of the smaller groups are part of physics or other related university departments, postgraduate education in astronomy is offered in 19 institutes.

There is not enough room here to characterise all these institutes in detail. However, it may be worthwhile to briefly enumerate the most important. With the IAG (see Figure 7), the University of São Paulo hosts the dominant research institute in astronomy in the country. It is home to about 20% of the total workforce mentioned above. This is twice

Figure 7. Urania, the Muse of Astronomy, from a picture window in the library on the former campus of the Institute of Astronomy and Geophysics of São Paulo University.

as many as the second most important, the venerable Observatório Nacional in Rio de Janeiro. Strong astronomy groups can also be found at INPE, located in São José dos Campos, the Federal University of Rio de Janeiro (distributed between the Observatório do Valongo and the Department of Physics), the Federal University of Rio Grande do Sul in Porto Alegre and the Federal University of Rio Grande do Norte in Natal. While all these astronomy centres carry out research in many fields, the Brazilian Centre of Physical Research (Centro Brasileiro de Pesquisas Físicas [CBPF]), Rio de Janeiro, which hosts the Brazilian branch of ICRAnet, focuses mainly on cosmology.

Administratively, the numerous astronomy groups are distributed between government institutions, which are directly subordinated to the federal Ministry of Science and Technology (CBPF, INPE, LNA, ON), entities belonging to federal or state universities, and (increasingly) private universities.

The community founded the Brazilian Astronomical Society (Sociedade Brasileira de Astronomia [SAB]) in 1974. The Society currently has 678 members.

As measured by the number of publications in refereed journals, scientific productivity was all but non-existent until the end of the 1960s, but as the number of active astronomers has increased, a steep and continuing rise in the number of published papers has been observed (Figure 8). The role of Brazil as a significant producer of scientific papers was recognised when it became a member of *Astronomy and Astrophysics*, the leading astronomical journal in Europe.

Although optical and infrared observational astronomy is predominant, Brazilian astronomy embraces a wide range of special fields. There are at least 16 major areas of astronomy that are being actively pursued by astronomers in Brazil and that have recently been identified in the context of a National Plan for Astronomy[1]. The relative importance of the various disciplines can be gauged from the number of publications that they have generated. Table 1 gives the percentages of papers by Brazilian authors in refereed journals by area in 2008.

Funding

Brazilian astronomy is largely publicly financed. Operating costs for facilities open to the entire community are borne exclusively by the Federal Government, normally through MCT research institutes. Funds for the development of new projects and capital investments (instrument development among them), come from the same sources, including the government funding agency FINEP (Financiadora de Estudos e Projetos), as well as from Brazilian state funding agencies, which normally do not fund the operation of astronomical infrastructure. While other states also contribute, FAPESP, the funding agency of São Paulo state, plays a dominant role.

CNPq (Conselho Nacional de Desenvolvimento Científico e Tecnológico), a branch of the MCT, is extremely important as a provider of stipends for students and grants for established scientists. A similar role is played by CAPES (Coordenação de Aperfeiçoamento de Pessoal de Nível Superior), a branch of the Ministry of Education. Apart from stipends and grants, CNPq also finances smaller scale projects for individual scientists, scientific meetings, etc. (as do the state agencies).

Specific funding by the federal and state governments, such as PRONEX (Programa a Núcleos de Excelência) and the Millennium Institutions (Institutos do Milênio) in the past, and the current (virtual) National Institutes of Science and Technology (INCT) has also greatly benefited Brazilian science. Two astronomy-related National Institutes have been created: INCT-A (A for astrophysics), which focuses on preparing the astronomical community for the challenges and opportunities of the future, and INCT-E (E for *espaço* [space]) which focuses on space technology and astronomy from space.

Direct personnel costs are, of course, carried by the employers, who are, in most cases, the federal or the state governments. However, the private sector is also involved through private (in general, non-profit) universities with research and higher education interests in astronomy.

Long-term strategic outlook

Brazil's young and vigorous community feels that it has gained an international reputation as a respected player in global astronomy. It is not seen as an accident that Rio de Janeiro was chosen to host the IAU General Assembly in 2009, but rather as recognition of the achievements of Brazilian science. The community is

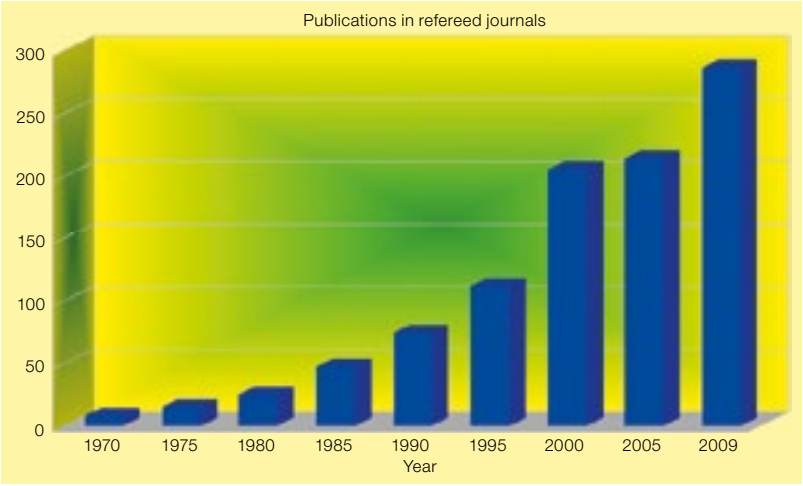

Figure 8. Evolution of the number of publications by Brazilian astronomers in refereed journals over the past decades.

aware that worldwide astronomy is characterised more than ever by international collaborations. Consequently, success for a national community depends decisively on its participation in the international community.

Moreover, it is understood that the growing necessity for international collaborations, the numerous scientific opportunities that present themselves in the worldwide scenario, combined with the elevated costs for large-scale scientific projects, call for a medium- and long-term strategic plan for astronomy to direct and coordinate the further development of the field in Brazil. Therefore, with the active support of the Ministry of Science and Technology, in 2010 the community elaborated a National Plan for Astronomy[1] as a guideline for the future of astronomy in the country, aligned to the general policy for science and technology of the federal government.

Among many other issues, this document emphasises the need to maintain access to a competitive observational infrastructure, on penalty of losing the respected position gained by Brazilian astronomers. Different ways of achieving this purpose have been studied by the INCT-A and a special commission created by the MCT. Based on these results the broad majority of the astronomical community came to the conclusion that the association of Brazil with ESO would be the most effective of all the available options. More than any other alternative, the association with ESO benefits the country in many ways, the most important advantages being that:

– it gives Brazil immediate access to ESO's existing telescopes, fostering scientific collaboration (and competition!) with scientists of other member states, and enlarging the scope of instruments already at the disposal of Brazilian astronomers significantly, thus eliminating some limitations felt by parts of the community;
– it meets one of the main recommendations of the National Plan for Astronomy by guaranteeing access to the future generation of giant telescopes, i.e. the European Extremely Large Telescope, and opening up opportunities for Brazilian industry to take part in its development and construction;
– it provides access to ALMA, satisfying and fostering the development of a community of radio astronomers who have not benefited from significant investments similar to those made in optical astronomy during the past three decades;
– it opens up a wide range of opportunities for the participation in technological development as part of the instrumentation programme for ESO telescopes.

Optical and infrared stellar astronomy	28.8 %
Theoretical cosmology	17.4 %
Optical and infrared extragalactic astronomy	11.9 %
Physics of asteroids	5.8 %
Theoretical stellar astrophysics	4.3 %
Chemical evolution of stellar systems	4.3 %
Dynamical astronomy	4.3 %
Solar radio astronomy	3.2 %
Instrumentation	3.2 %
Exoplanets	2.7 %
Other	13.2 %

Table 1. Percentage of papers published in refereed journals by area in 2008.

It is felt that the development model for optical astronomy which Brazil has followed in the past, i.e., offering its scientists a suite of instruments with diverse characteristics on small and medium-sized telescopes up to to the 8-metre-class Gemini giants, although with limited access in the case of the larger instruments, has lifted the astronomical community to a level of maturity. This progress now permits the next step — or rather leap — in its evolution: the ascent to a new and higher level in scientific, technological and instrumental terms, which is expected to be the natural consequence of Brazil's association with the strongest organisation in ground-based astronomy in the world. We are confident that not just optical astronomy will be strengthened, but that the fertile environment of partnership with ESO will benefit Brazilian astronomy as a whole, as well as related technological fields.

References

de Zeeuw, P. T. 2011, The Messenger, 143, 5
Prazeres, A. 2004, *Georg Marcgrave, e o desenvolvimento da astronomia moderna na América Latina, na cosmopolita Recife de Nassau*, http://www.liada.net/NASSAU%20&%20GEORG%20MARCGRAVE.pdf
Videira, A. A. P. 2007. *História do Observatório Nacional: a persistente construção de uma identidade científica*. Río de Janeiro: Observatorio Nacional

Links

[1] National Plan for Astronomy: http://www.lna.br/PNA-FINAL.pdf

The first European ALMA antenna from the AEM Consortium (Thales Alenia Space, European Industrial Engineering and MT-Mechatronics) being carried on an ALMA transporter during the handover to the ALMA Observatory at the Operations Support Facility (OSF). After testing at the OSF, it will be moved to the ALMA Operations Site on the Chajnantor plateau. See Announcement ann11022 for more details.

The Science Impact of HAWK-I

Ralf Siebenmorgen[1]
Giovanni Carraro[1]
Elena Valenti[1]
Monika Petr-Gotzens[1]
Gabriel Brammer[1]
Enrique Garcia[1]
Mark Casali[1]

[1] ESO

HAWK-I is ESO's most efficient near-infrared camera, and after two and a half years of operations we review its science return and give some future directions in the context of the Adaptive Optics Facility. The instrument underwent major technical challenges in the early phase of its operations: there was a problem with the entrance window, which was replaced, and radioactive events occur in the material of two of the four detectors. A number of high quality science papers based on HAWK-I data have been published, indicating a good performance and scientific return. HAWK-I is well-suited for a variety of attractive science cases and a project is in development to provide a faster readout, which would improve the capabilities for Galactic observations. When combined with the laser-assisted ground layer adaptive optics system, HAWK-I will become an excellent facility for challenging follow-up observations of exoplanetary transits.

Instrument overview and performance

HAWK-I is a cryogenic wide-field camera installed at the Nasmyth A focus of the VLT Unit Telescope 4 (UT4). The field of view is 7.5 by 7.5 arcminutes, with a cross-shaped gap of 15 arcseconds between the four 2RG 2048 × 2048 detectors. The pixel scale is 0.106 arcseconds. The instrument is offered with ten filters in two filter wheels: four broadband filters (*Y*, *J*, *H* and K_s), which are identical to the filters used in VIRCAM/VISTA, and six narrowband filters (Brγ, CH_4, H_2, 1.061 µm, 1.187 µm, and 2.090 µm). The image quality is seeing-limited down to at least 0.4 arcseconds. Typical limiting magnitudes (Vega) to reach a signal-to-noise ratio (S/N) of five on a point source in one-hour on-source integration are: 23.9 in *J*, 22.5 in *H* and 22.3 in K_s.

The efficiency, defined as the proportion of photons converted into electrons passing the telescope, instrument optics and detector, is computed for various near-infrared (NIR) instruments and is shown in Figure 1 for the NIR cameras SOFI, VISTA, ISAAC, CONICA and HAWK-I. The efficiency of the HAWK-I instrument is 70–80 % and so it is the most efficient NIR camera in ESO's instrumentation suite. The stability of the zero point is important for absolute photometry. For HAWK-I, there is a small periodic scatter in the zero point of $\Delta J \sim 0.1$ mag over a period of a year, significantly lower than that of either CONICA or ISAAC.

Along with the distortion caused by the instrument optics, atmospheric refraction produces a geometrical shrinkage of the field of view with increasing zenith distance. The differential achromatic refraction is ~0.6 arcseconds, as measured over the full 7.5 by 7.5 arcminute field size of HAWK-I and for a zenith distance between 0° and 60°.

During science operations three technical challenges were identified: the entrance window, radioactive events in the detector material and the instrumental distortion correction. The instrument was first installed in July 2007. At the beginning of the observing period P81 in 2008 the instrument suffered from a damaged coating of the entrance window. This defect was fixed by a replacement window installed during an intervention in the summer of 2008. The instrument also suffered from radioactive events which contaminated two of the four chips of the detector mosaic (Finger, 2008). The contamination can be seen in the dark exposures. One of the four detectors shows on average a well-localised decay every 75 s. The event affects an area of 7 × 7 pixels and is eliminated by a cleaning algorithm in the pipeline. Another detector is similarly affected, and, although the events are much less frequent, they generate charge which is not localised to within a few pixels, but spreads in a diffuse charge cloud with an unpredictable location, resulting in glitches that cannot be cleaned during data analysis. However, the sensitivity limit of the individual detectors shows that there is no major degradation of the detection limit caused by these radioactive events.

The HAWK-I instrument team has recently undertaken observations to assess the relative sensitivities of the four HAWK-I detector chips, using observations of the high Galactic latitude field around the $z = 2.7$ quasar B0002-422 (α 00^h 04^m 45^s, δ −41° 56′ 41″) taken during technical time. The observations consisted of four sets of 11 × 300 s sequences in the NB1060 filter; details of such an observational set-up are discussed in the HAWK-I User Manual. The four sequences are rotated by 90° in order that a given position on the sky is observed by each of the four chips of the HAWK-I detector. The jitter sequences are reduced following the standard two-pass background subtraction work flow described in the HAWK-I pipeline manual. Objects

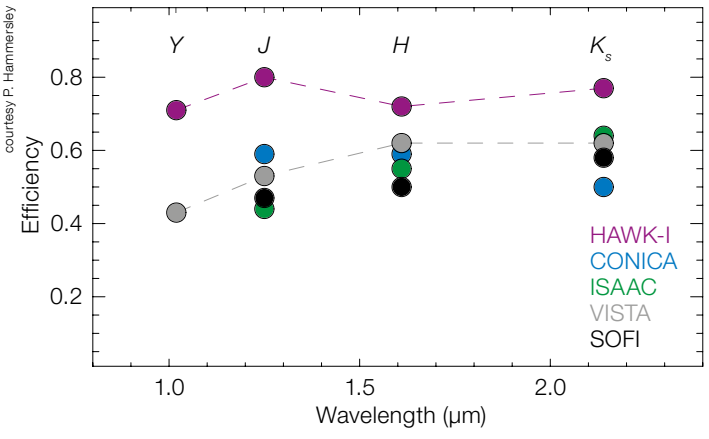

Figure 1. Comparison of the efficiency of the NIR instruments SOFI, VISTA, ISAAC, CONICA and HAWK-I is shown.

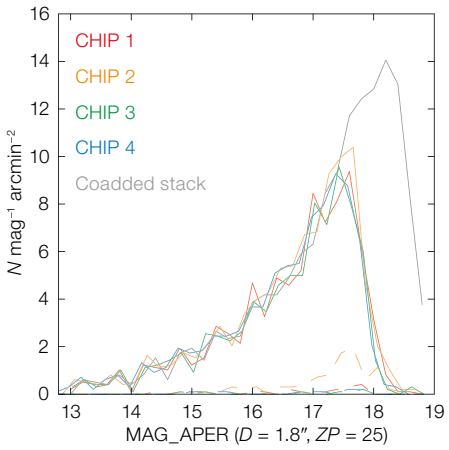

Figure 2. Number counts as a function of aperture magnitude of the four HAWK-I detectors: chip1 (red line), chip2 (orange), chip3 (green), chip4 (blue line) and the co-addition of all four chips (black line). Dashed lines give the number of spurious detections. Radioactive events are most common for chip 2, which nevertheless has a similar detection probability as the other chips, but an enhanced number of spurious detections at faint flux (> 17 mag) levels (shown as dashed orange).

are detected using the SExtractor software. The resulting number counts as a function of aperture magnitude observed by each detector are shown in Figure 2. The limiting magnitudes, here taken to be the magnitude where the number counts in Figure 2 decrease sharply, provide a proxy for the individual detector sensitivities. The sensitivities agree to within 10% between the individual chips. We also show in Figure 2 the number counts for a deep co-added stacked image of the four rotated and aligned jitter sequences which are a factor of two deeper than the individual sequences. We used the co-added stack to assess the number of spurious sources detected on each individual detector: objects matched from the single chip image to the deeper image are considered to be real, while objects that only appear on the single chip images are considered spurious. The image artefacts on detector 2, which are caused by radioactive events, do result in an elevated number of spurious detections at faint magnitudes, reaching 20% at the limiting magnitude.

AOF and GRAAL

The Adaptive Optics Facility (AOF; see Lelourn et al., 2010; Paufique et al., 2010 and Arsenault et al., 2010) will provide a correction of the ground layer turbulence, improving the image quality of HAWK-I. The resulting point spread function (PSF) diameter that collects 50% encircled energy is reduced by 21% in the K_s-band, and by 11% in the *Y*-band, under median seeing conditions at Paranal of 0.0.87 arcseconds at 500 nm. Hence, the AOF will provide better seeing statistics. When installing the AOF on UT4, the secondary mirror of the telescope will be replaced by a deformable secondary mirror (DSM) with more than 1000 actuators. In addition, four laser guide stars will be installed on the telescope structure, and a wavefront sensor system, GRAAL (ground layer adaptive optics assisted by lasers), will be used to measure the turbulence from artificial guide stars. GRAAL will be installed between HAWK-I and the Nasmyth flange. HAWK-I's field of view is not affected by GRAAL. It is planned to begin installing the AOF in 2013, with a total telescope downtime of a few months (subject to the exact distribution of technical time) due to the installation of the new secondary mirror, the lasers and GRAAL. The schedule anticipates that the AOF will be operational from 2015.

Normal adaptive optics systems aim at correcting atmospheric turbulence down to the diffraction limit of the telescope. The price to be paid is a limit in corrected field of view (less than 1 arcminute) and a limit in sky coverage (less than 50%) since a bright guide star is required even when using laser guide stars. The AOF ground layer adaptive optics mode (GLAO) does not provide diffraction-limited image quality, but it does correct the full 7.5 by 7.5 arcminute field of view and the sky coverage is practically 100%.

HAWK-I science return

When HAWK-I was conceived, the selected science cases, according to the document, Science Case for 0.9–2.5 μm infrared imaging with the VLT (ESO/STC-323), were:

1. Galaxy evolution from deep multi-colour surveys;
2. Multi-wavelength observations of normal and active galaxies;
3. Structure and evolution of nearby galaxies;
4. Galactic star and planetary formation;
5. Outer Solar System bodies.

HAWK-I started to operate regularly in April 2008. A significant number of observations executed during P81 were affected by the damaged entrance window coating, and were re-executed by ESO. In the period from mid-2008 until end of 2010, 26 refereed papers were published containing HAWK-I results. They have 350 citations to date and an h-index of 10. Of these 26 papers, two were published in *Nature*, seven in *ApJ*, four in *ApJ Letters*, one in *AJ*, four in *MNRAS*, and 12 in *A&A*. The two *Nature* papers, Tanvir et al. (2009) and Hayes et al. (2010), resulted in ESO press releases. To evaluate the science impact of HAWK-I, we have compared the number of papers based on data obtained at the other NIR VLT instruments during their first 2.5 years of science operations. The rate of publication turns out to be fairly similar among all the VLT instruments considered (NACO, ISAAC, SINFONI and CRIRES). The science output of HAWK-I up to the end of 2010 can be summarised as follows:

1) In most cases, publications which are based on HAWK-I present results on extragalactic, high redshift astrophysics. The most relevant papers being the characterisation of the galaxy populations around $z \sim 2$ (Galametz et al., 2010; Hayes et al., 2010; and Lidman et al., 2008) and beyond redshift $z \sim 6$ (Vanzella et al., 2010; Fontana et al., 2010; Castellano et al., 2010a,b; and Bouwens et al., 2010). Such a burst of results for extremely high redshift targets was not expected at the time when defining the HAWK-I science cases, while the results at intermediate redshifts were expected from science case #1.
2) The other fields explored so far are Milky Way stellar populations (Brasseur et al., 2010), trans-Neptunian objects (Snodgrass et al., 2010), gamma-ray bursts (D'Avanzo et al., 2010) and quasars (Letawe & Magain, 2010). Stellar

population studies have been hampered by HAWK-I's large minimum detector integration time (DIT), which causes saturation on bright sources and almost completely prevents observations in the Galactic disc.

3) No papers were published in the field of star formation and structure of nearby galaxies (science cases #3 and #4) in the period up to and including 2010, in spite of the fact that several programmes have been queued and successfully executed.
4) Contrary to expectations, HAWK-I was intensively used to study exoplanets, via transit or occultation techniques (Gibson et al., 2010; Anderson et al., 2010; and Gillon et al., 2009), and to conduct supernova search campaigns (Goobar et al., 2009) for spectroscopic follow-up. Transit observations, in particular, are expected to be increasingly important in the nearby future as a windowed readout of the detectors has been implemented.
5) The majority of the observations published require or benefit from the large field of the instrument.

In Figure 3 we give two examples of JHK_s colour-composite maps highlighting the superb image quality of the HAWK-I camera.

ESO/M. Gieles, Acknowledgement: Mischa Schirmer

Figure 3. Three colour (J [1.25 μm], H [1.65 μm] and K_s [2.15 μm]) composite maps obtained with HAWK-I. The upper image shows the nearby galaxy Messier 83, total exposure time was 8.5 hours and field of view 13 arcminutes squared. On the bottom, an image of 6 by 5.2 arcminutes of two stellar clusters in the Carina Nebula is shown, obtained during HAWK-I science verification.

Future directions: HAWK-I + GRAAL

It is anticipated that HAWK-I will be equipped with GRAAL and routinely operate in GLAO mode from 2015 onwards, which will open up new paths for competitive science cases in the coming years. The image quality delivered by HAWK-I + GRAAL is expected to be 20% better in comparison with today. For seeing in the K_s-band of 0.6 arcseconds, the GRAAL-supported instrument is expected to deliver a resolution of 0.5 arcseconds on a regular basis. Given HAWK-I's pixel scale of 0.106 arcseconds, the PSF delivered by HAWK-I + GRAAL will still be Nyquist-sampled, which is particularly important for precise PSF-photometry, astrometry and the analysis of morphological structures on sub-arcsecond spatial scales. Currently, half of the HAWK-I K_s-band images show an image quality (full width at half maximum, FWHM) on point sources larger than 0.6 arcseconds. This arises from the fact that 70% of the HAWK-I observations were executed during DIMM (differential image motion monitor) seeing worse than 0.83 arcseconds. Half of the HAWK-I observations were performed at a median DIMM seeing of almost 1 arcsecond. The poorer than average seeing conditions prevalent during most HAWK-I observations is a result of the demand for good seeing conditions for NACO and SINFONI. Observing with HAWK-I together GRAAL will result in a much better image quality performance. The question arises: what kind of scientific projects will be feasible with HAWK-I + GRAAL that are currently not feasible with HAWK-I, or only under very rare conditions, when the seeing is exceptionally good. We outline three selected science cases of HAWK-I + GRAAL.

1. Cosmological surveys

A deep, wide-field NIR imaging survey complementing the HST/CANDELS cosmological survey is required. CANDELS[1] is the largest single project in the history of the Hubble Space Telescope, with 902 assigned orbits of observing time and obtains images at *J*- and *H*-band over a total field of view of 30 × 30 arcminutes. The survey will be completed in 2014. As the scientific exploitation also relies on multi-colour imaging, HAWK-I + GRAAL is an ideal instrument to complement the survey with very deep K_s- and *Y*-band imaging, as well as with narrowband imaging aimed at searching for very high redshift galaxies. Morphological studies of galaxies at intermediate and high *z* are a particular goal of the project that can be pursued only with a spatial resolution of < 0.5 arcseconds over a wide area. A wide field of view is essential in such a study, since structural properties are analysed on sufficiently large statistical samples. HAWK-I observations in the *Y*-band, complementing the first two CANDELS fields, have already been scheduled.

VISTA does offer the requested wide-field capability, but delivers neither the spatial resolution nor the required sensitivity. In order to reach the same limiting magnitude, VISTA requires an integration time 16 times longer than HAWK-I + GRAAL. However, the NIRCAM[2] instrument onboard JWST will have a field of view almost six times smaller than HAWK-I, but will offer at least a factor 15 in improved sensitivity. JWST is expected to become operational in ~2016.

2. Nearby wide-field imaging

Stellar population studies, both in nearby galaxies and in Galactic fields, currently suffer most from crowding and will benefit from an improved K_s image quality provided by HAWK-I + GRAAL. High spatial resolution coupled with a wide field of view is an important requirement for stellar population studies. A problem of current HAWK-I observations, when targeting crowded stellar populations, is that the relatively large minimum DIT of 1.7 s causes saturation on the brightest sources, which are numerous when observing towards the Galactic disc. The HAWK-I instrument operation team is at present testing a new windowed detector readout scheme that allows very short exposure times on the brightest pixels and, in parallel, long exposures for the remaining field. Such a new detector readout mode in combination with HAWK-I + GRAAL's improved seeing capabilities should lead to an increase of HAWK-I observations in this research field.

3. Exoplanets and transits

HAWK-I has recently proved to be an excellent instrument with which to perform challenging observations of exoplanetary transits. In order to obtain an overall picture of an exoplanet's atmospheric properties, occultation data in many photometric bands are required. With a continuously growing number of newly discovered planets and planetary candidates, there is a high demand for comprehensive follow-up observations by NIR imaging. Crucial requirements for such observations are a wide field of view, allowing for a large number of reference sources for precise relative photometry, and an instrument sensitive enough to collect a sufficient number of photons, typically for a S/N > 1000, in a short time. From space the CoRoT satellite (Moutou et al., 2008) is a mission particularly designed to discover transiting exoplanets. CoRoT has already found several hundred systems with candidate transiting planets. The mission will continue beyond 2015 and will possibly be followed up by PLATO (Roxburgh & Catala, 2006), an ESA project study due to be launched in 2018. Similarly, from the ground, there are robotic search projects ongoing on small telescopes. Instrumentation includes wide-field imaging capabilities covering several degrees in optical bands. The goal is to discover a large sample of candidate planetary transits which will be followed up on larger telescopes by radial velocity studies or NIR imaging. Examples are: WASP (Cameron et al., 2009) which has already detected 16 systems and will continue for several years; or HAT-South, which is the first global network dedicated to search for transiting planets.

The increase in sensitivity of HAWK-I + GRAAL will allow exoplanetary transits to be followed up around stars significantly fainter than those observed at the moment (K_s of 8–11 mag). Therefore a larger volume of planet–host star systems can be probed, so that potential exoplanets detected by CoRoT come within reach of the VLT and hence provide important NIR constraints on the physical nature of the planets. Observations with VISTA will not have the required sensitivity to perform such investigations. Since the large field of view is important for precision photometry, there is no strong advantage in using JWST/NIRCam instead.

References

Anderson, D. R. et al. 2010, A&A, 513, 3
Arsenault, R. et al. 2010, The Messenger, 142, 12
Bakos, G. A. et al. 2011, AAS Meeting 217, 253.02
Bouwens, R. J. et al. 2010, ApJ 725, 1587
Brasseur, C. A. et al. 2010, AJ, 140, 1672
Cameron, A. C. et al. 2009, IAU Symposium, Volume 253, 29
Castellano, M. et al. 2010a, A&A, 511, 20
Castellano, M. et al. 2010b, A&A, 524, 28
Coppin, K. E. K. et al. 2010, MNRAS, 407, L103
D'Avanzo, P. et al. 2010, A&A, 422, 20
Decarli, R. et al. 2009, ApJ, 703, L76
Finger, G. Reports on HAWK-I detectors available at: http://www.eso.org/~gfinger/marseille_08/AS08-AS12-9_H2RG_mosaic_gfi_final.pdf http://www.eso.org/~gfinger/hawaii_1Kx1K/crosstalk_rock/crosstalk.pdf
Fontana, A. et al. 2010, ApJL, i725, 205
Galametz, A. et al. 2010, A&A, 522, 58
Gibson, N. P. et al. 2010, MNRAS, 404, L104
Gillon, M. et al. 2009, A&A, 506, 359
Gogus, E. et al. 2010, ApJ, 718, 331
Goobar, A. et al. 2009, A&A, 507, 71
Greiner, J. et al. 2009, ApJ, 693, 1610
Hayes, M. et al. 2010, Nature, 464, 562
Hayes, M. et al. 2010, A&A, 509, L5
Hickey, S. et al. 2010, MNRAS, 404, 212
Le Louarn, M. et al. 2010, SPIE, 7736, 111
Letawe, G. & Magain, P. 2010, A&A, 515, 84
Lidman, C. et al. 2008, A&A, 489, 981
Mattila, S. et al. 2008, ApJ, 688, L91
McLure, R. J. et al. 2010, MNRAS, 403, 960
Moutou, C. et al. 2008, A&A, 488, L47
Paufique, J. et al. 2010, SPIE, 7736, 57
Roxburgh, I. W. & Catala C. 2006, IAUJD, 17, 32
Snodgrass, C. et al. 2010, A&A, 511, 72
Stanishev, V. et al. 2009, A&A, 507, 61
Tanvir, N. R. et al. 2009, Nature, 461, 1254
Vanzella, L. et al. 2010, ApJL, 730, 35

Links

[1] CANDELS: www.candels.ucolick.org
[2] JWST NIRCam: www.ircamera.as.arizona.edu/nircam

p3d — A Data Reduction Tool for the Integral-field Modes of VIMOS and FLAMES

Christer Sandin[1]
Peter Weilbacher[1]
Ole Streicher[1]
Carl Jakob Walcher[1]
Martin Matthias Roth[1]

[1] Leibniz-Institut für Astrophysik Potsdam (AIP), Germany

The second release of the data reduction tool p3d now also supports the integral-field modes of the ESO VLT instruments VIMOS and FLAMES. This article describes the general capabilities of p3d and how its different tools can be invoked, with particular reference to its use with data from VIMOS and FLAMES.

p3d is a general and highly automated data reduction tool for fibre-fed integral field unit (IFU) spectrographs. Based on an early proprietary version, p3d was rewritten from scratch to be more versatile, user-friendly, extendable and informative (Sandin et al., 2010). The first release supported four IFUs: the lens array and PPAK of the PMAS spectrograph at the Calar Alto Observatory; SPIRAL at the AAOmega spectrograph at the Australian Astronomical Observatory; and VIRUS-P at the McDonald Observatory. The second release of p3d supports most of the remaining instruments, including the four higher resolution IFU modes of VIMOS (HR-Blue, HR-Orange, HR-Red, and MR), as well as all the setups for the three IFU modes of FLAMES (ARGUS, and the two sets of mini IFUs).

Data reduction features

All the reduction capabilities of p3d, with supporting test studies, are described in detail in Sandin et al. (2010). p3d itself is available at the project website[1]. In Table 1 we outline the available features of p3d and the two ESO pipelines for VIMOS (version 6.2) and FLAMES (i.e. GIRAFFE; version 2.8.7). Cosmic-ray hits in single images, or in images that cannot be combined, are not removed by p3d. Instead, for ESO data, we recommend using the DCR program (Pych, 2004) first, and thereafter, if required, combining the resulting images in p3d using an average. All extracted images of p3d are accompanied by an error image.

Feature	ESO pipelines	p3d
Logging, at different levels of verbosity	x	x
Configuration by a plain text file	x	x
Combination of raw-data images	partly	all recipes
Dark current subtraction	x	–
Spectrum extraction: regular/deconvolution methods	x/–	x/2
Spectrum extraction: subtraction of a scattered-light component	–	x
Fully automatic spectrum tracing	x	x
Creation of a dispersion mask	automatic	interactive
Flat-field normalisation	partly	x
Flux calibration	x	–
Full error propagation	partly	x
Interactive inspection of intermediate and final products	–	x
Reduction using a GUI/scripts	x/x	x/x

Table 1. Comparison between features of p3d and the IFU modes of the ESO VIMOS (version 6.2) and FLAMES (version 2.8.7) pipelines.

By default p3d shows graphical results of the spectrum tracing, the cross-dispersion profile fits (used later when deconvolving overlapping spectra), the quality of the dispersion solution, and the optimally extracted spectra. Figure 1 shows an example. This makes it easy to check that the outcome is correct and satisfactory; and if it is not these plots will quickly provide important clues for a solution to the problem. p3d comes with an integrated spectrum viewer that works with any IFU (row-stacked) spectrum image, together with a fibre position table.

The algorithms used in p3d are described in Sandin et al. (2010). With this new release all parts of p3d are now thoroughly documented. The installation procedure is described in the distribution README file, and the various recipes are, together with all the options, described in detail in the headers of the respective files. A more appealing version of the same documentation is available at the project

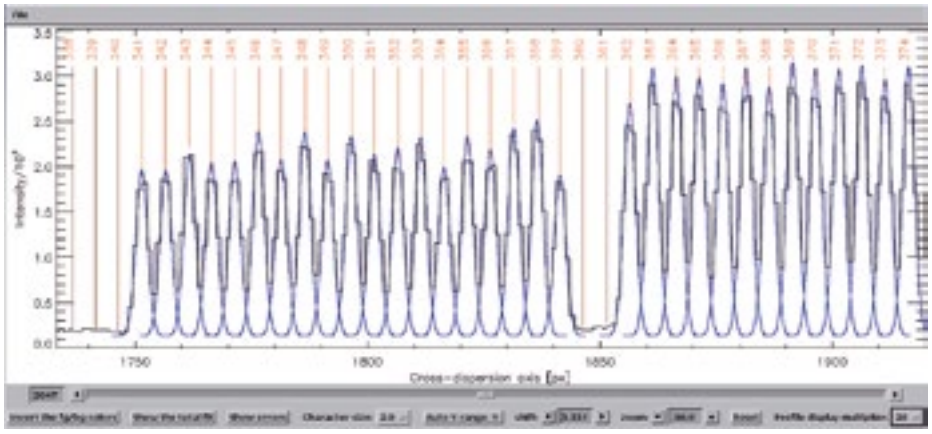

Figure 1. The fitted cross-dispersion line profiles for a set of the spectra in the VIMOS fourth quadrant (with grism HR-orange). The different lines are: intensity (in raw counts) at the middle column of the bias-subtracted continuum image (black line); the fitted Gaussian profiles (blue lines); the initial position of each spectrum (vertical red lines); and the vignetted spectra, which were not fitted (vertical blue lines).

<ob900000.sh>

```
#!/bin/bash

cpath=`pwd`
path="/data/user/VLT-P87/C/2011-04-27"
cd $path

name="ngc1-hr-blue-T1-1a"
parfile="${p3d_path}/data/instruments/vimos/nvimos_hr.prm"
userparfile="../p3dred/user_p3d.prm"
opath="../p3dred/odata/$name"
mkdir -p $opath

df1="\
VIMOS_IFU_OBS117_0001_B.1.fits.gz,\
VIMOS_IFU_OBS117_0002_B.1.fits.gz,\
VIMOS_IFU_OBS117_0003_B.1.fits.gz,\
VIMOS_IFU_OBS117_0004_B.1.fits.gz"
group=1,1,1,2 # Files 1-3 are combined, file 4 is used single

# Extracting the object spectra for quadrant 1:
logfile="../p3dred/logs/dred_${name}_objx_q1.log"
masterbias="../p3dred/odata/VIMOS_SPEC_BIAS118_0001_B_mbias1.fits.gz"
tracemask="${opath}/VIMOS_IFU_LAMP118_0001_B_imcmb1_trace1.fits.gz"
 dispmask="${opath}/VIMOS_IFU_WAVE118_0001_B.1_dmask1.fits.gz"
flatfield="${opath}/VIMOS_IFU_LAMP118_0001_B_imcmb1_flatf1.fits.gz"
${p3d_path}/vm/p3d_cobjex_vm.sh $df1 $parfile masterbias=$masterbias \
 tracemask=$tracemask dispmask=$dispmask flatfield=$flatfield \
 userparfile=$userparfile opath=$opath detector=0 \
 logfile=$logfile loglevel=2 group=$group & \
# Click away the popup window (for a 1600x1200 screen):
sleep 1 && xdotool mousemove 800 600 && xdotool click 1
```

<ob900000.pro>

```
cd,cur=cpath
path='/data/user/VLT-P87/C/2011-04-27'
cd,cpath

name='ngc1-hr-blue-T1-1a'
parfile=!p3d_path+'/data/instruments/vimos/nvimos_hr.prm'
userparfile='../p3dred/user_p3d.prm'
opath='../p3dred/odata/'+name
file_mkdir,opath

df1=[, $
 'VIMOS_IFU_OBS117_0001_B.1.fits.gz', $
 'VIMOS_IFU_OBS117_0002_B.1.fits.gz', $
 'VIMOS_IFU_OBS117_0003_B.1.fits.gz', $
 'VIMOS_IFU_OBS117_0004_B.1.fits.gz']
group=[1,1,1,2] ; Files 1-3 are combined, file 4 is used single

; Extracting the object spectra for quadrant 1:
logfile='../p3dred/logs/dred_'+name+'_objx_q1.log'
masterbias='../p3dred/odata/VIMOS_SPEC_BIAS118_0001_B_mbias1.fits.gz'
tracemask=opath+'/VIMOS_IFU_LAMP118_0001_B_imcmb1_trace1.fits.gz'
 dispmask=opath+'/VIMOS_IFU_WAVE118_0001_B.1_dmask1.fits.gz'
flatfield=opath+'/VIMOS_IFU_LAMP118_0001_B_imcmb1_flatf1.fits.gz'
p3d_cobjex,df1,parfile,masterbias=masterbias, $
 tracemask=tracemask,dispmask=dispmask,flatfield=flatfield, $
 userparfile=userparfile,opath=opath,detector=0, $
 logfile=logfile,loglevel=2,group=group
```

Figure 2. An example of a script that can be used to extract object spectra in VIMOS data. The script on the left-hand (right-hand) side is used from the shell (IDL command line).

website[1]; these web pages are updated with each new release.

p3d is based on the Interactive Data Language (IDL)[2], which must be installed on the system. All computing platforms supported by IDL can be used with p3d. There are three ways to invoke p3d. The first is through the graphical user interface (GUI), which can be started either from the IDL command line or using the shell script provided. This approach corresponds to the ESO tool Gasgano. The second is to run the individual recipes from the command line, and the third is to use the shell scripts provided; this last approach most closely corresponds to the ESO tool Esorex. The shell scripts use the IDL Virtual Machine together with the compiled binary files that are provided, with or without an IDL license. The shell scripts work on all platforms with a bash shell.

The GUI method is an easy entry point for the new user. By comparison, the two script methods allow the more experienced user to save time, since she or he can simply execute the scripts anew, after any change to the procedure or the code. Figure 2 shows an example of a simple script, using both methods, which can be used to reduce VIMOS data.

Details regarding VIMOS and FLAMES

When p3d is used with FLAMES and VIMOS some care is required in the configuration procedure to produce the most accurate outcome possible. We emphasise that the required modifications are small when comparing data that were extracted either before or after the respective refurbishments (cf. Hammersley et al., 2010; Melo et al., 2007). Here we note the details of each instrument separately, beginning with VIMOS.

VIMOS

With VIMOS data the reduction is done for each of the four quadrants individually. The data from the four quadrants are combined in a final step — after the data have been flux calibrated — to produce a datacube image with all 1600 spectra. Data from quadrants one, two and four, are all traced well, without any required user interaction. The third quadrant sometimes requires a manual parameter adjustment to trace all the spectra properly; this is caused by the spectrum pattern, which is less well defined than in the other quadrants. The tracing plots show that the tracing procedure sometimes misses one spectrum in the last group of spectra. With pre-refurbishment data, a similar problem is only found in data from the fourth quadrant. The scattered-light subtraction should be used in all spectrum extraction procedures to set the zero background level properly; we recommend a zeroth-order polynomial fit.

We found that the first-guess dispersion solution of p3d allows the emission lines that are required to create an accurate dispersion mask to be easily identified for all grism setups and quadrants. For our data from P86 (PI: Lundqvist), the maximum residual (for HR-blue and HR-orange) between the true wavelength and the fitted wavelength of any arc line was 0.002–0.007 nm for a fifth-order polynomial. Larger residuals are found in

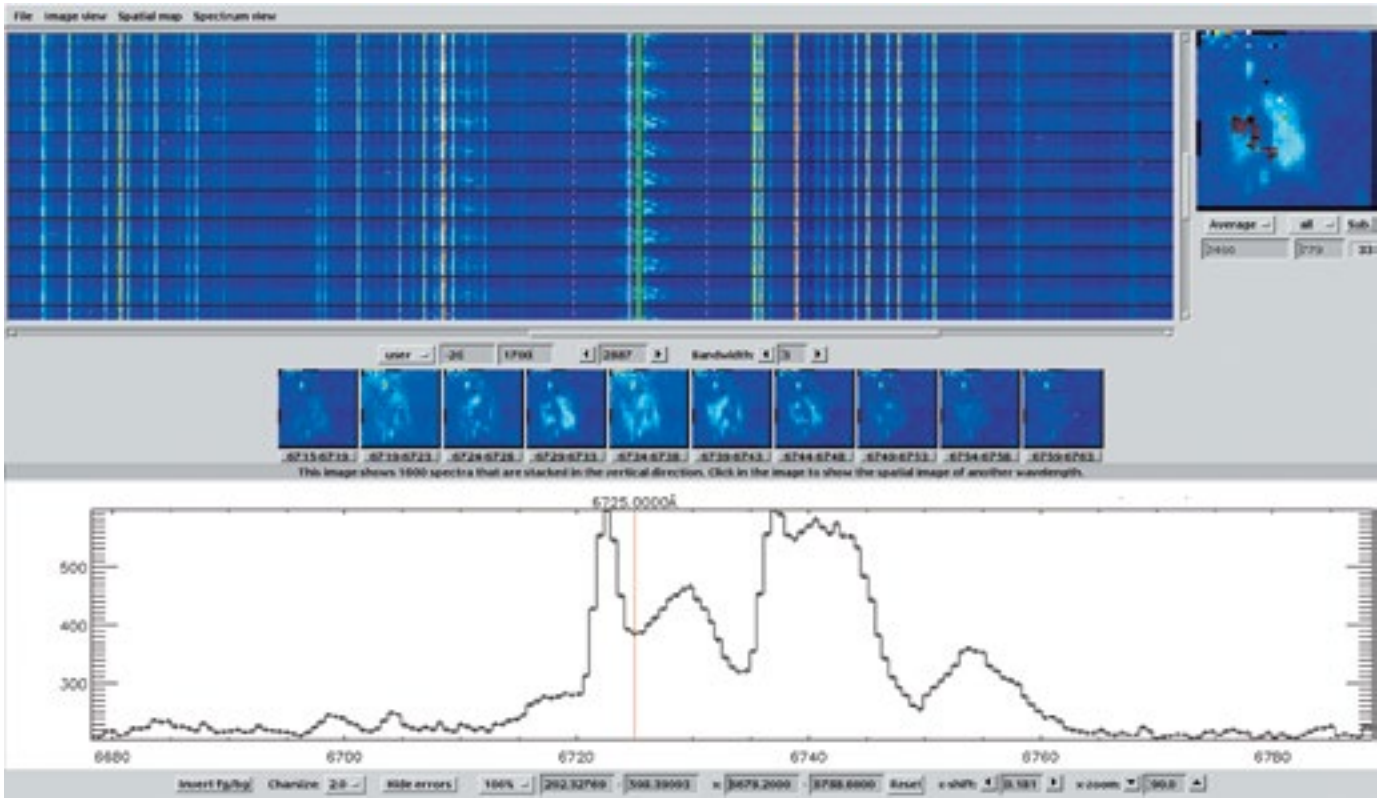

Figure 3. The p3d spectrum viewer showing an extracted datacube, where all four quadrants of VIMOS have been combined. The four different panels show: the spectrum image (upper left); the spatial map at a selected wavelength (upper right; north is up and east left); ten stored spatial maps of different wavelengths (middle panels); the selected spectrum, in this case the average of the 33 spectra that are marked in the spatial map (bottom panel).

low-transmission spectra. We also found that the highest accuracy level can be achieved in more spectra if cosmic-ray hits are removed in the arc image before creating the dispersion mask.

Noise reduction is a good reason to replace an extracted flat-field image with a smoothed version. Such a replacement proved impossible with VIMOS, due to the strong fringing at red wavelengths. With the new data the fringing effects are smaller, but still present. The default is therefore to avoid any smoothing of the flat-field image. Moreover, if twilight flat-field images are available, it is possible to use their transmission correction and correct the data further. In Figure 3 we show the spectrum viewer display for an extracted and combined dataset of a supernova remnant (using HR-orange).

The data were not flux-calibrated, but the data from the separate quadrants were re-normalised using the mean flat-field spectrum of each quadrant.

FLAMES

The three different IFU modes of FLAMES use the same instrument configuration file. Since there is only one detector, all spectra are reduced at once. We have found that the tracing works well in all cases, although the last sky fibre is always outside the CCD. The calibration fibres are reduced along with the other fibres, but are never used by p3d. Furthermore, p3d provides a linear first-guess dispersion solution for the same set of arc lines that is used by the GIRAFFE pipeline. However, in order to enable easy identification of all the arc lines to be used, it is advisable to restrict the set of arc lines to the brightest before the reduction is begun. In our data from P83 (programme ID 083.B-0279, PI: Neumayer), the maximum residual, between the true wavelength and the fitted wavelength of any arc line, is constant at about 0.005–0.006 nm, for a fourth-order polynomial using about 20 lines and the LR02 setup. While the fringing effects in the red wavelength range are lower with the refurbished instrument than previously, one should still not smooth the flat-field data to remove the fringes more completely.

Our reduced data of the nuclear region of the galaxy NGC 3621 were fitted with stellar population models and are shown in Figure 4; specifically we used the pixel-fitting code PARADISE (Walcher et al., 2009), as well as a preliminary version of

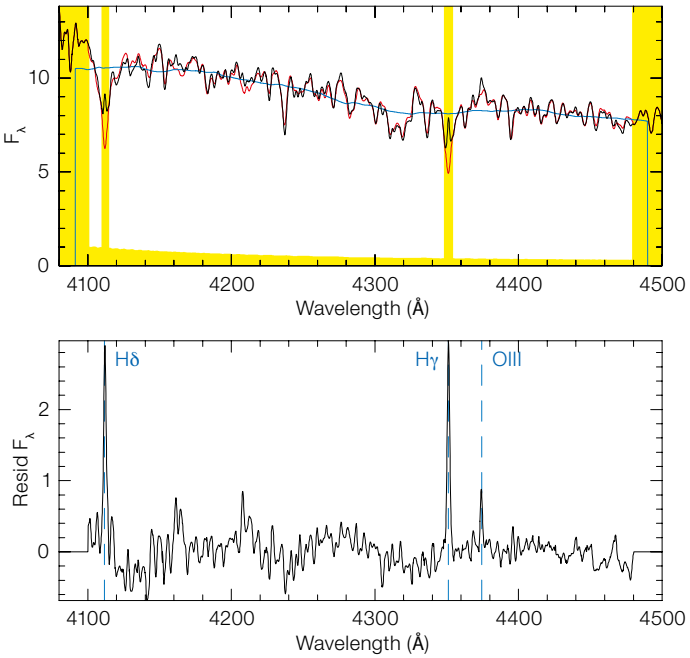

Figure 4. A spectrum of the circum-nuclear disc of the galaxy NGC 3621. The data (black line) are fitted with a stellar population model (red line). The blue line is the continuum used to normalise the data. Yellow areas mark wavelengths masked from the fit. The lower panel shows the fit residuals.

the Charlot & Bruzual (in prep.) stellar population model (see Gonzalez et al., 2010). The lower panel shows the residuals of the fit, i.e. a pure emission line spectrum. Note the presence of [O III] at 436.3 nm and of Wolf–Rayet features at 415–422 nm. This plot demonstrates the excellent quality of the data and of the reduction procedure, allowing even the faintest features to be identified reliably.

Both VIMOS and FLAMES benefit from optimal extraction. The associated profile-fitting stage in p3d makes use of modern multi-core workstations for improved processing speed. Instrument-specific guidelines on how to tailor the extraction are provided on the p3d Wiki[3].

Outlook

The old version of p3d has already been used successfully to reduce and publish data from various instruments (Roth et al., 2004) — including first data from the VIMOS–IFU (Monreal-Ibero et al., 2005). While the new version of p3d already contains a high level of functionality, there are many features that could still be included. For example, flux calibration, automated dispersion-mask creation, and an integrated line-fitting tool. With sufficient interest from the community we would consider adding full support also for the two remaining fibre-fed IFUs, *viz*. IMACS (Magellan) and Integral (WHT).

Acknowledgements

We thank Peter Lundqvist and collaborators for providing us with data from the refurbished VIMOS instrument (programme ID 086.D-0992).

References

González-López lira, R. A. et al. 2010, MNRAS, 403, 1213
Hammersley, P. et al. 2010, The Messenger, 142, 8
Markwardt, C. B. 2009, ASP Conf. Ser., 411, 251
Melo, C. et al. 2007, The Messenger, 133, 17
Monreal-Ibero, A. et al. 2005, ApJ, 628, L139
Pych, W. 2004, PASP, 116, 148
Roth, M. M. et al. 2004, ApJ, 603, 531
Sandin, C. et al. 2010, A&A, 515, A35
Walcher, C. J. et al. 2009, MNRAS, 398, 44

Links

[1] p3d project website: http://p3d.sourceforge.net.
[2] IDL can be downloaded free from: http://www.ittvis.com.
[3] p3d Wiki: http://sourceforge.net/apps/mediawiki/p3d/index.php?title=Main_Page

MPG/ESO 2.2-metre telescope image of the spiral galaxy NGC 3621 taken with the Wide Field Imager (WFI). NGC 3621 is a nearby Sd galaxy with a high inclination, situated at a distance of 6.2 Mpc. The centre hosts a Seyfert 2 active galactic nucleus and a nuclear star cluster. The colour image was formed from broad-band (*B*, *V* and *R*) and narrowband ([O III] and Hα) images selected from the ESO archive by Joe DePasquale as part of the *Hidden Treasures* competition (Hainaut et al. 2011, *The Messenger*, 143, 57). See image eso1104a for more details.

Phase 3 — Handling Data Products from ESO Public Surveys, Large Programmes and Other Contributions

Magda Arnaboldi[1]
Jörg Retzlaff[1]
Remco Slijkhuis[1]
Vincenzo Forchí[1]
Paulo Nunes[1]
Diego Sforna[1]
Stefano Zampieri[1]
Thomas Bierwirth[1]
Fernando Comerón[1]
Michèle Péron[1]
Martino Romaniello[1]
Dieter Suchar[1]

[1] ESO

Phase 3 represents the final step in the execution of ESO large programmes and public surveys, which starts with the submission of the letters of intent for public surveys and proposals for large programmes, i.e. Phase 1, and continues with the preparation and submission of observing blocks for service mode observations, i.e. Phase 2. In this paper we present the new Phase 3 infrastructure deployed on 10 March 2011. This infrastructure supports the reception, validation and publication of data products from the public survey projects and large programmes to the ESO Science Archive Facility.

Access to the survey data products by the astronomical community

The ESO public survey projects on the near-infrared 4-metre VLT Infrared Survey Telescope for Astronomy (VISTA) (Emerson et al., 2006) and the optical 2.6-metre VLT Survey Telescope (VST) (Capaccioli et al., 2005) are ambitious projects that range from very wide area surveys with short exposures, like the VISTA Hemisphere Survey (VHS), which aims at covering the whole southern hemisphere, to deep surveys concentrating on small areas or even a single pointing on the sky, and going very deep. Typical examples of the latter are the UltraVISTA and VIDEO surveys (for an overview of the six VISTA and the three VST public surveys see Arnaboldi et al. [2007]). A plot reproducing the survey areas of the six VISTA surveys is shown in Figure 1. In addition to the imaging surveys, ESO opened a call for spectroscopic public surveys and the selected projects will soon follow the same policies and procedures for telescope operations, access to data products and publication.

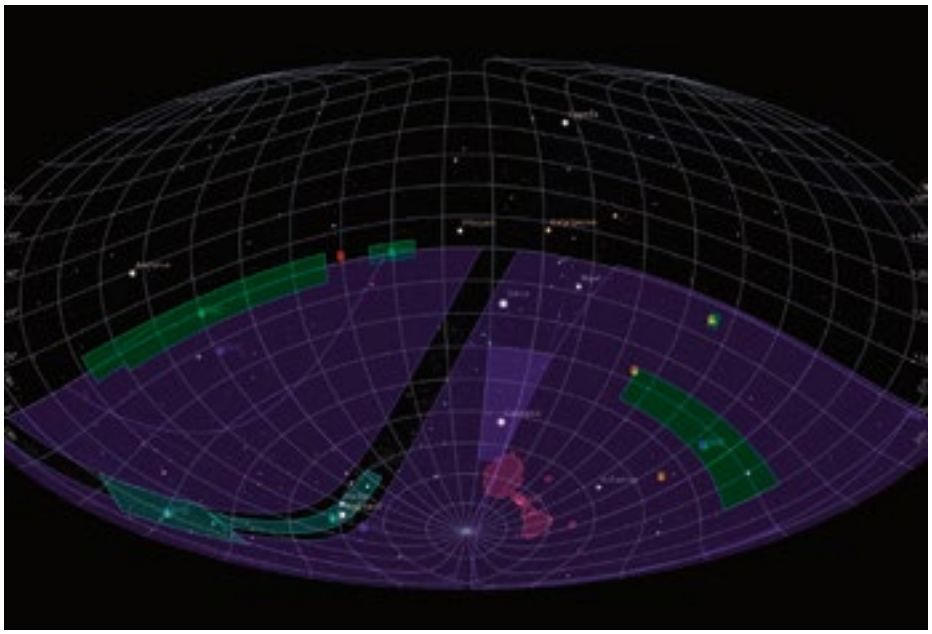

Figure 1. Summary of the regions of the sky covered by the six VISTA surveys: VHS is shown as the blue shaded areas; VIKING areas in light green; VVV areas in light blue; VMC areas in purple; and the ULTRAvista and VIDEO fields in red and yellow, respectively.

The raw data collected at the survey telescopes for the different projects amounts to about 700 GB per month, which in turn are condensed into a few terabytes of data products each year. Because of the legacy value of the public survey projects, ESO's policy is to ensure their long-term archival value by supporting easy access to the data products and fostering their wide scientific use by the astronomical community at large, beyond those projects initially identified by the survey teams.

Phase 3 policies and concepts

Policies

As stated in the ESO Council document on the VLT/VLTI science operation policies (Meeting#104, 17–18 December 2004), the ESO Science Archive Facility (SAF) is the collection point for the survey products and the primary point of publication/availability of these products to the ESO community. As part of the implementation of the Council's recommendations, a dedicated group within the Data Products Department (DPD) was set up to oversee the definition of the requirements for Phase 3 and their implementation for the validation, ingestion and publication of data products from the various ESO projects in the SAF. The Phase 3 tools, user manuals and definitions of data standards are all available on the ESO website[1].

The dependencies between telescope time allocation and the delivery of data products to the ESO SAF is made explicit in the policies for public surveys. In fact, further allocation of observing time at the survey telescopes beyond the first year and a half, and the scientific follow-up at the VLT of the public survey targets is subject to timely delivery of the survey products and their compliance to the specifications detailed during Phase 1. The Public Survey Panel that initially took part in selecting the public survey projects will periodically review the progress of the surveys and report to the OPC for any additional allocation of telescope time to these projects.

Concepts

The Phase 3 concepts provide the framework that supports the data submission process and facilitates data access

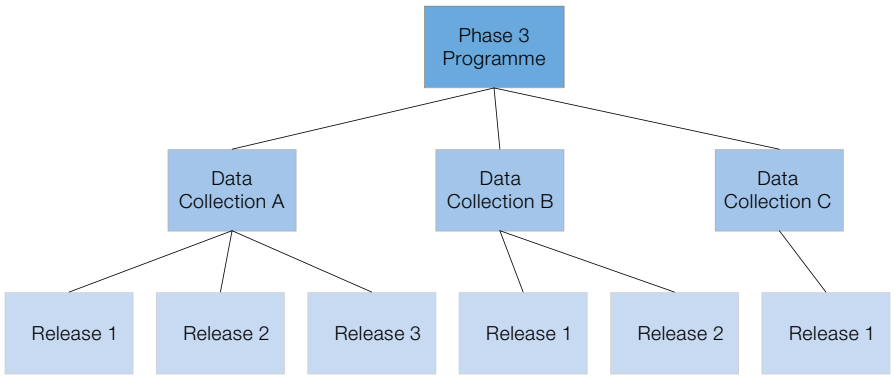

Figure 2. Block diagram illustrating the hierarchy of the Phase 3 concepts: from Phase 3 programme to collection and data release.

through the ESO archive. They form a simple hierarchical structure where the Phase 3 programme is at the top, followed by data *collection* and data *releases* at the bottom. A data release must be associated to one, and only one, data collection. The hierarchy of the Phase 3 concepts is illustrated in Figure 2. The data collection allows the data from a given programme to be organised according to high-level criteria into self-consistent groups, which the archive user then can browse and access.

As an example of the application of these concepts, a Phase 3 programme is then one of the survey projects (e.g., VHS), one data collection of which may correspond to one target object, or a target region in case of a survey (e.g., the South Galactic Pole for the VHS survey). The collection name must be defined when starting data submission and cannot be revised at a later stage by the user. Each data release must also be supported by a release description that specifies content, data properties and form.

The individual data release may be considered to be a version of the data collection. Subsequent data releases for the same collection may follow the initial release to add more data according to the progress of the observing programme (e.g., Release 2, 3, etc.). The Phase 3 infrastructure allows the data provider to complement, update or supersede a previous release according to the PI's strategy for data publication.

Phase 3 process and tools

The Phase 3 process consists of the following steps that are carried out by the PI/CoI and the ESO staff working in the External Data Products (EDP) group. PI/CoI activities include the definition of new data collections and releases, data preparation and validation, data upload to the ESO staging area, creation and upload of the release description, and finally closing the release. The PI of an ESO programme can delegate the Phase 3 process to one or more people to distribute the effort of data submission and release preparation. Multiple delegates can, in principle, work on the same data release but it is the sole responsibility of the PI to finally ensure the overall consistency.

On the ESO side, the EDP's activities are to create the Phase 3 programme, validate the submitted data, then carry out their archival and publication. The validation of the submitted data includes the automatic validation of the data against the published format standards for data products, including their header keywords, as a first step, and the verification of the data release content as a second step. During scientific validation, the completeness and consistency of the data release description with respect to the submitted products is examined and spot checks of the metadata content and the reported quality parameters are carried out. A summary diagram of the Phase 3 process and the various responsibilities is shown in Figure 3.

Tools

The Phase 3 infrastructure consists of the following components:

— a web application — the Phase 3 release manager — that allows the PI to manage the Phase 3 delegation, and define collections and releases;
— the release validator, which is a command-line application that verifies the data standard and validity of the header keywords against predefined rules;
— the FTP server (phase3ftp.eso.org) that is used in the Phase 3 process by the PI/CoI.

On the ESO side, the release manager is accessed in "operator mode" at the beginning of the Phase 3 process, to create a new Phase 3 programme, and at the end, after the data products pass the science validation, for their ingestion into the ESO archive. Applying for the automatic ingestion of the data products extracts the header information and loads this information into the ESO metadata repository, while all data files are sent to the bulk storage system in the ESO archive. Two independent copies of all the data are kept for reasons of safety. A summary showing the different interfaces of the Phase 3 infrastructure with users and the archive facility is displayed in Figure 4.

An important aspect of the support provided by the EDP group is the monitoring of the submitted data products with respect to the executed observations. To this end a dedicated application is used, which accesses the metadata repository and allows the association between data

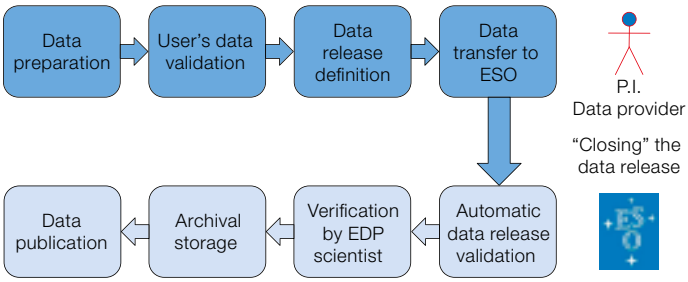

Figure 3. Schematic diagram illustrating the Phase 3 process and responsibilities.

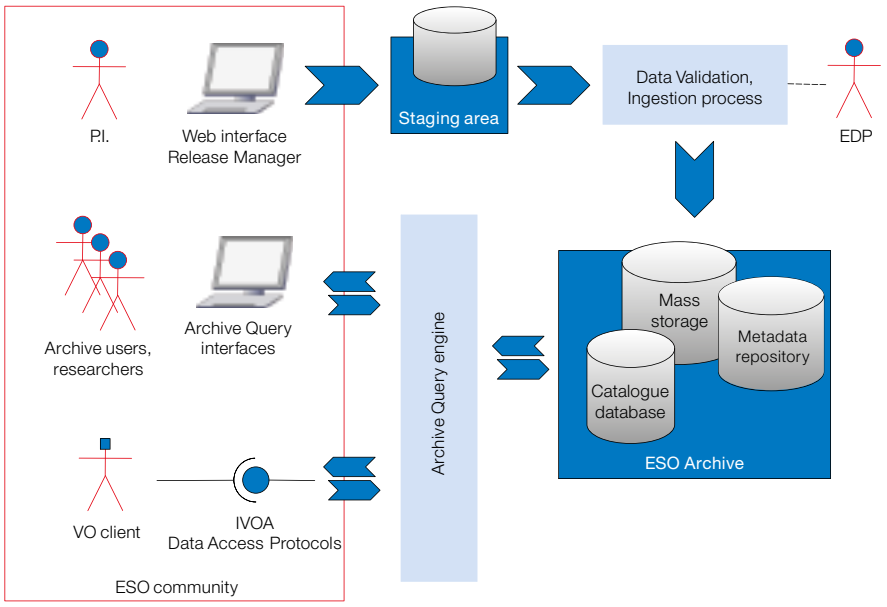

Figure 4. Diagram illustrating the Phase 3 data flow and intefaces with users and the ESO Science Archive Facility. The staging area provides 15 TB of disk space.

product files and the successfully executed OBs at the survey telescopes stored in the Phase 2 database.

Data standards

The definition of data standards and the deployment of the rules as the basis of the automatic validation are key responsibilities of the EDP group. Data standards are required to characterise the level of data reduction and calibration, to track provenance, which allows ESO to monitor survey progress, and finally to support the query for specific data products and VO protocols via the ESO archive interfaces.

For the VISTA data, a number of product types were identified: tiles, pawprints, stripe images, weight maps and source lists. Their definition and relevant keywords are illustrated on the Phase 3 webpage[1].

What's next? Publication of catalogues and internal data products

While supporting the Phase 3 process for ESO programmes and developing new data standards, the EDP group is engaged in further developing the Phase 3 infrastructure so as to be able to accept catalogues and internal data products (IDPs).

Catalogues

As high-level data products, the resulting source catalogues from the public survey projects represent particularly important results. They are delivered at the milestones set by the major survey releases, the first of which is on 1 October 2011, a year and a half after the beginning of science operation with VISTA. Source catalogues require the data from different bands and tiles to be merged and a global calibration across tiles to be applied. The catalogues are different from the source lists, which are per-tile products and can be downloaded as entire FITS tables. The catalogue contents will be searchable via a dedicated query interface in the ESO archive. Basic functionalities will be supported to allow the archive user to carry out searches by position as well as by non-positional source parameters for sources in any areas of the southern sky, for further scientific selection and investigation on the user's computer.

IDPs

An important aspect of the Phase 3 concepts is that they were developed to support the publication of the data products generated by ESO as part of the quality control process. The DPD foresees that the first IDPs to be ingested and accessible by the community will be those generated by the most advanced pipelines. These IDPs will be made available via the query interfaces in the science archive domain dedicated to data products.

Phase 3 in operation

The Phase 3 tools were developed by the Data Flow Infrastructure Department, and the operational deployment was carried out by the Operations Technical Support Department within ESO. The project manager for the Phase 3 Infrastructure is Remco Slijkhuis, in collaboration with the EDP group.

Inputs from public survey users were collected during a dedicated one-day workshop on VISTA data products at ESO on 30 November 2010. The presentation of the Phase 3 infrastructure and tutorials were followed by a joint discussion with the VISTA survey teams, and whenever possible, the requests by PIs for extra functionality were implemented in the Phase 3 infrastructure that was deployed on 10 March 2011.

The current Phase 3 submission for the VISTA public surveys is ongoing with 6.8 terabytes of data products currently uploaded on the Phase 3 staging area. Once the scientific validation is completed by the EDP group, these data products will be safely stored, and then become available for community access via the archive query interfaces.

For enquiries on the Phase 3 process or to initiate a Phase 3 submission, please contact usd-help@eso.org, quoting Subject: Phase 3.

References

Arnaboldi, M. et al. 2007, The Messenger, 127, 28
Capaccioli, M., Mancini, D. & Sedmak, G. 2005, The Messenger, 120, 10
Emerson, J., McPherson, A. & Sutherland, W. 2006, The Messenger, 126, 41

Links

[1] Phase 3 web information: http://www.eso.org/sci/observing/phase3.html

Colour-composite image of the nearby Carina dwarf spheroidal galaxy formed from the combination of thousands of images in *U*, *B*, *V* and *I* with many telescopes and imagers including the MPG/ESO 2.2-metre telescope and Wide Field Imager. See the article by Stetson et al. (p. 32) for more details.

A VISIR Mid-infrared Imaging Survey of Post-AGB Stars

Eric Lagadec[1]
Tijl Verhoelst[2]
Djamel Mekarnia[3]
Olga Suarez[3, 4]
Albert A. Zijlstra[5]
Philippe Bendjoya[3]
Ryszard Szczerba[6]
Olivier Chesneau[3]
Hans Van Winckel[2]
Michael J. Barlow[7]
Mikako Matsuura[7, 8]
Janet E. Bowey[7]
Silvia Lorenz-Martins[9]
Tim Gledhill[10]

[1] ESO
[2] Instituut voor Sterrenkunde, Katholieke Universiteit Leuven, Belgium
[3] Fizeau, OCA/UNS/CNRS, Nice, France
[4] Instituto de Astrofisica de Andalucia, Granada, Spain
[5] Jodrell Bank Centre for Astrophysics, University of Manchester, United Kingdom
[6] N. Copernicus Astronomical Center, Torun, Poland
[7] University College London, United Kingdom
[8] Mullard Space Science Laboratory, Univerisity College London, United Kingdom
[9] Universidade Federal do Rio de Janeiro, Brazil
[10] University of Hertfordshire, United Kingdom

Post asymptotic giant branch (AGB) stars are key objects for the study of the dramatic morphological changes that low- to intermediate-mass stars undergo during their evolution from the AGB towards the planetary nebula stage. There is growing evidence that binary interaction processes may play a determining role in shaping many objects, but so far direct evidence for binarity is still weak. We report on a systematic study of the dust distribution around a large sample of post-AGB stars that probes the symmetry-breaking in the nebulae around these systems.

According to our current understanding of stellar evolution, all stars with main sequence masses in the range 1–8 $M_{\odot}$ evolve via the asymptotic giant branch phase to the planetary nebula (PN) stage. As they ascend the AGB, their mass-loss rate increases from solar-like values of 10^{-14} $M_{\odot}$/yr up to 10^{-4} $M_{\odot}$/yr. The integrated mass lost from these stars is an essential component of galactic evolution, as it is the main source of *s*-process elements in the Universe and the main producer of carbon. AGB stars are also the main contributors to the dust phase of the interstellar medium (ISM). During the last stages of AGB evolution, the remains of the convective hydrogen envelope are ejected during final, quiescent and sporadic mass-loss events. Dust grains and molecules, predominantly CO, form in their winds, forming large circumstellar envelopes that can be detected in the infrared and millimetre domains.

A departure from spherically symmetric mass-loss is observed in a substantial fraction of suspected AGB to PN transition objects. In particular, multipolar structures are often associated with protoplanetary nebulae (PPNe). The three-dimensional morphologies of these objects are projected on the sky, thus making it difficult to determine the intrinsic morphology of PPNe and PNe. But it is estimated that around 80 % of all PNe show aspherical morphologies. Hubble Space Telescope observations of PNe, for example, show a large range of morphologies, including elliptical, bipolar, multipolar or round nebulae.

Hydrodynamical models explain many of the observed structures from a structure-magnification mechanism, where a fast wind from the central star of the PN ploughs into the earlier slow AGB wind, amplifying any density asymmetry already present: this is the generalised interacting stellar wind model (GISW). Another model has also been proposed to explain the shaping of PNe. In this model shaping occurs at the end of the AGB phase, when fast collimated jets are triggered and shape a bipolar nebula. If the direction of the jets changes with time, then multipolar nebulae can be formed. Such jets could be formed through interaction with a companion, e.g., in an accretion disc (see Balick & Frank [2002] for a review).

Much of the theory of the shaping of PN and PPN relies on the presence of circumstellar material in either a dusty torus or a disc. Our team has discovered some discs/tori in the heart of PNe (Lagadec et al., 2006; Chesneau et al., 2006; Matsuura et al., 2006; Chesneau et al., 2007) using adaptive optics on ESO's Very Large Telescope (VLT) and mid-infrared (MIR) interferometry at the Very Large Telescope Interferometer (VLTI). But the role of these discs/tori in the shaping of the nebulae is still unclear, as we know neither the fraction of the total dust mass that is present in these central cores, nor the fraction of objects exhibiting such a disc/torus structure.

In order to observe the inner region of post-AGB stars, we need MIR observations, as the dust optical depth is smaller at longer wavelengths. The MIR is the only wavelength range at which we can observe the inner morphology of stars from the AGB to the PPN phase. Furthermore, the main source of radiation for these sources in the MIR is direct emission from dust, while at shorter wavelengths it is scattered light. Mid-infrared imaging is thus the best way to study the dusty structures inside these evolved stars.

Many MIR imaging observations of post-AGB stars have been made in the past. But the only available MIR imaging survey (Meixner et al., 1999) has been made with 3-metre-class telescopes and suffers from limited angular resolution for the morphological study of the observed objects; in addition the survey selection is biased, as known bipolar nebulae were observed. The survey consisted of only 17 resolved sources. Some work has been done using 8-metre-class telescopes, but always focusing on particular individual bright, well-known objects.

Here we present the results from the first mid-infrared *N*-band imaging survey of a large number of post-AGB stars with 8-metre-class telescopes. We aim at a systematic survey probing the inner dusty regions of post-AGB stars.

Target selection and observations

The large sample of observations came from five distinct observing runs from VISIR/VLT, Michelle/Gemini North and T-Recs/Gemini South.

Our sample contains the brightest post-AGB stars observable from Paranal and includes PPNe, R CrB stars, RV Tauri stars and "Water Fountains". R CrB stars are hydrogen-deficient post-AGB stars with known obscuration events. RV Tauri stars are pulsating post-AGB stars, located at the high luminosity end of the Population II Cepheid instability strip. These RV Tauri stars are likely to harbour compact dusty discs. Water Fountains are oxygen-rich PPNe characterised by the presence of blue and red-shifted OH and H_2O masers, hence their curious class name. Some *bona fide* PN and evolved massive stars were also observed.

Most of the observations were obtained with the MIR instrument VISIR on the VLT. The excellent observing conditions during our run (0.43 mm of precipitable water vapour in the atmosphere), combined with the burst mode on VISIR, allowed us to obtain high quality diffraction-limited images. The burst mode readout allows every single frame of an exposure to be saved. In this way it is possible to follow rapidly evolving events or to improve the spatial resolution by taking short enough exposures to freeze atmospheric turbulence, as in lucky imaging (e.g., Law et al., 2006). This mode can be used only for objects that are bright enough to provide a high enough signal-to-noise (S/N) in a single elementary frame.

We thus observed 93 evolved stars in a quasi-uniform way in the mid-infrared, with a spatial resolution of the order of 0.3 arcseconds (which is the diffraction limit at this wavelength).

Two kinds of objects: resolved cores and detached shells

From the set of 93 objects we observed, 59 appear as point sources. Among the extended targets, we resolved a wealth of different structures, such as resolved central cores, dark central lanes, detached shells, S-shaped outflows. If we consider only the PPNe from our sample, we arrive at a sample of 52 detected objects.

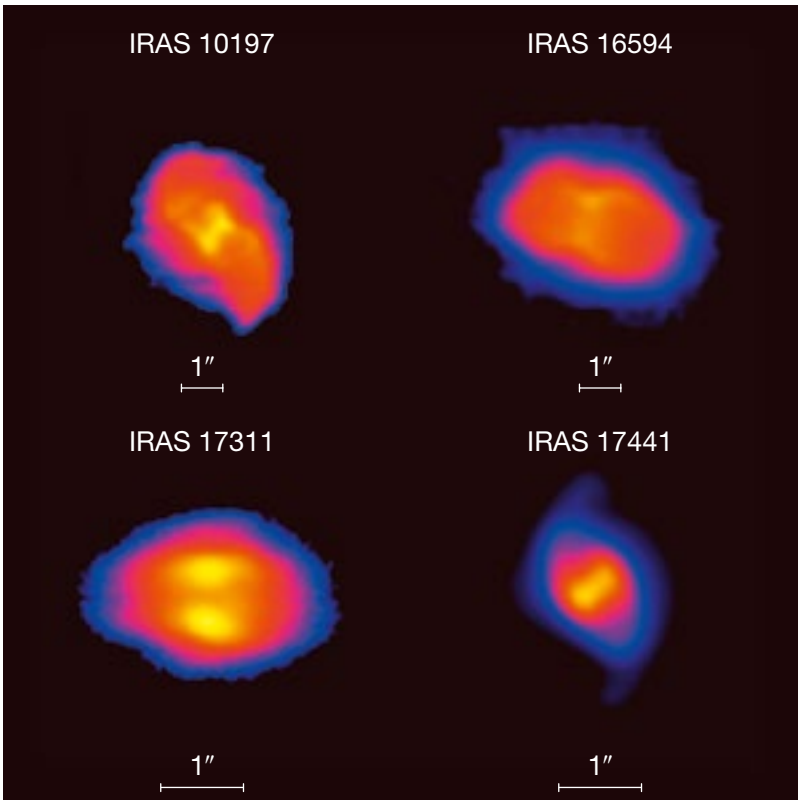

Figure 1. VISIR 10 µm images of a sample of post-AGB stars with resolved central cores. The designation of each target is given and the spatial scale is shown.

For the largest objects that are clearly resolved, we notice that the PPNe can be divided into two categories. On the one hand the objects with a dense central core, in the form of a bright central source or a dark lane, with most of the emission coming from the poles, indicate the presence of a large amount of dust, making the central regions optically thick even in the MIR. Four examples are shown in Figure 1. On the other hand, some objects do not have such a dominant central core, and we can observe either a detached shell or the central star (examples in Figure 2). The objects without a central core all have an elliptical morphology, while the objects with a central core are either bipolar or multipolar. Both types of sources are differentiated in their spectral energy distribution (SED): the objects with a dense central core or an equatorial dark lane have a rather flat SED in the near-infrared wavelength range, due to the presence of hot dust close to the central star; the objects with detached shells are characterised by the presence of a clear double-peaked distribution to the SED, with a first peak at a wavelength shorter than 1 µm due to the central star, and a second peak due to the cool dust in the shell. The flux is much lower in the near-IR due to the absence of dust close to the central star. Figure 3 shows examples of both SEDs.

The very strong correlation between the presence of a dense core and the bipolar morphology is an indication that the dense cores play a role in the shaping of the nebulae. Two main classes of models have been proposed to explain the shaping of nebulae. The first class of models is based on the GISW models and here a fast wind from the central star of a PPN or PN interacts with a slower wind, a remnant of the AGB phase, assumed to be toroidal. In the second class of models, the primary shaping agents are high-speed collimated outflows or jets that are created at the end of the AGB phase or at the beginning of the PPN phase. The interaction of these jets with a spherical AGB wind will create lobes that are in fact

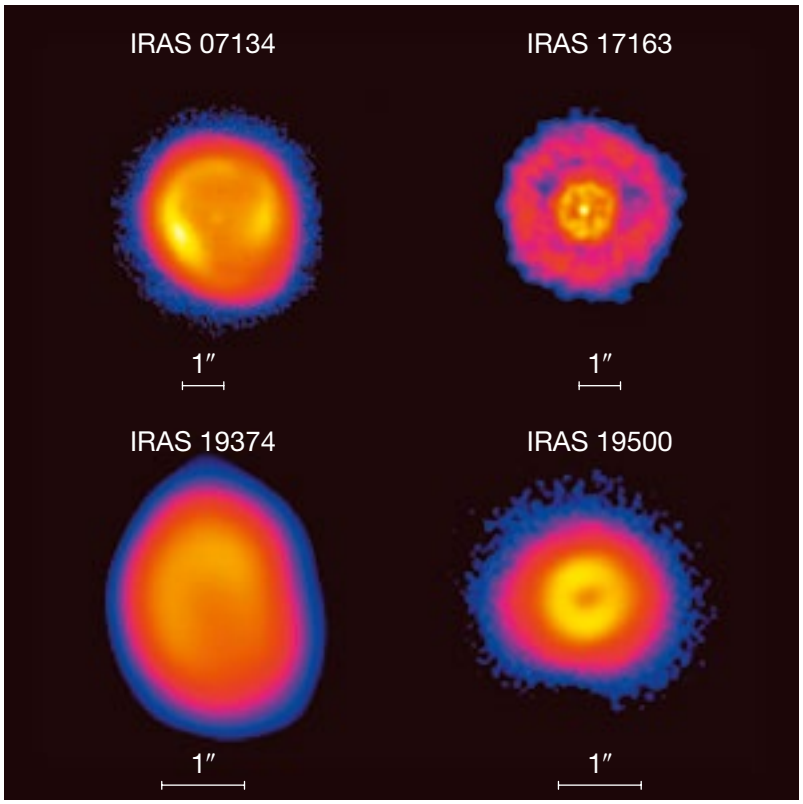

Figure 2. VISIR 10 μm images of a sample of post-AGB stars with detached shells. Annotations are as in Figure 1.

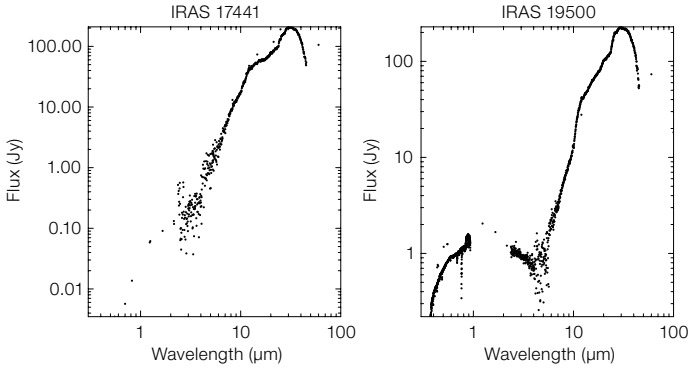

Figure 3. Typical spectral energy distributions of the two classes of objects observed. Left: an object with a dense equatorial dusty torus and a bipolar/multipolar morphology. Right: an object with a detached shell and an elliptical morphology.

cavities. If the direction of the jets changes with time, multipolar nebulae can be shaped.

Both models require the presence of a central torus/disc in the core of the nebula. Our observations clearly indicate that the bipolar and multipolar nebulae do have such a central structure in their core.

Departure from circular symmetry

All the PPNe we resolved in our survey show a clear departure from circular symmetry. Some circular shells are resolved, but only around massive evolved stars. A dramatic change in the distribution of the circumstellar material is often observed when a star evolves from the AGB to the PN phase (Balick & Frank, 2002).

Most AGB stars have a large-scale circularly symmetric morphology, while PNe display a variety of morphologies from elliptical to bipolar or multipolar. Optical imaging surveys of PNe indicate that 80% of the PNe show a clear sign of departure from circular symmetry, and thus that approximately 20% of PNe are spherical. The shaping of the PNe is thought to occur at the very end of the AGB phase or the beginning of the PPN phase. It is thus surprising that in our sample of 25 resolved PPNe, we do not find any circular ones.

The fact that we do not observe any circular PPNe could be a sample selection effect. We selected our targets as bright IRAS 12 μm sources. To be a bright emitter at these wavelengths, an object needs to have dust with a temperature of approximately 300 K, which must therefore be located close to the central star. This is the case for the stars with a central core, which are aspherical. The spherical PPNe are fainter than the non-spherical ones in the mid-infrared, due to the lack of a central torus/disc emitting in this wavelength range. At the end of the AGB phase, the envelopes of the AGB progenitors of circular PPNe are ejected and rapidly cool down while expanding. There are thus very few spherical PPNe that are bright in the mid-infrared. Furthermore those bright PPNe are compact and thus difficult to spatially resolve. The best way to detect such spherical envelopes is thus at longer wavelengths, and such detached shells are actually observed in the far infrared with the Herschel Space Observatory.

Formation of point-symmetric structures

A few objects that we resolved display a point-symmetric morphology, with an S-shaped envelope. One of our targets, IRAS 17441 (shown lower right in Figure 1), displays a tilt between the orientation of the resolved central dusty torus and the tips of the observed S-shaped structure. Such a tilt was observed by Volk et al. (2007), and measured to be almost 90 degrees. They suggested that a precession of the dusty torus could explain the observed S-shaped structure of the nebula. They estimated

the dynamical age of the envelope, assuming a distance of 1 kpc and an expansion velocity of 100 km/s, to be approximately 100 yr. According to this model, the torus should thus precess with a rate of around 1°/yr. As our observations were made four years after the observations presented by Volk et al. (2007), we should see a tilt of the torus of about 4° between the two observations. The images provided by these authors show that the orientation of the torus that they observed is exactly the same as the one we observed. The torus in the core of IRAS 17441 is thus not precessing at such a high rate.

It appears that we cannot explain the observed S-shaped structures with a precession of the central tori. This could be due to the fact that we underestimated the dynamical age of the nebula or that another mechanism is responsible for the S-shaped structure. A more plausible explanation is that the S-shaped structure is not due to the precession of the torus itself, but to precessing outflows inside this torus. The presence of such outflows has been observed in the PN NGC 6302, which has a morphology very similar to that of IRAS 17441 (Meaburn et al., 2008). These outflows are of a Hubble-type, which means that their velocity is proportional to the distance from the source. A torus similar to the ones observed in the core of these objects is also seen in the core of NGC 6302. The properties of such outflows can be theoretically described by a sudden ejection of material, a "bullet". Such bullets naturally account for multipolar flows, which could arise naturally from the fragmentation of an explosively driven polar-directed shell. We postulate that the S-shaped structure observed in IRAS 17441 is due to high speed outflows triggered at the end of the AGB phase, or the beginning of the PPN phase, likely during an explosive event.

Chemistry and morphology

Amongst the PPNe clearly resolved in our survey, 18 have known dust chemistry: either oxygen-rich, carbon-rich or a dual dust chemistry with both carbonaceous and oxygeneous dust grains in their envelopes. For the oxygen-rich sources, we find that 10 out of 11 are bipolar or multipolar, while the remaining one is elliptical. For the carbon-rich sources, we find that two are bipolar or multipolar and two elliptical. The three objects with a dual dust chemistry are multipolar or bipolar. This is in agreement with the recent work by Guzman-Ramirez et al. (2010), which shows a strong correlation between dual dust chemistry and the presence of an equatorial overdensity. The dual dust chemistry could be due either to the formation of PAHs in an oxygen-rich torus after CO photodissociation, or to the presence of a long-lived oxygen-rich disc formed before the star turned carbon-rich due to the third dredge-up.

Stanghellini et al. (2007) also studied the correlation between dust composition and morphologies. They determined, from a study of 41 Magellanic Cloud PNe, that all PNe with oxygen-rich dust are bipolar or highly asymmetric. Our study agrees with this finding, and it seems that oxygen-rich PPNe appear to be bipolar or multipolar. The low C/O ratio of these bipolar nebulae could be due to the interaction with a binary companion during a common envelope phase, or, in the case of single star evolution, result from conversion of carbon to nitrogen. The common envelope interaction will lead to the ejection of the envelope earlier than in the single star evolution scenario, leading to a less efficient dredge-up of carbon, and thus a lower C/O ratio. The conversion of carbon to nitrogen occurs for massive AGB stars in the hot bottom-burning process. It is thus likely that the bipolar PPNe have progenitors with larger masses than the elliptical ones. This is in agreement with the work by Corradi & Schwartz (1995), who showed that bipolar PNe tend to have a higher progenitor mass. Soker (1998) proposed that this result could be explained in the paradigm of binary system progenitors, as primaries that undergo a common envelope phase, and thus become bipolar, tend to have a higher mass.

Future directions

A large fraction of the dust in galaxies is produced during the late stages of the evolution of low- and intermediate-mass stars. This dust is ejected into the ISM during the PPN phase. Our observations show the existence of two paths for this dust ejection, via a detached shell or an expanding torus. It is now becoming clear that the bipolar objects with an equatorial torus have been formed via the interaction with a binary companion. This opens up a new field of research to study the impact of the presence of a binary companion on the dust formation by evolved stars. In order to better understand the importance of PPNe for the life cycle of dust, it would be interesting to study how these different paths affect the dust production by these objects. Spatially resolved VISIR mid-infrared spectra of these sources will allow us to study the dust composition at different locations in these PPNe, enabling us to better understand the evolution of dust during the PPNe phase, from its formation to its ejection, and how the presence of a dense dusty disc affects its composition.

Finally, the mass loss from evolved stars is a key ingredient for our understanding in many fields of astrophysics, including stellar evolution and the enrichment of the ISM via stellar yields. The aim of an ongoing ESO large programme (PI: C. Paladini), which will combine MIDI + VISIR + Herschel observations of a sample of evolved stars, is to constrain the geometry of this mass loss at different spatial scales. We will then be able to fully understand the dust evolution from its formation in a circumstellar envelope until its injection into the ISM, and better understand the life cycle of dust.

References

Balick, B. & Frank, A. 2002, ARA&A, 40, 439
Chesneau, O. et al. 2006, A&A, 455, 1009
Chesneau, O. et al. 2007, A&A, 473, L29
Corradi, R. L. M. & Schwarz, H. E. 1995, A&A, 293, 871
Guzman-Ramirez, L. et al. 2011, MNRAS
Lagadec, E. et al. 2006, A&A, 448, 203
Lagadec, E. et al. 2011, MNRAS, in press
Law, N. M. et al. 2006, MNRAS, 368, 1917
Matsuura, M. et al. 2006, ApJl, 646, L123
Meaburn, J. et al., 2008, MNRAS, 385, 269
Meixner, M. et al. 1999, ApJS, 122, 221
Stanghellini, L. et al. 2007, ApJ, 671, 1669
Soker, N. 1998, ApJ, 496, 833

The VISTA Near-infrared *YJKs* Public Survey of the Magellanic Clouds System (VMC)

Maria-Rosa Cioni[1, 2]
Gisella Clementini[3]
Leo Girardi[4]
Roald Guandalini[1]
Marco Gullieuszik[5]
Brent Miszalski[1]
Maria-Ida Moretti[6]
Vincenzo Ripepi[7]
Stefano Rubele[4]
Gemma Bagheri[1]
Kenji Bekki[8]
Nick Cross[9]
Erwin de Blok[10]
Richard de Grijs[11]
Jim Emerson[12]
Chris Evans[13]
Brad Gibson[14]
Eduardo Gonzales-Solares[15]
Martin Groenewegen[5]
Mike Irwin[15]
Valentin Ivanov[16]
Jim Lewis[15]
Marcella Marconi[7]
Jean-Baptiste Marquette[17, 18]
Chiara Mastropietro[19]
Ben Moore[20]
Ralf Napiwotzki[1]
Tim Naylor[21]
Joana Oliveira[22]
Mike Read[9]
Eckhard Sutorius[9]
Jacco van Loon[22]
Mark Wilkinson[23]
Peter Wood[24]

[1] University of Hertfordshire, Physics Astronomy and Mathematics, United Kingdom
[2] University Observatory Munich, Germany
[3] INAF, Osservatorio Astronomico di Bologna, Italy
[4] INAF, Osservatorio Astronomico di Padova, Italy
[5] Royal Observatory of Belgium, Belgium
[6] University of Bologna, Department of Astronomy, Italy
[7] INAF, Osservatorio Astronomico di Capodimonte, Italy
[8] ICRAR, University of Western Australia, Australia
[9] University of Edinburgh, Institute for Astronomy, United Kingdom
[10] University of Cape Town, South Africa
[11] Peking University, Kavli Institute for Astronomy and Astrophysics, China
[12] Queen Mary, University of London, United Kingdom
[13] UK Astronomy Technology Centre, United Kingdom
[14] Centre for Astrophysics, University of Central Lancshire, United Kingdom
[15] University of Cambridge, Institute of Astronomy, United Kingdom
[16] ESO
[17] UPMC, University of Paris, Institut d'Astrophysique de Paris, France
[18] CNRS, Institut d'Astrophysique de Paris, France
[19] LERMA, Observatoire de Paris, France
[20] University of Zurich, Institute of Theoretical Physics, Switzerland
[21] University of Exeter, School of Physics, United Kingdom
[22] University of Keele, School of Physical and Geographical Sciences, United Kingdom
[23] University of Leicester, United Kingdom
[24] Mount Stromlo Observatory, RSSA, Australia

The VISTA public survey project VMC targets the Large Magellanic Cloud, the Small Magellanic Cloud, the Bridge and two fields in the Stream. The VMC survey is a uniform and homogeneous survey in the *Y, J* and K_s near-infrared filters. The main goals are the determination of the star formation history and the three-dimensional structure of the Magellanic system. The survey is therefore designed to reach stars as faint as the oldest main sequence turn-off point and to constrain the mean magnitude of pulsating variable stars such as RR Lyrae and Cepheids. We provide a brief overview of the survey strategy and first science results. Further details are given in Cioni et al. (2011).

Introduction

The Magellanic Clouds offer an excellent laboratory for near-field cosmology. They represent the closest prototype for studies of interacting galaxies and their low metallicity and high gas content provide information about galaxies at an early stage of evolution. The Magellanic Clouds have experienced an extended star formation history (SFH) and their dynamical interaction may be responsible for the formation of the Magellanic Bridge. The origin of the Magellanic Stream is under debate as to whether it is also of tidal origin from the interaction of the Large Magellanic Cloud (LMC) with the Small Magellanic Cloud (SMC), or produced by ram pressure between the two galaxies.

The VMC[1] survey is acquiring near-infrared (NIR) data of unprecedented sensitivity in the Magellanic system that is of immense value for the astronomical community. The survey represents the only NIR counterpart to existing optical surveys and for the large number of unclassified objects observed with the Spitzer Space Telescope in the mid-infrared. The VMC will cover the bulk of the Magellanic system as opposed to the tiny regions sampled by the Hubble Space Telescope, and the limited area covered by most of the other ground-based observations at the same sensitivity.

Figure 1. VMC logo

Current open questions about the formation and evolution of the Magellanic Clouds will be addressed by the VMC survey, such as: How have the SFHs of the LMC and SMC been influenced by interaction? Does the geometry of the Magellanic system depend on age and metallicity? Why is there a significant difference in structure between the gas and stars in the SMC?

Observations and data reduction

VISTA[2] (Emerson et al. 2006) is the largest wide-field NIR imaging telescope designed to perform survey operations. The performance during commissioning is presented by Emerson et al. (2010), while science verification programmes are summarised in Arnaboldi et al. (2010).

The VMC survey parameters are listed in Table 1. VMC uses three filters, *Y*, *J* and K_s for the analysis of colour–colour diagrams; the wider colour spacing in $Y–K_s$ provides a good characterisation of the sub-giant branch population for deriving the SFH. Monitoring of variable sources is performed in the K_s-band, where variable stars obey a clear period–magnitude relation. The VMC survey area is shown in Figure 2. It covers the area to a limiting *B* magnitude of 25 mag arcsec^{-2} for both galaxies and encompasses the major features traced by the distribution of stars and gas.

Here we focus on observations obtained during the dry-run period (November 2009–March 2010) when VISTA was tested and survey operations were still being defined. Six VMC fields were observed in the LMC. One field covers the famous 30 Doradus region, one field corresponds to the South Ecliptic Pole (SEP) region, there are a pair of fields located in the northern outer part of the LMC disc while the remaining two fields are located towards the Bridge. The progress of the VMC survey observations up to 4 March 2011 is provided in Table 2.

The VISTA raw images are reduced by the VISTA Data Flow System (VDFS) pipeline at the Cambridge Astronomical Survey Unit (CASU[3]). Standard reduction steps are performed and quality control parameters are calculated for both monitoring and evaluating observing conditions retrospectively. A tile image is produced by combining different pawprint images adjusted for astrometric and photometric distortions as well as different sky levels. Tile catalogues are produced following the application of a nebulosity filter in order to remove diffuse varying background on scales of 3 arcseconds or larger (Irwin 2010). The average VMC parameters from all single-tile images are given in Table 3 where the magnitude limit is at 5σ. This set comprises observations obtained up to the end of November 2010 but does not distinguish between crowded and uncrowded fields for which the VMC has different observing requirements.

Astrometry is based on the positions of the many 2MASS sources within each detector. The median astrometric root-mean-square is 80 milliarcseconds (mas) and is dominated by uncertainties on 2MASS coordinates. Residual systematic distortions across the VISTA field of view are present at the 25 mas level. The photometric calibration relies on the observation of stars from the 2MASS catalogue with magnitudes in the range 12–14 in all bands. The calibration in the *Y*-band is possible where the extinction is not too high, i.e. $E_{B-V} < 1.5$ (Hodgkin et al. 2009). Figure 3 shows the behaviour of VISTA photometric uncertainties in a VMC field. Uncertainties are reduced by about 50% compared to those for individual tiles and will reduce further for deep tiles. A morphological classification flag is also included in the catalogue.

The data reduced by the VDFS pipeline are ingested into the VISTA Science Archive[4] (VSA). At present these data are reduced with the version 1.0 of the pipeline and include all VMC data observed until end of November 2011. At the VSA the data are archived to produce standardised data products: individual passband frame association and source association to provide multi-colour, multi-epoch source lists; cross-associations with external catalogues; and deeper stacking. The position and magnitude of each source in a given table refers to the astrometrically and photometrically calibrated measurements using the parameters specified in the image headers. In addition the magnitude of the brightest stars ($K_s < 12$ mag.) are recovered for saturation effects (Irwin 2009). Figure 4 shows the K_s magnitude difference for stars in a VMC field compared to 2MASS before and after saturation correction.

Table 1. VMC survey parameters.

Filter	*Y*	*J*	K_s	Filter	*Y*	*J*	K_s
Central λ (μm)	1.02	1.25	2.15	Exposure time per epoch (s)	800	800	750
Bandwidth (μm)	0.10	0.18	0.30	No. of epochs	3	3	12
DIT (s)	20	10	5	Total exposure time (s)	2400	2400	9000
No. of DITs	4	8	15	Sensitivity per epoch (Vega)	21.3	20.8	18.9
No. of exposures	1	1	1	S/N per epoch	5.7	5.9	2.9
Micro-stepping	1	1	1	Total sensitivity (Vega)	21.9	21.4	20.3
No. of jitters	5	5	5	Total S/N	10	10	10
Pawprints in tile	6	6	6	Saturation (Vega)	12.9	12.7	11.4
Pixel size (arcsec)	0.339	0.339	0.339	Area (deg^2)	184	184	184
System FWHM	0.51	0.51	0.51	No. of tiles	110	110	110

Description	VMC	LMC	SMC	Bridge	Stream
No. of tiles	110	68	27	13	2
No. of epochs	1980	1224	486	234	36
No. of Y epochs	330	204	81	39	6
No. of J epochs	330	204	81	39	6
No. of K_s epochs	1320	816	324	156	24
Observed *Y* epochs	59	37	8	8	6
Observed *J* epochs	58.5	38.5	6.5	7.5	6
Observed K_s epochs	98.5	75	5	4.5	14
No. of observed epochs	216	150.5	19.5	20	26
Completion in *Y*	17.9%	18.1%	9.9%	20.5%	100%
Completion in *J*	17.7%	18.9%	8%	19.2%	100%
Completion in K_s	7.5%	9.2%	1.5%	2.9%	58.3%
Total completion	10.9%	12.3%	4%	8.5%	72.2%

Table 2. VMC survey progress up to 4 March 2011. (Items in blue refer to the complete survey.)

Filter	FWHM	Ellipticity	Zero-point	Mag. Limit
Y	1.03 (0.14)	0.06 (0.01)	23.44 (0.10)	21.00 (0.49)
J	1.01 (0.13)	0.06 (0.01)	23.68 (0.14)	20.55 (0.44)
K_s	0.92 (0.10)	0.05 (0.01)	23.00 (0.19)	19.25 (0.30)

Table 3. VMC survey tile quality up to 30 November 2010.

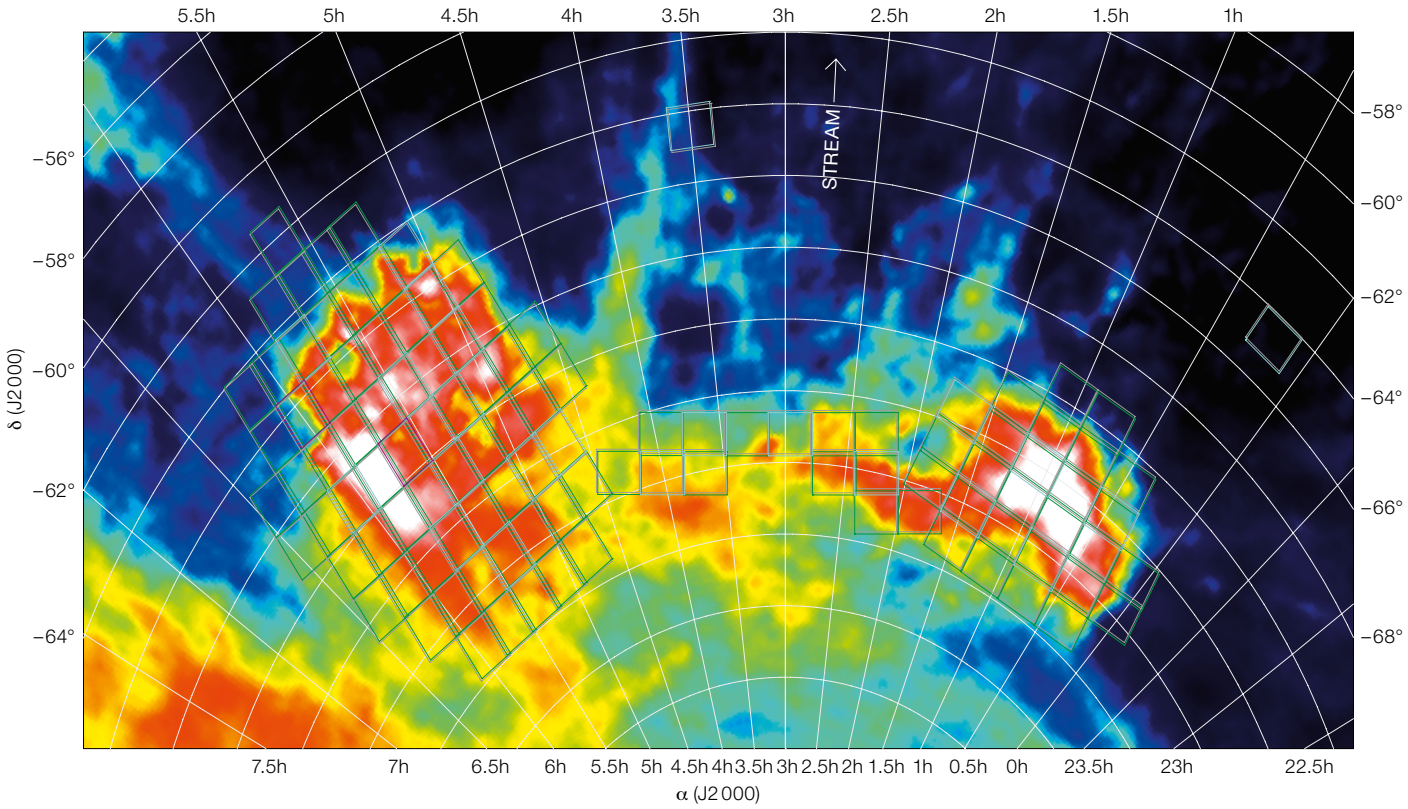

Figure 2. (Top) Magellanic system area tiled for VMC observations superimposed on the distribution of HI gas (McClure-Griffiths et al. 2009). Tiles are colour coded as follows: purple: completed; cyan: observations in progress; green: to be observed.

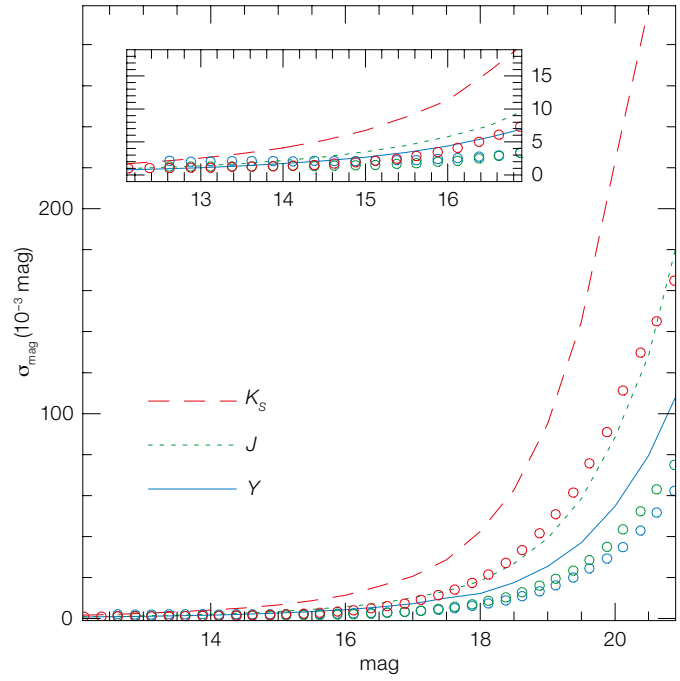

Figure 3. (Bottom left) Photometric uncertainties in the VMC data for stacked pawprints (dashed, dotted and continuous lines in the K_s-, J- and Y-bands respectively) and tiles (red, green and blue circles in the K_s-, J- and Y-bands respectively) in one field are shown.

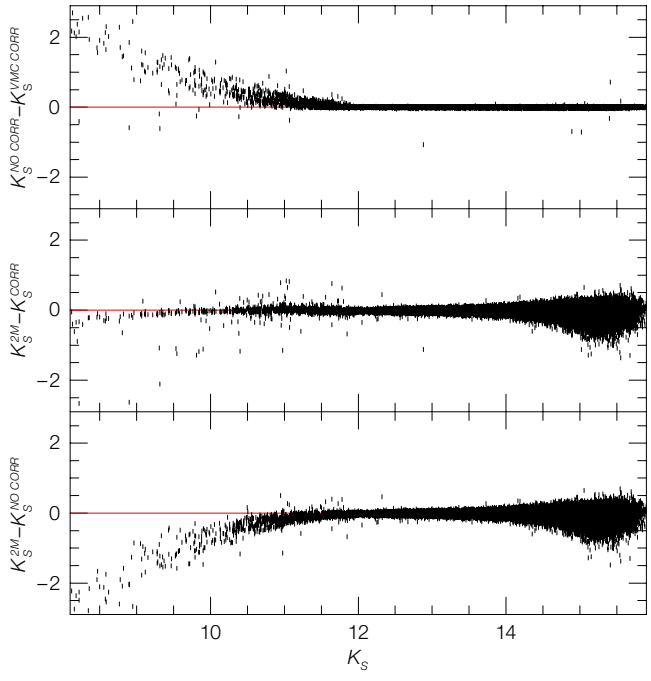

Figure 4. (Bottom right) Magnitude difference for stars in common between VMC and 2MASS before (bottom) and after (middle) recovering the magnitude of VMC stars approaching the saturation limit; the adjustment applied is shown at top.

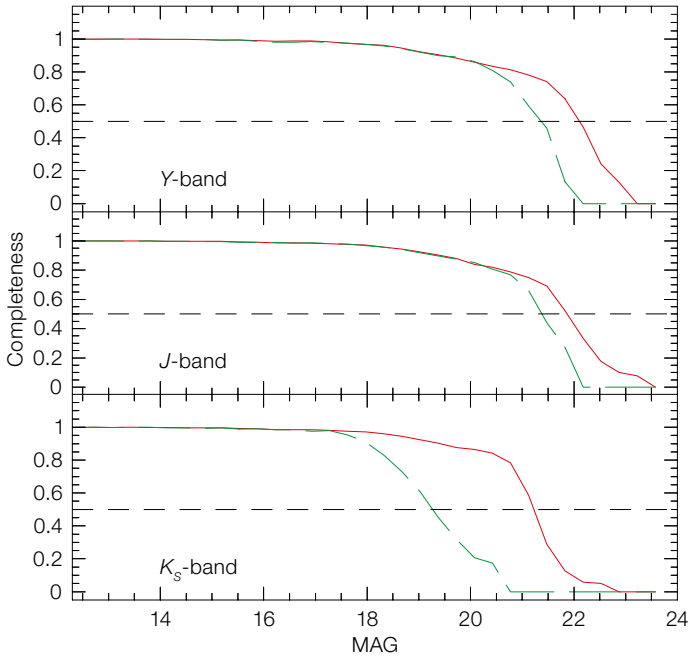

Figure 5. Completeness results for the South Ecliptic Pole (SEP) field are shown for single epoch (in green) and deep stacked images (in red).

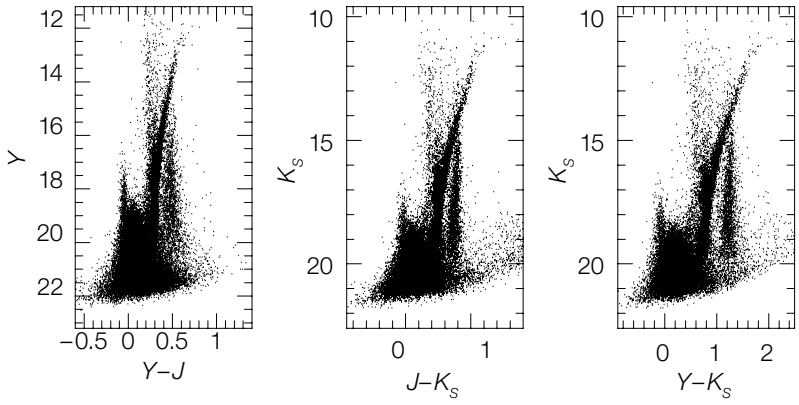

Figure 6. Colour–magnitude diagrams of VMC sources in the SEP field.

The completeness of the stellar photometry as a function of location across the Magellanic sytem and position in the colour–magnitude diagrams is estimated via the usual procedure of adding artificial stars of known magnitudes and positions to the images, then comparing them in the derived photometric catalogues. For this work tile images are created and regions equivalent to 1/12 of the area are selected for performing PSF photometry. Then, artificial stars are added randomly at a mutual distance of > 30 pixels, so as not to increase the typical crowding of the images. Artificial stars spanning smaller bins are later grouped together to estimate the number ratio between added and recovered stars. The results of this process are shown in Figure 5.

Colour–magnitude diagrams

Figure 6 shows the colour–magnitude diagrams (CMDs) of VMC stellar and probable stellar sources in the SEP field. These data were extracted from the VSA. The exposure times per band correspond to 2400 s in *Y*, 2800 s in *J* and 9400 s in K_s.

The distribution of stars in the CMDs shows different stellar populations. The bluest conic structure, bending to red colours at bright magnitudes, is formed by main sequence (MS) stars of increasing mass with increasing brightness. The MS joins, via the sub-giant branch, the red giant branch (RGB) beginning at ~2 mag below the red clump, the approximately circular region described by the highest concentration of stars. The RGB continues beyond the red clump at brighter magnitudes describing a narrow structure bending to red colours. The abrupt change in source density at the tip of the RGB marks the transition to brighter asymptotic giant branch (AGB) stars. The broad vertical distribution of stars below the RGB is populated by Milky Way (MW) stars that are easily distinguished from LMC stars. Cepheid and supergiant stars occupy the region of the diagram to the bright and blue side of the RGB, while RR Lyrae stars are somewhat fainter than the red clump and lie more or less parallel to the sub-giant branch.

The Ant diagram

Figure 7 shows the observed colour-colour diagram, and the corresponding CMDs, of the VMC data in the SEP field. The distribution of sources in the colour–colour diagram resembles the body of an ant, with different parts distinguished:

- *Gaster* ($-0.1 < (Y-J) < 0.3$ and $-0.3 < (J-K_s) < 0.3$), shown in red, the lower part of the ant body corresponds to the location of MS stars in the LMC, with the youngest being at the bluest extremity.
- *Mesosoma* ($0.2 < (Y-J) < 0.4$ and $0.4 < (J-K_s) < 0.75$), shown in blue, the middle part of the ant body corresponds to the main locus of helium-burning giants in the LMC. Most of them are in the red clump.
- *Petiole* ($0.15 < (Y-J) < 0.3$ and $0.3 < (J-K_s) < 0.4$), shown in green, is a small thin extension of the mesosoma at its red side, and is mainly caused by foreground bright stars in the MW
- *Head* ($0.4 < (Y-J) < 0.55$ and $0.65 < (J-K_s) < 0.85$), shown in magenta. Its main blob is defined by foreground low-mass stars in the Milky Way.
- *Upper antenna* ($0.42 < (Y-J) < 0.6$ and $0.85 < (J-K_s) < 1.1$), shown in cyan, being formed by the more luminous RGB stars in the LMC close to the tip of the RGB, extending up to $(J-K_s) = 1$ mag.
- *Lower antenna* ($(Y-J) > 0.55$ and $0.6 < (J-K_s) < 0.85$), shown in yellow, corresponding to the $(Y-J)$ redward

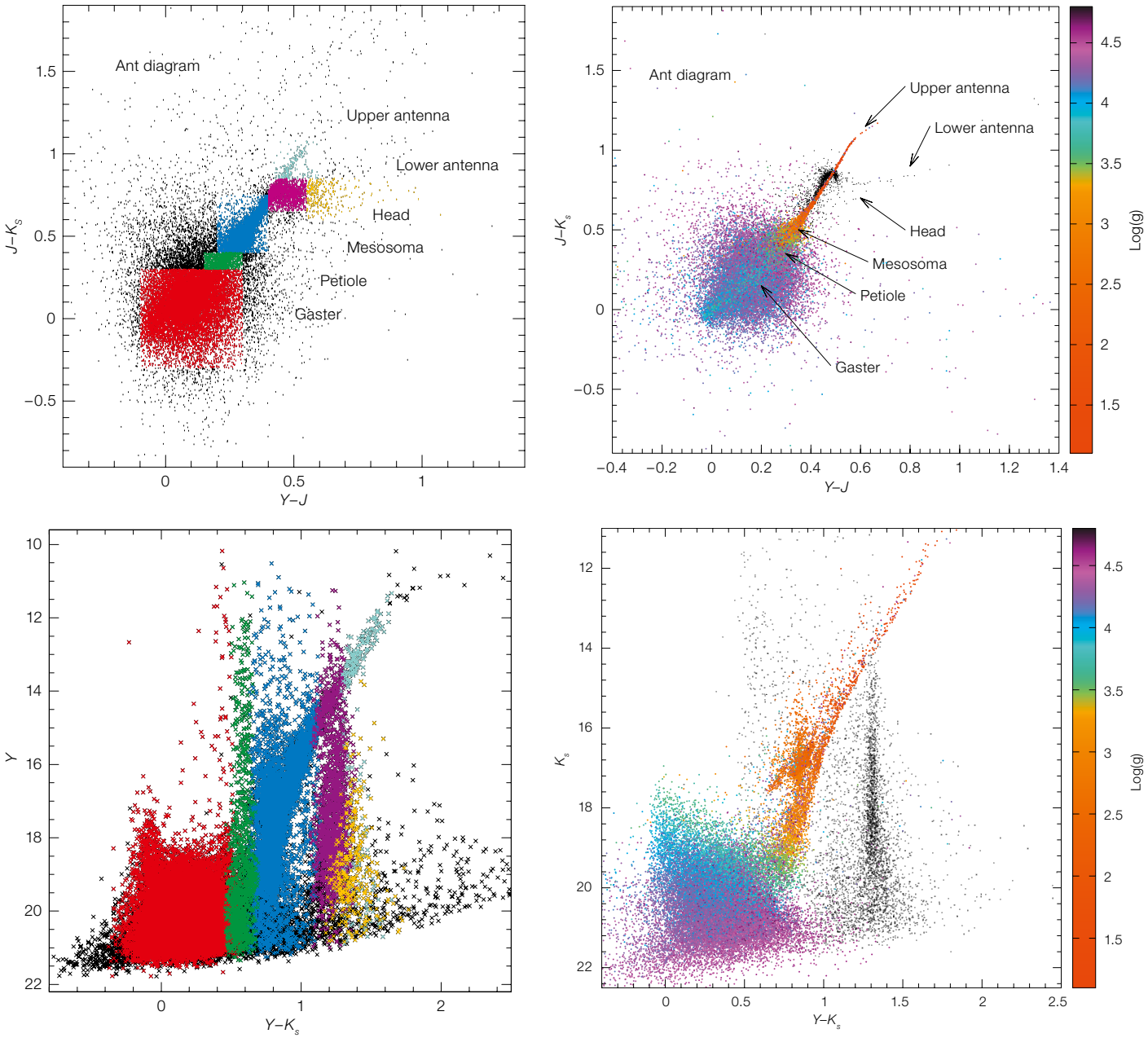

Figure 7. Colour–colour ("Ant diagrams") and colour–magnitude (CM) diagrams of VMC sources in the SEP field are shown for observed magnitudes (upper and lower left) and simulated magnitudes (upper and lower right). In the observed magnitude plots (left column), the coloured points correspond to the morphological selection outlined in the text and labelled in the upper plot. The mapping of stellar surface gravity to the simulated colour–colour and CM diagrams is shown in the right column.

extension of foreground low-mass stars in the MW.

The simulated Ant diagram is also shown in Figure 7, where colours now represent the stellar surface gravity.

RR Lyrae stars and Cepheids

Radially pulsating stars obey a period-mean density relation that forms the basis of their use as standard candles to measure the distance to the host system. In particular, RR Lyrae stars obey a period–luminosity–metallicity relation in the *K*-band that is only weakly affected by evolutionary effects, the spread in stellar mass within the instability strip and uncertainties in reddening corrections. Similarly, the Cepheid period–luminosity relation in the *K*-band is much narrower than the corresponding optical relations, and less affected by systematic uncertainties in reddening and metal content.

In the context of the VMC survey, the K_s photometry is taken in time series mode in order to obtain mean K_s magnitudes

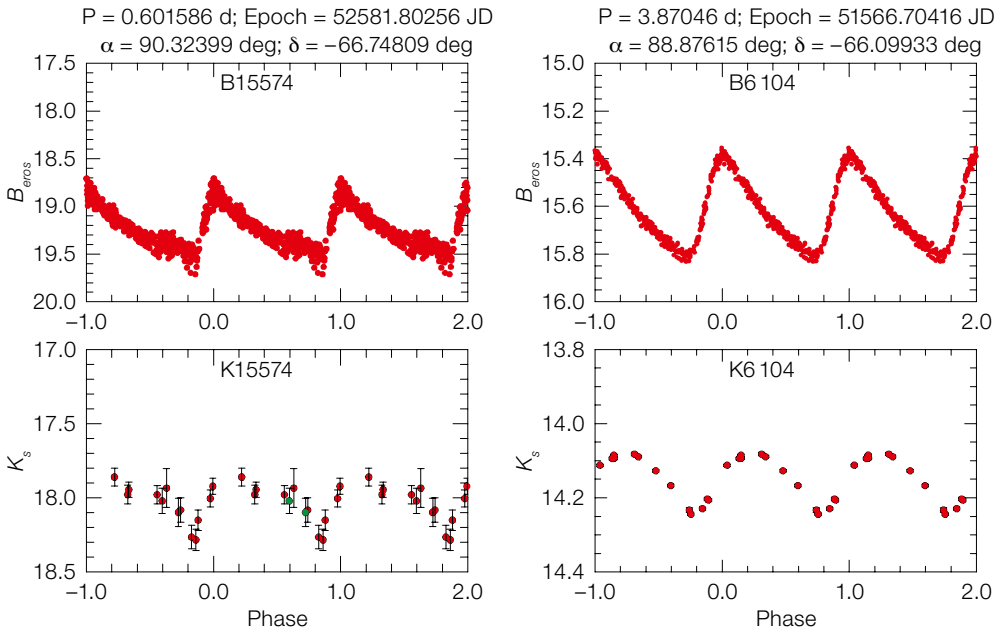

Figure 8. B_{EROS} and K_s VMC light-curves for an RR Lyrae star (left) and a Cepheid (right) in the SEP field.

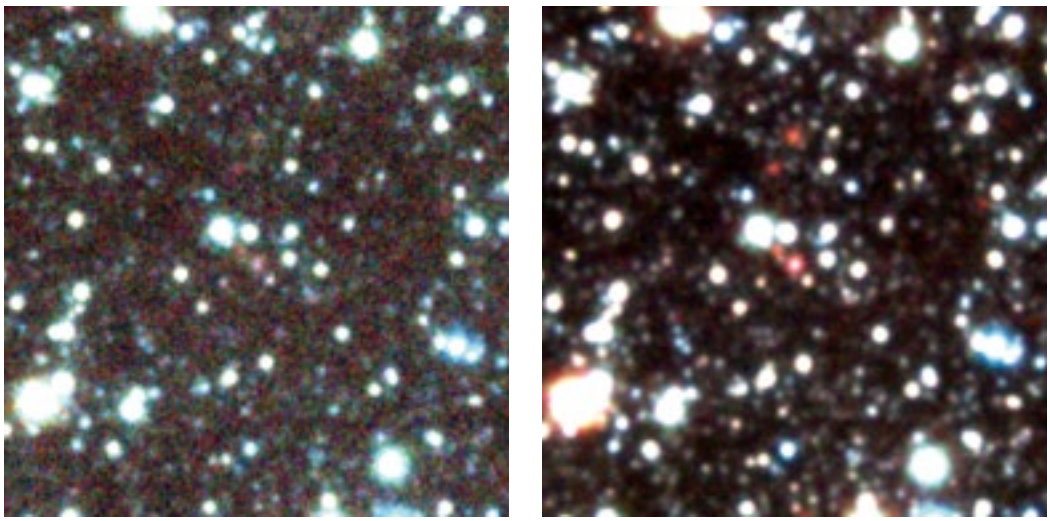

Figure 9. Colour-composite image of LMC PN MG 60 made from single (left) and stacked (right) exposures in *Y* (blue), *J* (green) and K_s (red) pass-bands.

for RR Lyrae stars and Cepheids over the whole Magellanic system. Their period–luminosity relations will be used to measure distances and construct a 3D map of the stellar distribution. The identification, period and epoch of maximum light for these objects are taken from micro-lensing surveys (EROS, MACHO and OGLE) of the LMC and SMC while in the Bridge we plan to use the VST data themselves (Cappellaro, 2005).

The location of the SEP field at the periphery of the LMC overlaps with EROS-2 (Tisserand et al., 2007). There are 117 RR Lyrae and 21 Cepheids in common between EROS-2 and VMC. EROS-2 periodicities were confirmed by analysing their B_{EROS} light-curves with GRATIS (Clementini et al. 2000). Figure 8 shows B_{EROS} and VMC light-curves of the RR Lyrae star #15574 (P = 0.601586 days) and the Cepheid variable #6104 (P = 3.87046 days). For the RR Lyrae star there is one point per night and the magnitude is the weighted average of all available observations, while for the Cepheid two points, corresponding each to a different detector, are shown. Both light-curves are well sampled, including shallower observations (shown in green), confirming the soundness of our observing strategy, and allowing us to derive mean magnitudes without using template light-curves. The average of individual K_s measures corresponds to 18.02 +/– 0.12 mag. and 14.17 +/– 0.06 mag. for the RR Lyrae star and Cepheid, respectively.

Planetary nebulae

Planetary Nebulae (PNe) are well known for their role in the development of the extragalactic standard candle planetary

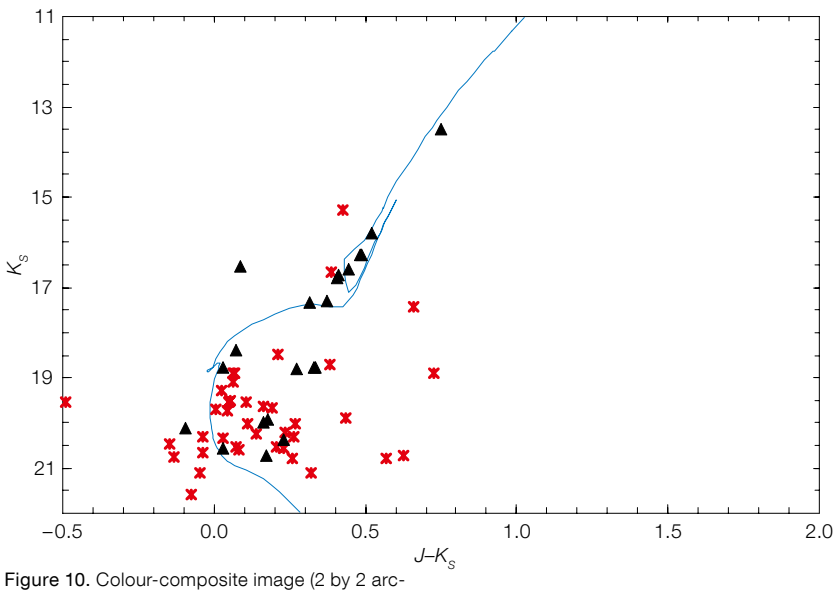

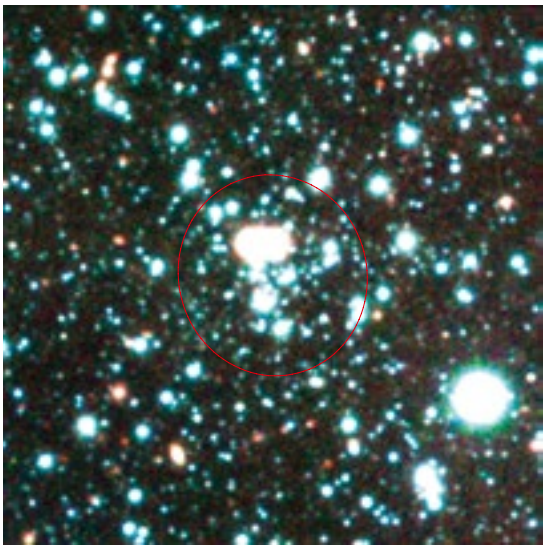

Figure 10. Colour-composite image (2 by 2 arcminutes, shown right) and CMD (shown left) of the stellar cluster KMHK 1577. The isochrone corresponds to an age of 0.63 Gyr and a metallicity of $Z = 0.004$.

nebula luminosity function (PNLF). Distances can be measured from the near-universal bright end cut-off across all galaxy types, but it remains difficult to explain how old stellar populations that lack recent star formation episodes could produce progenitors massive enough to power the high star luminosities populating the bright end.

Magellanic Cloud PNe are well positioned to further advance our understanding of the PNLF. The deep NIR photometry provided by the VMC survey will allow new PNe to be detected and the enhanced sensitivity to dust resulting from observation in the NIR will enable identification of contaminating compact H II regions and symbiotic stars. The synoptic nature of the VMC survey, which allows variability to be measured, will enable identification of pulsating Mira stars in the most obscured symbiotic stars, thus supporting the cleaning of the PNe sample.

Within the first six VMC tiles in the LMC, a combination of optical imaging, OGLE light-curves, the VMC NIR data and SAGE mid-infrared observations, reveals that only ~50% of the objects previously catalogued as PNe appear to be genuine. These are characterised by the colours $0.4 < (J–K_s) < 2$ and $0.0 < (Y–J) < 0.5$. The non-PNe identified in the sample are mainly misclassified field stars, compact H II regions or long-period variables. The strongest emission lines in the NIR for PNe include: H I at 1.083 μm in *Y*-band, Pa β in *J*, while K_s contains Br γ, multiple H I and molecular H_2 lines. Figure 9 shows the impact of stacking individual VMC exposures to detect PNe.

Stellar clusters

Stellar clusters are among the primary targets of the VMC survey. The detection of known stellar clusters will be examined and new clusters will be searched for. The analysis of stellar clusters will be centred on CMDs to estimate their ages and metallicities as well as on the comparison with results obtained from optical surveys. Ages, masses and metallicities of stellar clusters will allow us to discuss the SFH of the Magellanic Clouds and radial abundance gradients.

Here we show results obtained for cluster KHMK 1577 (Kontizas et al. 1990) in the SEP field. The properties of this cluster are unknown and it was chosen because of its favourable location at the centre of a pawprint. The image and CMD of the cluster are shown in Figure 10. The exposure time was 2400 s in *Y*, 2800 s in *J* and 9400 s in K_s; triangles indicate stellar sources and asterisks extended objects.

Acknowledgements

The VMC survey is supported by ESO and the UK STFC. This research has made use of Aladin, EROS-2 and 2MASS data. The UK's VISTA Data Flow System comprising the VISTA pipeline at CASU and the VISTA Science Archive at the Wide Field Astronomy Unit (WFAU) in Edinburgh has been crucial in providing us with calibrated data products for this paper.

References

Arnaboldi, M. et al. 2010, The Messenger, 134, 42
Cappellaro, E. 2005, The Messenger, 120, 13
Cioni, M.-R. L. et al. 2011, A&A, 527, A116
Clementini, G. et al. 2000, AJ, 120, 2054
Emerson, J. et al. 2006, The Messenger, 126, 41
Emerson, J. et al. 2010, The Messenger, 139, 2
Hodgkin, S. T. et al. 2009, MNRAS, 394, 675
Irwin, M. 2009, UKIRT Newsletter, 25, 15
Irwin, M. 2010, UKIRT Newsletter, 26, 14
Kontizas, M. et al. 1990, A&A, 84, 527
McClure-Griffiths, N. et al. 2009, ApJS, 181, 398
Tisserand, P. et al. 2007, A&A, 469, 387

Links

[1] VMC survey: http://star.herts.ac.uk/~mcioni/vmc/
[2] VISual and Infrared Telescope for Astronomy (VISTA): http://www.vista.ac.uk
[3] CASU: http://casu.ast.cam.ac.uk/surveys-projects/vista
[4] VISTA Science Archive (VSA): http://horus.roe.ac.uk/vsa/login.html

The Carina Dwarf Spheroidal Galaxy: A Goldmine for Cosmology and Stellar Astrophysics

Peter B. Stetson[1]
Matteo Monelli[2, 3]
Michele Fabrizio[4]
Alistair Walker[5]
Giuseppe Bono[4, 6, 7]
Roberto Buonanno[4, 8]
Filippina Caputo[6]
Santi Cassisi[9]
Carlo Corsi[6]
Massimo Dall'Ora[10]
Scilla Degl'Innocenti[11, 12]
Patrick François[13]
Ivan Ferraro[6]
Roberto Gilmozzi[7]
Giacinto Iannicola[6]
Thibault Merle[14]
Mario Nonino[15]
Adriano Pietrinferni[9]
Pier Prada Moroni[11, 12]
Luigi Pulone[6]
Martino Romaniello[7]
Frederic Thévenin[14]

[1] DAO/HIA/NRC, Victoria, Canada
[2] IAC, Tenerife, Spain
[3] Univ. La Laguna, Tenerife, Spain
[4] Univ. Tor Vergata, Roma, Italy
[5] NOAO/CTIO, La Serena, Chile
[6] INAF–OAR, Monte Porzio Catone, Italy
[7] ESO
[8] ASDC. Frascati, Italy
[9] INAF–OACTe, Teramo, Italy
[10] INAF–OAC, Napoli, Italy
[11] Univ. Pisa, Pisa, Italy
[12] INFN, Pisa, Italy
[13] Obs. de Paris-Meudon, Paris, France
[14] Obs. Côte d'Azur, Nice, France
[15] INAF–OAT, Trieste, Italy

We present deep and precise multiband (*U*, *B*, *V*, *I*) optical data for the Carina dwarf spheroidal galaxy. Data were collected using three different ground-based telescopes (4-metre Blanco CTIO, MPG/ESO 2.2-metre, 1.5-metre CTIO) and cover the entire body of the galaxy. We discuss the reliability of the absolute photometric zero-point calibrations of images collected with large-format and mosaic CCD cameras. The typical precision for the *B*- , *V*- and *I*-bands is better than 0.01 mag. The *U*-band is a little worse. A preliminary comparison with scaled-solar and α-enhanced evolutionary predictions covering a broad range of ages and chemical compositions seems to support previous photometric evidence that both the old (12 Gyr) and the intermediate-age (4–6 Gyr) subpopulations show a limited spread in chemical composition. The use of the Carina galaxy field as a possible standard stellar field is outlined.

Introduction

Dwarf galaxies play a fundamental role in several astrophysical problems. Current cosmological simulations predict dwarf satellite populations significantly larger than the number of dwarfs observed near giant spirals like the Milky Way and M31. This discrepancy is known as the missing satellite problem and challenges the current most popular cosmological model: the Lambda Cold Dark Matter paradigm (Madau et al., 2008). However, it is not yet known whether this discrepancy is due to limitations in the theoretical modelling or to observational bias at the faint end of the galaxy luminosity function (Kravtsov, 2010).

The distribution of dwarf galaxies in multi-dimensional parameter space indicates that they follow very tight relations. In particular, Prada & Burkert (2002) suggested that Local Group (LG) dwarf galaxies show strong correlations (Fundamental Line [FL]) between mass-to-light (M/L) ratio, surface brightness and metallicity (*Z*). They explained the correlation between M/L ratio and *Z* using a simple chemical enrichment model where the hot metal-enriched gas, at the end of the star formation epoch, is lost via galactic winds (Mac Low & Ferrara, 1999; Woo et al., 2008). Furthermore, the FL of dwarf irregulars (dIs) in a five-dimensional parameter space (total mass, surface brightness, rotation velocity, metallicity and star formation rate) is linear and tight, and extends the scaling relations of giant late-type galaxies to lower mass. On the other hand, the FL of dwarf spheroidals (dSphs) in a four-dimensional parameter space (total mass, surface brightness, rotation velocity and *Z*) is also linear and very tight, but is not an extrapolation of the scaling relations of giant early-type galaxies.

Carina plays a key role among the LG dSph galaxies for many reasons:

i) it is relatively close, and its central density is modest;
ii) it shows multiple star formation episodes, separated in time and in the amount of stellar mass involved (Monelli et al., 2003);
iii) it hosts a broad variety of variable stars ranging from low- and intermediate-mass hydrogen-burning dwarf Cepheids to low- and intermediate-mass helium-burning stars (Anomalous Cepheids; Dall'Ora et al., 2003);
iv) high resolution spectra are available for fewer than a dozen bright red giants (RGs). The mean metallicity is [Fe/H] = –1.69 with a spread of 0.5 (Koch et al., 2008);
v) calcium triplet measurements based on medium resolution spectra are also available for a large sample (437) of RG stars (Koch et al., 2006) with a peak at [Fe/H] = –1.72, but ranges from –2.5 to –0.5. Using the same spectra, but different selection criteria, Helmi et al. (2006) found a metallicity distribution from about –2.3 to –1.3.

However, we are facing a stark discrepancy between the spread in metallicity suggested by spectroscopic measurements and photometric metallicity indicators. Deep and accurate colour–magnitude diagrams (CMDs) of Carina indicate that the width in colour of the red giant branch (RGB) is quite limited (Monelli et al., 2003; Harbeck et al., 2001). This evidence was further supported in a recent investigation by Bono et al. (2010) employing a large number of multiband (*U*, *B*, *V*, *I*) CCD images from ground-based telescopes covering the entire body of the galaxy.

Photometric datasets and photometric calibration

The data were collected in various observing runs between December 1992 and January 2005. They include images from three telescopes: the Cerro Tololo Inter-American Observatory (CTIO) 1.5-metre telescope with a single Tektronix 2K CCD, the CTIO 4-metre Blanco telescope with the Mosaic II camera, and the MPG/ESO 2.2-metre telescope with the Wide Field Imager (WFI) camera (both

proprietary and archival data). The data discussed here represent 4152 individual CCD images with essentially complete coverage of the central regions of Carina (about 40 by 55 arcminutes, lacking only those regions obliterated by bright foreground stars). They were obtained in four photometric bands (*B* and *I* with the 1.5-metre telescope, and *UBVI* with both the 4-metre and 2.2-metre telescopes). The resulting colour image is shown on p. 20.

The photometric data were reduced using the DAOPHOT/ALLFRAME package (Stetson, 1987; 1994). Because of the multiple chips and pointings, any given star may have up to 17 calibrated measurements in *U*, 156 in *B*, 207 in *V*, and 70 in *I*. A total of 205 338 individual stars were catalogued and measured. Among these, 72 595 have photometric measurements in all four filters, while 129 230 have at least V and either *B–V* or *V–I*. The remainder, either extremely faint (*i.e.*, detectable in only one filter) or located near the periphery, have astrometry and instrumental magnitudes only.

The fundamental standard system of photometric magnitudes was established decades ago using photoelectric photometers on small telescopes — mostly of apertures 0.4–0.9 metres (e.g., Landolt, 1973; 1988; 1992; Graham, 1982; and references therein to the establishment of *UBV* by Johnson and *RI* by Cousins). One of the authors (PBS) has spent a significant part of his career attempting to ensure that measurements of very faint stars obtained with CCDs on large telescopes are on the same photometric system as measurements of very bright stars made with photomultipliers on small telescopes (Stetson, 2000; 2005)[1].

The question of whether the photometry discussed here is on the standard system breaks down into two parts:

i) the extent to which the CCD photometry, in general, is on the standard system; and
ii) the extent to which the photometry for Carina, in particular, is on the same system as the rest of the photometry. As of now, 2076 datasets have been homogeneously analysed through our software; among these, 1591 are considered to be of photometric quality, and 485 have been analysed in non-photometric mode (*viz*. data taken under non-photometric conditions).

Figure 1 shows the magnitude differences between the calibrated standard-system magnitudes from our own observations of the fundamental photometric standards, as compared to the published values for the same stars. In order to restrict the comparison to stars with the most reliable data, we consider only magnitudes based on at least five independent measurements obtained on photometric occasions, and having standard errors of the mean not greater than 0.02 mag based on the internal repeatability of the observations. For our measurements we were able to impose the additional condition that each star shows no evidence of intrinsic variation at a level greater than 0.05 mag root mean square (rms), when the data from all filters are considered.

The left panels of Figure 1 show the magnitude residuals (in the sense *published* minus *ours*) plotted versus apparent visual magnitude, while the right panels of Figure 1 plot the same residuals against the *B–I* colour. The differences show a systematic departure of a few hundredths of a magnitude between our photometric system and the standard system for stars brighter than approximately $V = 9$. We infer that the stars with $V \leq 9$ were simply too bright to be measured with our equipment, and we were unduly optimistic about these measurements. We therefore advise readers to ignore Stetson's results for standard stars with $V \leq 9$ and rely entirely upon the previously published photometric indices of such stars instead. Figure 1 demonstrates that our photometry matches the definitive published results with a high degree of fidelity over a dynamic range of ~600 in flux ($9 \lesssim V \lesssim 16$) and over the full available range of stellar temperature. Quantitatively, the weighted mean differences between the published results and ours are +0.0012 ± 0.0028, +0.0016 ± 0.0013, −0.0007 ± 0.0009 and −0.0025 ± 0.0013 mag in *U*, *B*, *V* and *I*, respectively, based upon 109, 209, 220 and

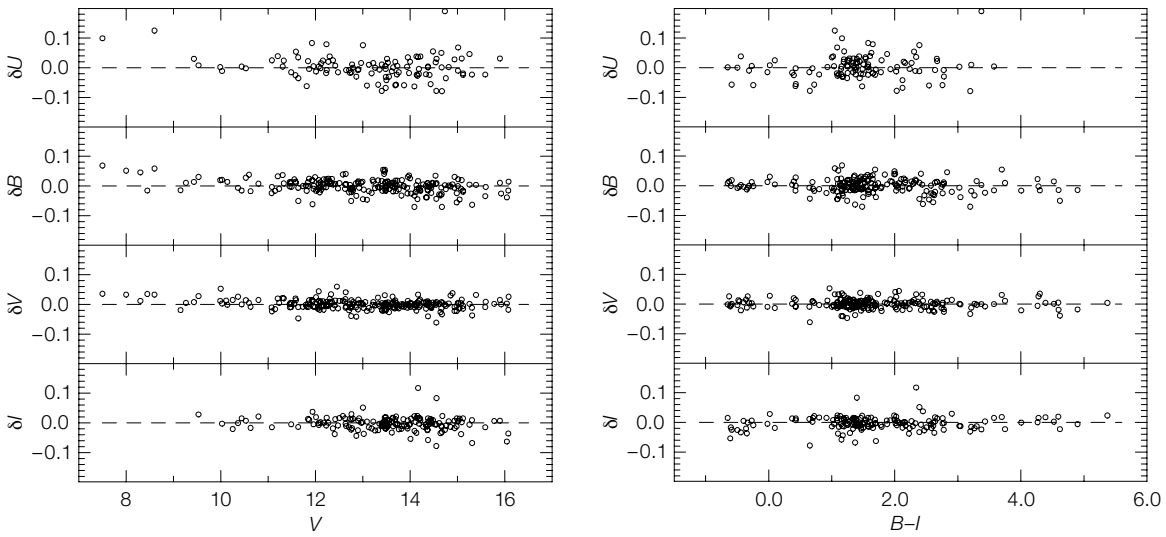

Figure 1. Left: From top to bottom, difference in *U*-, *B*-, *V*- and *I*-bands between standard system magnitudes and the current observations of the fundamental photometric standards as a function of the visual magnitude. Right: Same as the left, but the difference in magnitude is plotted as a function of *B–I*.

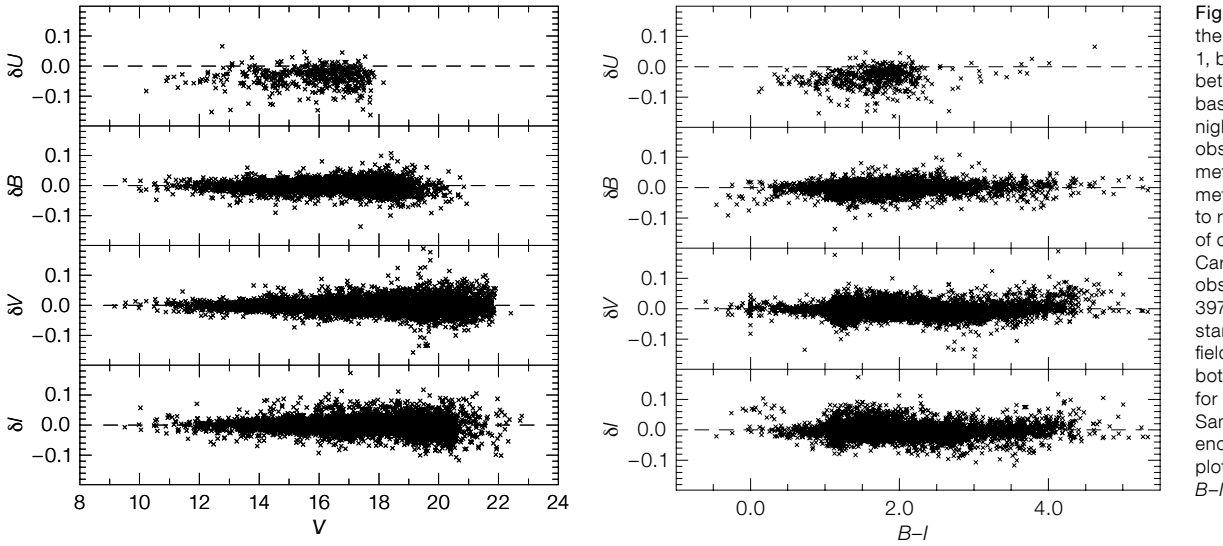

Figure 2. Left: Same as the left panels of Figure 1, but the difference is between magnitudes based on datasets from nights when Carina was observed (175 photometric, 88 non-photometric) as compared to results from the rest of our nights — when Carina was not observed (1416 clear, 397 cloudy) — for those stars in all our other fields that appear in both datasets. See text for more details. Right: Same as left, but difference in magnitude is plotted as a function of *B–I*.

151 stars. Expressed as a standard deviation, the average standard residual of one star is 0.027, 0.017, 0.012, 0.012 and 0.016 mag in *U*, *B*, *V*, *R* and *I*. It does not seem that these numbers can be reduced by obtaining more observations; rather, they represent a fundamental limit to the reliability with which any given *individual* star can be referred to a fundamental standard system, due to the fact that even though stars may have the same broadband colours in one photometric system, they can still have underlying spectral energy distributions that differ in detail, and that will be sampled differently by other filter sets.

Figure 2 provides the same sort of comparison for all stars in all fields in the Carina observations (263 in number: 175 photometric, 88 non-photometric) as compared to results for the same target stars appearing in our 1813 datasets obtained on nights when Carina was *not* observed (1416 clear, 397 cloudy). Again we have restricted the comparison to stars with at least five photometric observations, standard errors no larger than 0.02 mag and no evidence of intrinsic variation in excess of 0.05 mag rms when data from all filters are considered. These new comparisons show a few significant photometric outliers with magnitude differences > 0.10 mag, as expected in any large body of raw data, but the vast majority of stars show that the datasets that do include Carina observations are reasonably well matched to the rest of our CCD data *except* in the *U* filter. In this filter only, 451 stars common to the two samples — all of which lie in *only one* field, Selected Area 98 — show a systematic offset of 0.036 mag.

The Johnson *U* bandpass has always been a little problematic. Its classical implementation provided a bandpass defined by filter throughput on the long wavelength side, but by atmospheric opacity on the short wavelength side. Furthermore, the atmospheric extinction in the *U*-band is very high: ~0.5 mag per airmass on *good* nights at 2000 metres on mountaintops like Cerro Tololo or La Silla. Finally, this bandpass contains the Balmer convergence and jump in hot stars, and a multitude of strong metal lines (including Ca II H+K) and bands of molecules like CN in cool stars. All of these features make the *U* magnitudes sensitive to the exact placement and shape of the instrumental bandpass. We will continue to investigate the cause of this discrepancy, but for the present we expect that a correction of order one-tenth to one-half the difference should be applied to our *U*-band results for Carina to bring them closer to the standard system.

The problem is that we do not have many *other* nights of southern hemisphere observations that included measurements in the *U*-band, to which we could compare. Quantitatively, apart from *U*, the formal weighted mean magnitude differences are +0.0010, −0.0002, −0.0001 mag in *B*, *V* and *I*, respectively, based on 8795, 14 945, and 10 329 stars. The formal statistical confidence intervals on these numbers are all $< 1 \times 10^{-4}$ mag, but these are certainly underestimated; we still need to think harder about how to characterise our actual systematic uncertainties, given that so few independent points of comparison are available to us. However, the current evidence suggests that systematic differences between our Carina observations and the system of Landolt and Graham in *B*, *V* and *I* probably do not greatly exceed a few times 0.001 mag, and calibration issues will not be a significant limiting factor for our interpretations so long as we use *U* only for differential comparisons within our data.

Comparison between theory and observations

A detailed comparison between stellar populations in Carina with simple stellar populations belonging either to Galactic globular clusters (GCs) or to intermediate-age clusters in the Small Magellanic Cloud was presented in Bono et al. (2010). The discrimination between field and Carina stars was performed using the *U–V*, *B–I* colour–colour plane. Figure 3 shows three different CMDs of the candidate Carina stars. Note that after the selection there remain some field stars with colours similar to Carina's RGB

($V \leq 21.5$, $B–V \sim 0.5$ mag). The evolutionary properties of low- and intermediate-mass stars provide at least three independent metallicity indicators: the slope and the spread in colour of RGB stars; the spread in colour of red clump (RC) stars; and the spread in magnitude of blue and red horizontal branch (HB) stars. Data plotted in this figure show that both RGB and RC stars cover a very limited range in colour in the three adopted CMDs. The same observation applies to the spread in magnitude of blue and red HB stars.

The theoretical framework for both scaled-solar and α-enhanced evolutionary models is based on isochrones available in the BaSTI database (Pietrinferni et al., 2004; 2006). To compare theory and observations we adopted the distance modulus and the reddening available in the literature (Dall'Ora et al., 2003; Monelli et al., 2003). As a first working hypothesis, we are assuming that both the old and the intermediate-age subpopulations have scaled-solar chemical compositions. Spectroscopic investigations indicate that α-elements in dSph galaxies may be overabundant when compared with solar composition, but underabundant when compared with GCs of similar metallicity (Tolstoy et al., 2009; and references therein).

The left panels of Figure 4 show the comparison in the *V*, *B–V* CMD, at fixed chemical composition ([Fe/H] = –1.79, Y = 0.245), with two old (top; 10, 12 Gyr) and three intermediate-age (bottom; 2, 4, 6 Gyr) isochrones. Data plotted in these panels display that theory and observations, within the errors, agree quite well. The intermediate-age isochrones appear slightly bluer than the bulk of the RGB stars, but the difference is of the order of a few hundredths of a magnitude. The right panels of Figure 4 show the comparison at fixed age and different chemical compositions. In particular, the top right panel shows the comparison with three old isochrones of 12 Gyr and iron abundances ranging from –2.3 to –1.5 dex. Note that evolutionary models were constructed assuming a helium-to-metal enrichment ratio $\Delta Y/\Delta Z = 1.4$ and a mass-loss rate $\eta = 0.4$ (Pietrinferni et al., 2004). The colour range covered by the

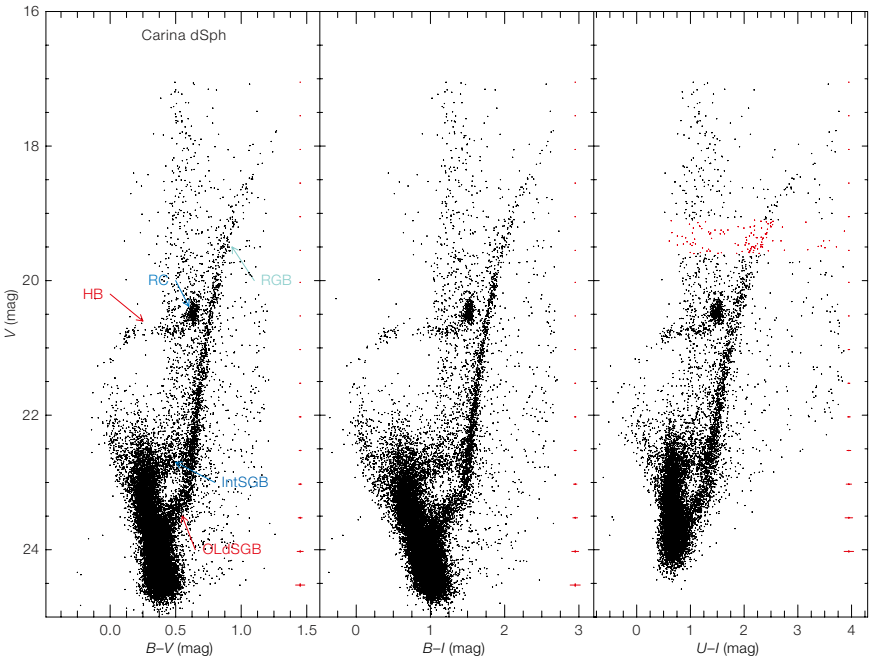

Figure 3. Left: *B–V*, *V* colour–magnitude diagram of candidate Carina stars based on optical images collected with the MOSAIC camera at the 4-metre Blanco telescope, with the WFI at the MPG/ESO 2.2-metre telescope and with the 1.5-metre CTIO telescope. The blue labels mark intermediate-age stellar tracers (SGB, RC), while the red ones the old stellar tracers (SGB, HB). The red bars plotted at the right display the intrinsic photometric error both in magnitude and in colour. Middle: Same as left, but candidate Carina stars are plotted in the *B–I*, *V* colour–magnitude diagram. Right: Same as left, but candidate Carina stars are plotted in the *U–I*, *V* colour–magnitude diagram.

isochrones is systematically larger than observed over the magnitude range of sub-giant branch (SGB) and RGB stars. The same outcome applies to the intermediate-age (6 Gyr) subpopulation. The current predictions with the most metal-poor composition attain colours that are similar to the red tail of RC stars. However, the observed CMDs show a well defined separation between RC and RGB stars.

To further constrain the impact of chemical composition on the evolutionary properties of Carina stellar populations, we assumed that both the old and the intermediate-age sub-populations are α-enhanced. The left panels of Figure 5 show the comparison with two old (top; 10, 12 Gyr) and three intermediate-age (bottom; 2, 4, 6 Gyr) isochrones constructed assuming the same iron content as the scaled-solar isochrones adopted in Figure 4, but an overabundance of α-elements: [α/Fe] = 0.4. The comparison between theory and observation appears slightly better than for the scaled-solar isochrones, since both the old and the intermediate-age predictions attain colours that are similar to the observed ones. In addition, we repeated the comparison using isochrones assuming different values of global metallicity ([M/H], see labelled values). The right panels of Figure 5 show the comparison with isochrones of 12 Gyr (top) for the old and of 6 Gyr for the intermediate-age sub-population.

The key advantage in the approach we adopted to compare theory and observations is that we are using theoretical predictions to constrain the *relative* difference and the *spread* in the heavy element abundances of Carina subpopulations. The above findings indicate that the possible abundance spreads of both the old and the intermediate-age subpopulations appear to be limited and of the order of 0.2–0.3 dex (Bono et al., 2010; Fabrizio et al., 2011), thus supporting the spread in iron abundances based on high resolution spectra provided by Shetrone et al. (2003). Theoretical and empirical uncertainties do not allow us to reach firm conclusions regarding

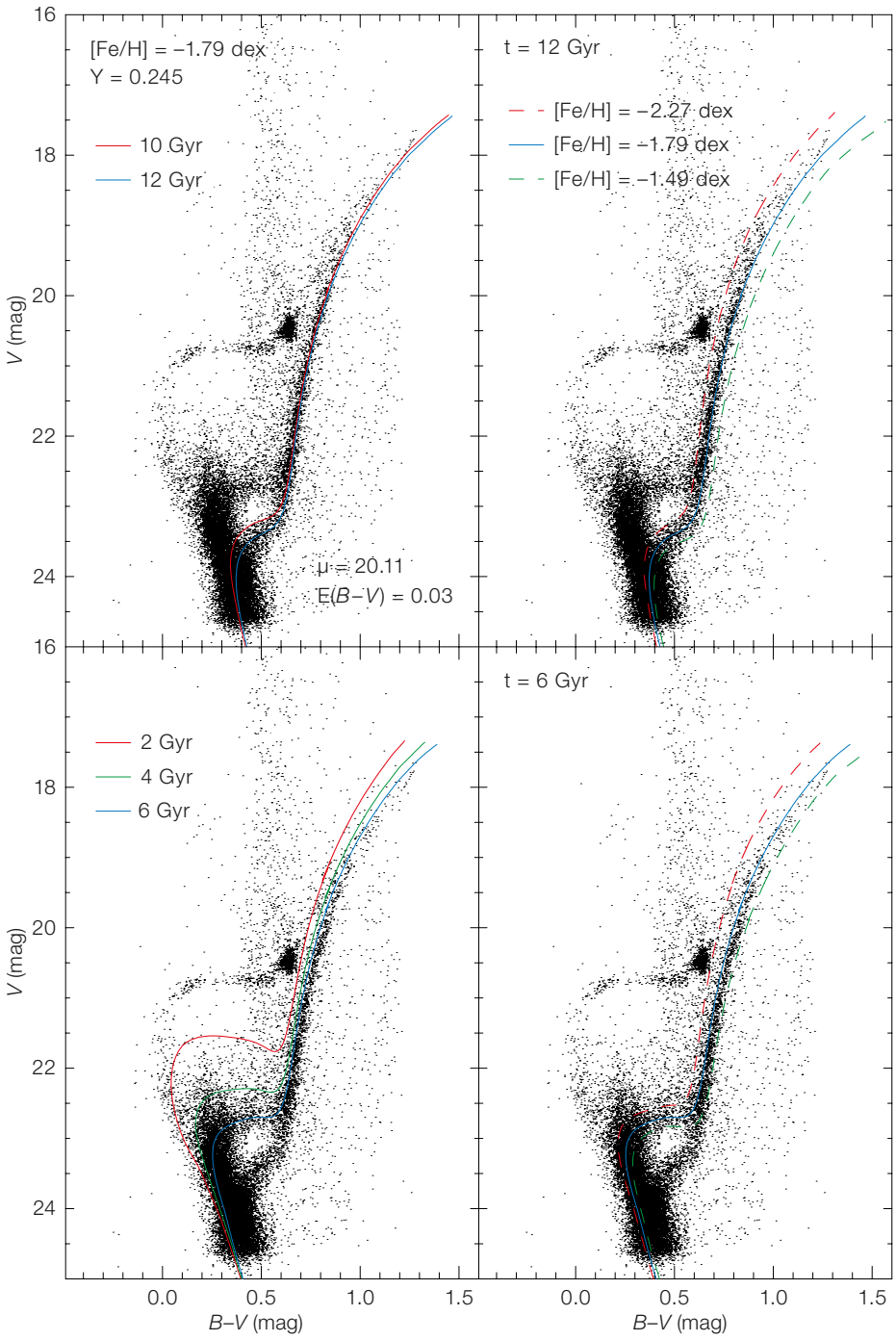

Figure 4. Left: *B–V*, *V* colour–magnitude diagram of Carina based on optical images. The solid coloured lines display two old (top) and three intermediate-age (bottom) scaled-solar isochrones at fixed iron abundance and different ages. The adopted true distance modulus and the reddening are also indicated. Right: Same as left panels, but comparison assumed an age of 12 Gyr for the old (top) and of 6 Gyr for the intermediate-age (bottom) subpopulation.

the possible occurrence of an α-element enhancement.

Future prospects

The identification of the physical mechanisms that drive the formation and the evolution of stars and stellar systems, and the interplay between Big Bang nucleosynthesis and the creation of chemical elements in stars is one of the landmark achievements in astrophysics. The former largely relies on photometry, the latter on spectroscopy. Many of the current open problems in stellar astrophysics are approached through a comparison between the theoretical and observational Hertzsprung–Russell diagrams. This comparison relies on three fundamental pillars: absolute distances, photometric calibrations, and input physics adopted in the stellar evolutionary and pulsation models.

There is a threefold motivation for the ongoing effort for precise photometric calibrations for stellar populations in nearby dwarf galaxies:

i) A systematic drift in photometric precision when moving from bright to faint RG stars might produce a spread in colour, and in turn, mimic a spread in metal content. Moreover, these systems are characterised by very low stellar densities, thus requiring that photometry be collected with large format and mosaic CCD cameras. Intense effort to achieve consistent zero-points across the field is mandatory to avoid spurious broadening of the key evolutionary sequences.

ii) Dwarf galaxies in the Local Group and in the local volume are often contaminated by foreground field stars. Their colours, unfortunately, are similar to the colours of Galactic RGs and main sequence (MS) stars, once again mimicking a broadening in colour due to a spread in age and/or in metallicity. The separation of field and Galactic stars can be performed using radial velocity and/or proper motions, but at present this approach is limited to relatively bright RGs. A robust cleaning of MS and SG sequences can be performed using colour–colour planes (Bono et al., 2010) and/or a statistical subtraction of a control field (Balbinot et al., 2010). These approaches require, once again, very precise calibration in different bands across multiple telescope pointings.

iii) The use of variable stars as distance indicators, stellar tracers and physics laboratories requires precise time series data and multiband calibrations.

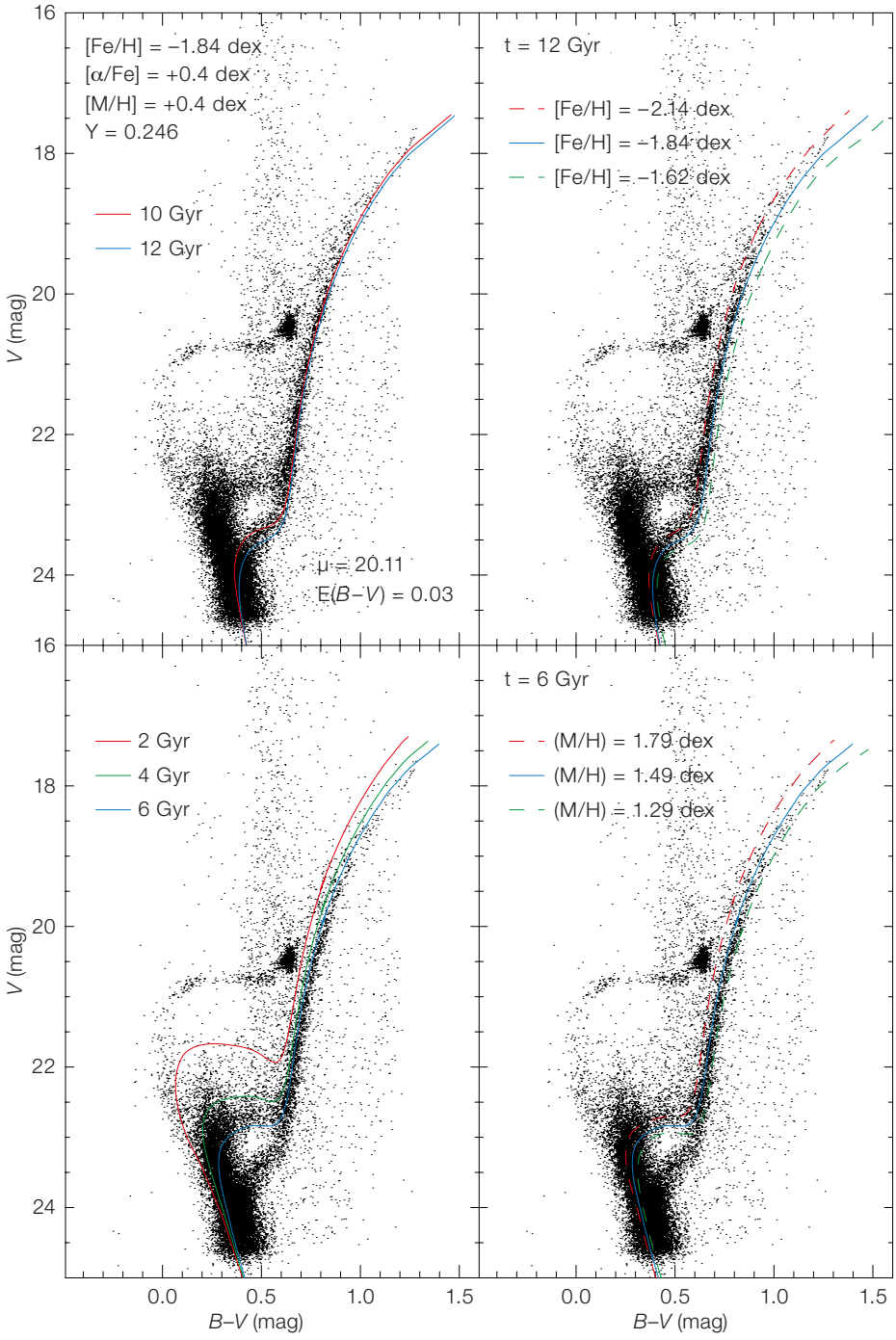

Figure 5. Left: Same as left panels of Figure 4, but comparison performed using isochrones constructed by assuming the same iron content ([Fe/H] = –1.84 dex) of the scaled-solar models, but with an α-enhanced chemical composition (see labelled values). Right: Same as left panels, but comparison performed using isochrones with different global metallicities ([M/H], see labelled values).

The way to easily overcome the above problems is to have a sizable sample of local standard stars covering a broad range of magnitudes and colours. Local standards are now available in a significant fraction of globular clusters. So far, only a few dwarf galaxies have precise local standard stars in the optical and in near-infrared (NIR) bands. All three Carina fields have 659 *U*-band, 5711 *B*- and *V*-band and 1467 *I*-band standard stars spanning a region 123 by 149 arcminutes. The brightest standard has $V = 13.95$; the median is $V = 19.27$; and the faintest $V = 22.42$ mag. The Carina region together with other regions[1] is thus a potential standard stellar field to calibrate the next generation of large CCD cameras.

The use of accurate and deep NIR data, together with the present dataset, can play a crucial role in the identification of field and Carina candidate stars using optical–NIR colour–colour planes. The stronger sensitivity to effective temperature of the optical–NIR colours can also provide a robust separation between old and intermediate-age stars. At the same time, a high-resolution, high signal-to-noise ratio spectroscopic study of a sizable sample of RG stars and He-burning (RC, HB) stars is mandatory to *measure* the abundance spread, if any, in old and intermediate-age stellar populations.

References

Balbinot, E. et al. 2010, MNRAS, 404, 1625
Bono, G. et al. 2010, PASP, 122, 651
Dall'Ora, M. et al. 2003, AJ, 126, 197
Fabrizio, M. et al. 2011, PASP accepted
Graham, J. A. 1982, PASP, 94, 244
Helmi, A. et al. 2006, ApJL, 651, L121
Koch, A. et al. 2006, AJ, 131, 895
Koch, A. et al. 2008, AJ, 135, 1580
Kravtsov, A. 2010, Advances in Astronomy, 2010,
Landolt, A. U. 1973, AJ, 78, 959
Landolt, A. U. 1983, AJ, 88, 439
Landolt, A. U. 1992, AJ, 104, 340
Mac Low, M. & Ferrara, A. 1999, ApJ, 513, 142
Madau, P. et al. 2008, ApJ, 679, 1260
Monelli, M. et al. 2003, AJ, 126, 218
Pietrinferni, A. et al. 2004, ApJ, 612, 168
Pietrinferni, A. et al. 2006, ApJ, 642, 797
Prada, F. & Burkert, A. 2002, ApJ, 564L, 73
Shetrone M. D., et al. 2003, AJ, 125, 684
Stetson, P. B. 1987, PASP, 99, 191
Stetson, P. B. 1994, PASP, 106, 250
Stetson, P. B. 2000, PASP, 112, 925
Stetson, P. B. 2005, PASP, 117, 563
Tolstoy, E., Hill, V. & Tosi, M. 2009, ARA&A, 47, 371
Woo, J., Courteau, S. & Dekel, A. 2008, MNRAS, 390, 1453

Links

[1] List of photometric standard fields: http://www3.cadc-ccda.hia-iha.nrc-cnrc.gc.ca/community/STETSON/standards/

(Top) Workshop participants hard at work during the ALMA simulator tutorial, see Randall & Testi, p. 39, for details. (Bottom) Photo of the participants at the worshop The Evolution of Compact Binaries, taken on the beach of Viña del Mar. See Schmidtobreick & Schreiber, p. 47.

Report on the Workshop

ALMA Community Days: Towards Early Science

held at ESO Headquarters, Garching, Germany, 6–7 April 2011

Suzanna Randall[1]
Leonardo Testi[1]

[1] ESO

ALMA is rapidly approaching Early Science operations, and is scheduled to start the first observing projects for the astronomical community in the autumn of 2011. The Call for Proposals for ALMA Early Science Cycle 0 was published on 30 March, inviting the community to submit observing proposals by the deadline of 30 June 2011. Held just after the Call for Proposals was issued, the ALMA Community Days were designed to optimally prepare the European ALMA Community for Cycle 0 proposal submission. The workshop included a broad range of scientific and technical presentations as well as hands-on software tutorials for the ALMA simulators and the Observing Tool.

ALMA, the Atacama Large Millimeter/submillimeter Array, is expected to be the world's leading observatory at millimetre and submillimetre (sub-mm) wavelengths over the coming decades. A global collaboration involving Europe, North America, East Asia as well as the host country Chile, ALMA will comprise at least 66 high-precision antennas equipped with receiver and digital electronics systems to observe in the frequency range from 30 GHz to 1 THz at angular resolutions as high as 5 milliarcseconds. Dynamic scheduling and innovative calibration strategies will ensure the most efficient use of the unique atmospheric qualities encountered at the 5000-metre-high site on the Chajnantor plateau in the northern Chilean Andes.

While Full Science operations are scheduled to begin in 2013, the increasing capabilities of the growing array will become available to the astronomical community following the start of Early Science operations in the autumn of 2011. Early Science operations will be divided into two observing periods, Cycle 0 and Cycle 1, each planned to last between nine and twelve months. It is expected that the capabilities of the array offered to the community will substantially increase from Cycle 0 to Cycle 1, and then again for Full Science operations.

The aim of this two-day workshop was to optimally prepare the European astronomical community for ALMA Early Science. The first day was dedicated to a series of technical and scientific presentations on the status of ALMA and the capabilities offered in Early Science, while the second day was taken up by hands-on tutorials on the two most important pieces of software for ALMA proposal preparation — the ALMA Observing Tool and the ALMA simulators. The ALMA Community Days were very well received by the European astronomical community, and the maximum capacity of 100 participants was easily reached (see Figure 1). The Community Days were followed by a dedicated workshop on massive star formation with the ALMA Early Science capabilities (see Longmore et al. p. 41). Interestingly, a large fraction (~40%) of the workshop participants described themselves as novices in radio/sub-mm interferometry, indicating that ALMA is eagerly awaited not only by radio/sub-mm astronomers, but also by the wider astronomical community.

ALMA Early Science and commissioning/science verification

The presentations on the first day were kicked off by L. Testi, who reported on the current status of ALMA and the capabilities offered during Early Science. In Cycle 0, a minimum of 16 antennas will be working together in two configurations with baselines up to 125 metres and 400 metres. Four receiver bands will be offered, covering the frequency ranges 84–116 GHz (around 3 mm; Band 3), 211–275 GHz (around 1.3 mm; Band 6), 275–373 GHz (around 850 μm; Band 7) and 602–720 GHz (around 450 μm; Band 9). One major limitation in Cycle 0 is the time available for scientific observations: accepted programmes will be scheduled for up to one third of the time

Figure 1. The participants at the 2011 ALMA Community Days gathered outside the ESO Headquarters.

on a best-effort basis, while the completion of the array is given priority. Single dish observations, polarisation measurements and solar observations are not yet offered, but are planned for Cycle 1.

The audience was given a first-hand impression of the current commissioning and science verification activities at the ALMA site in Chile by T. van Kempen and L. Humphreys. While some remarkable commissioning data had been obtained in the second half of 2010, progress slowed during the first quarter of 2011 due to a particularly severe altiplanic winter and the deployment of a major software upgrade. However, the situation has now improved, and the first science verification data (focussing on TW Hya and NGC 3256) will be released to the public at the beginning of June.

The European ALMA Regional Centre

User support for the European ALMA community is handled by the European ALMA Regional Centre (ARC), which currently consists of seven ARC nodes distributed across Europe and a central coordinating node hosted at ESO. The European ARC, its staff and the services offered to the scientific community were introduced by P. Andreani, while the individual nodes and the face-to-face support offered there were presented by M. Zwaan. An overview of the proposal review process was given by G. Mathys. In Cycle 0, it is expected that around 100 proposals will be accepted, with an average execution time of 5–10 hours each. Projects not completed will not be carried over to Cycle 1, therefore the ideal Cycle 0 project will produce immediately publishable results, highlighting the unique capabilities of Early Science ALMA with only a few hours of observations.

Comprehensive technical information on ALMA capabilities, proposal preparation and relevant software is available online via the ALMA Science Portal[1], as was explained by F. Stoehr. Any technical or scientific questions/comments relating to ALMA should be addressed to the ALMA Helpdesk, which was presented by S. Randall. Accessible via the ALMA Science Portal, the Helpdesk contains a regularly updated knowledge base with answers to frequently asked questions and allows registered users to submit tickets that will receive a customised reply.

The ALMA Science Portal gives access to a suite of ALMA-related software. During the first stages of proposal preparation, the ALMA simulators, introduced by E. van Kampen, can be used to estimate the image fidelity achieved in a given observing time for the Cycle 0 array configurations. Similarly, the sensitivity calculator can be used to estimate the integration time needed to achieve a given sensitivity goal. Proposals must be prepared and submitted with the ALMA Observing Tool (OT), which was presented by A. Biggs. Finally, the data obtained in Cycle 0 will be reduced using CASA scripts, while in the future an automatic ALMA data reduction pipeline will become available, as outlined by D. Petry.

Science with ALMA

Observations obtained with ALMA are expected to have a significant impact on a broad range of current research topics in astronomy. As convincingly demonstrated by A. Rushton, even Galactic high-energy astrophysics, normally associated with much higher or lower frequency observations, can benefit from the unique capabilities of ALMA. ALMA test data for Sgr A*, obtained with five antennas during commissioning as part of a self-calibration test, reveal a number of molecular absorption and hydrogen recombination lines and are already comparable or superior in quality to spectroscopy taken with existing facilities, such as Owens Valley Radio Observatory. ALMA will also be a powerful tool for studying asymptotic giant branch stars, in particular their envelopes, as explained by M. Maercker. Spectroscopy taken as part of commissioning on the evolved star R Dor showed a far lower noise level than equivalent data obtained with a higher integration time with HIFI/Herschel. ALMA band 3 test data were also successfully used to detect a detached shell around R Scl (see Figure 2).

Extragalactic astrophysics and cosmology has always been one of the main scientific drivers behind ALMA. L. Cortese showed beautiful commissioning data on NGC 253 (see the image in *The Messenger* 142, p. 17), which was observed in all the four bands that will be available in Cycle 0. These data were used for continuum mapping at different wavelengths as well as velocity mapping from a number of the strong transition lines detected. ALMA test data on extragalactic sources also include NGC 3256, PKS 1830-211, BRI 0952, and the Cosmic Eyelash. In all cases, the ALMA test data obtained with just 4–8 antennas are comparable or superior in quality to those obtained with existing facilities, such as the Sub-Millimeter Array (SMA) or the Plateau de Bure Interferometer. The potential of

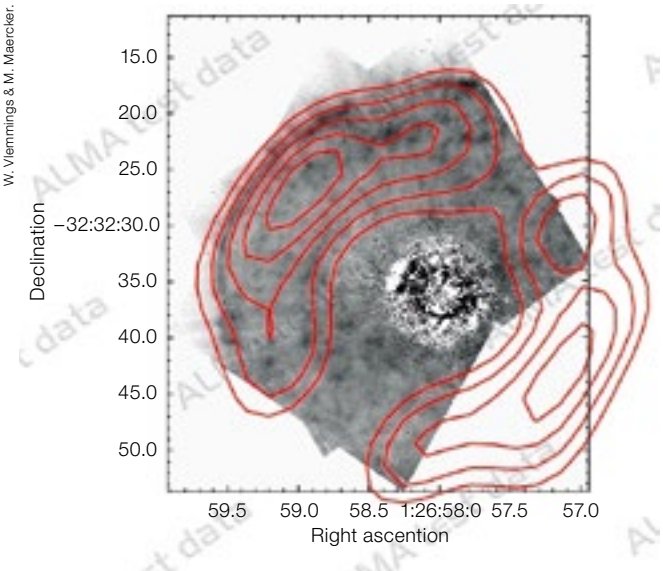

Figure 2. CO(1-0) test data of the detached shell around R Scl observed with ALMA with five antennas (red contours). The grey-scale image shows stellar light scattered by dust particles in the detached shell observed with the ACS on HST (Olofsson et al., 2010).

ALMA for Solar System science was briefly outlined by M. Zwaan. Since solar observations will not be offered in Cycle 0, the current focus is expected to lie in observations of the atmospheres of planets and their moons, Kuiper Belt and trans-Neptunian objects, and the study of comets. Ironically, the only ALMA test data currently available for a Solar System body are single-dish observations of the Sun taken during a period of particularly bad weather, when the thick cloud cover effectively acted as a solar filter!

Star formation, both at low- and high-mass, is another research area that will benefit extensively from ALMA's unique capabilities, as shown by J. Pineda and P. Klaassen. ALMA band 7 test data have already revealed outflows for a number of molecular species in NGC 1333 IRAS4B, and the unprecedented sensitivity achievable even during Early Science is expected to have a strong impact on our understanding of core formation, fragmentation, disc and planet formation, to give just a few examples. A 14.7 GHz wide band 7 spectral sweep of the Orion Kleinmann–Low region, taken during ALMA commissioning as part of a spectral scan test, impressively illustrates the potential of ALMA for spectral line detection. With the large bandwidth covered and the high sensitivity achieved, the ALMA test observations already entirely surpass SMA data (see Figure 1 of Longmore et al. p. 42).

Hands-on software tutorials

The second and last day of the workshop was devoted entirely to hands-on software tutorials. Around 80 interested participants were split into two groups depending on their previous experience in radio/sub-mm interferometry. Each group was given a hands-on tutorial on the two major pieces of software relevant to ALMA proposal preparation: the OT and the ALMA simulators. While the tutorials were held simultaneously for the two groups, those for the novice users were slightly longer and included an introduction to radio/sub-mm concepts (presented by A. Biggs) and interferometry basics (given by A. Richards) in the OT and the simulator sessions respectively. Both groups were given software-specific presentations and live demonstration sessions (with presenters A. Avison, A. Biggs, E. van Kampen and S. Randall), followed by a few hours in which tutees could experiment with the software, with the help of a number of tutors (see upper figure on p. 38).

The enthusiastic response of the European astronomical community to this workshop and the lively discussions among the participants indicate that the groups specialising in the radio/sub-mm, and other wavelength regimes, are eagerly awaiting ALMA and Early Science operations. We look forward to a flood of excellent observing proposals and some spectacular scientific results during Cycle 0 — and beyond!

The presentations and most of the tutorial material are available in electronic form from the conference website: http://www.eso.org/sci/meetings/2011/alma_es_2011.html.

Acknowledgements

The organisation of the ALMA Community Days would not have been possible without the help of C. Stoffer, who took care of many of the practical aspects of the workshop and kept an overview at all times. We would also like to thank the members of the Organising Committee, S. Longmore, the entire ESO ARC staff and the ESO Garching IT Helpdesk staff for their help. The tutorials on the second day could not have taken place without the tutors: A. Biggs, A. Bridger, V. Casasola, B. Dabrowski, L. Humphreys, A. Kospal, S. Muller, S. Randall (OT) ; A. Avison, A. Richards, A. Rushton, E. van Kampen, M. Zwaan (Simulators). Finally, we would like to thank all the speakers for putting so much work into their presentations. The workshop was sponsored by ESO and Radionet, which provided travel support to a number of speakers and tutors.

References

Olofsson, H. et al. 2010, A&A, 515, 270

Links

[1] ALMA Science Portal: www.almascience.org

Report on the

ALMA Early Science Massive Star Formation Workshop

held at ESO Headquarters, Garching Germany, 8 April 2011

Steven Longmore[1]
Leonardo Testi[1]
Pamela Klaassen[1]

[1] ESO

With the deadline for ALMA Early Science Cycle 0 proposals fast approaching, a workshop was held for members of the European massive star formation community to discuss ideas for potential ALMA Early Science projects. The workshop began with short summary talks on the ALMA Early Science capabilities, the multi-wavelength large-area survey data available as ALMA source-finder charts and the modelling/analysis tools that are available to help interpret future ALMA data. The rest of the meeting was spent discussing science ideas and proposal strategies. There was general agreement on the main science questions to be addressed, the basic observing strategies required to achieve the goals and the future steps needed to develop the ideas into proposals.

With the deadline for ALMA Early Science Cycle 0 proposals fast approaching[1], a dedicated workshop was organised, providing a forum for members of the European massive star formation community to get together and discuss ideas for potential ALMA Early Science projects. The workshop, which followed the ALMA Community Days (see Randall et al. p. 39), was attended by 35 participants from many institutions across Europe[2] (see Figure 2).

High-mass star formation is one of the key science topics that will exploit the order of magnitude improvements in sensitivity, resolution, dynamic range and image fidelity offered by ALMA over existing millimetre and submillimetre interferometers. ALMA will excel at providing images in unprecedented detail and is the obvious follow-up instrument for lower-resolution, large-scale surveys.

The workshop therefore began with review talks on the many single-dish Galactic Plane surveys that have been conducted over the past few years; these surveys will act as ALMA source-finder charts. The advent of new facilities and instrumentation means that these surveys are now available over most of the electromagnetic spectrum, both in continuum from centimetre to near-infrared wavelengths (CORNISH[3], BGPS[4], ATLASGAL[5], Hi-GAL[6], HOBYS[7], MIPSGAL[8], GLIMPSE[9], RMS[10], UKIDSS[11]) and for spectral-line emission (HOPS[12], MALT90[13]). The typical angular resolution of these surveys range from one to a few times the ALMA primary beam. This makes ALMA an ideal

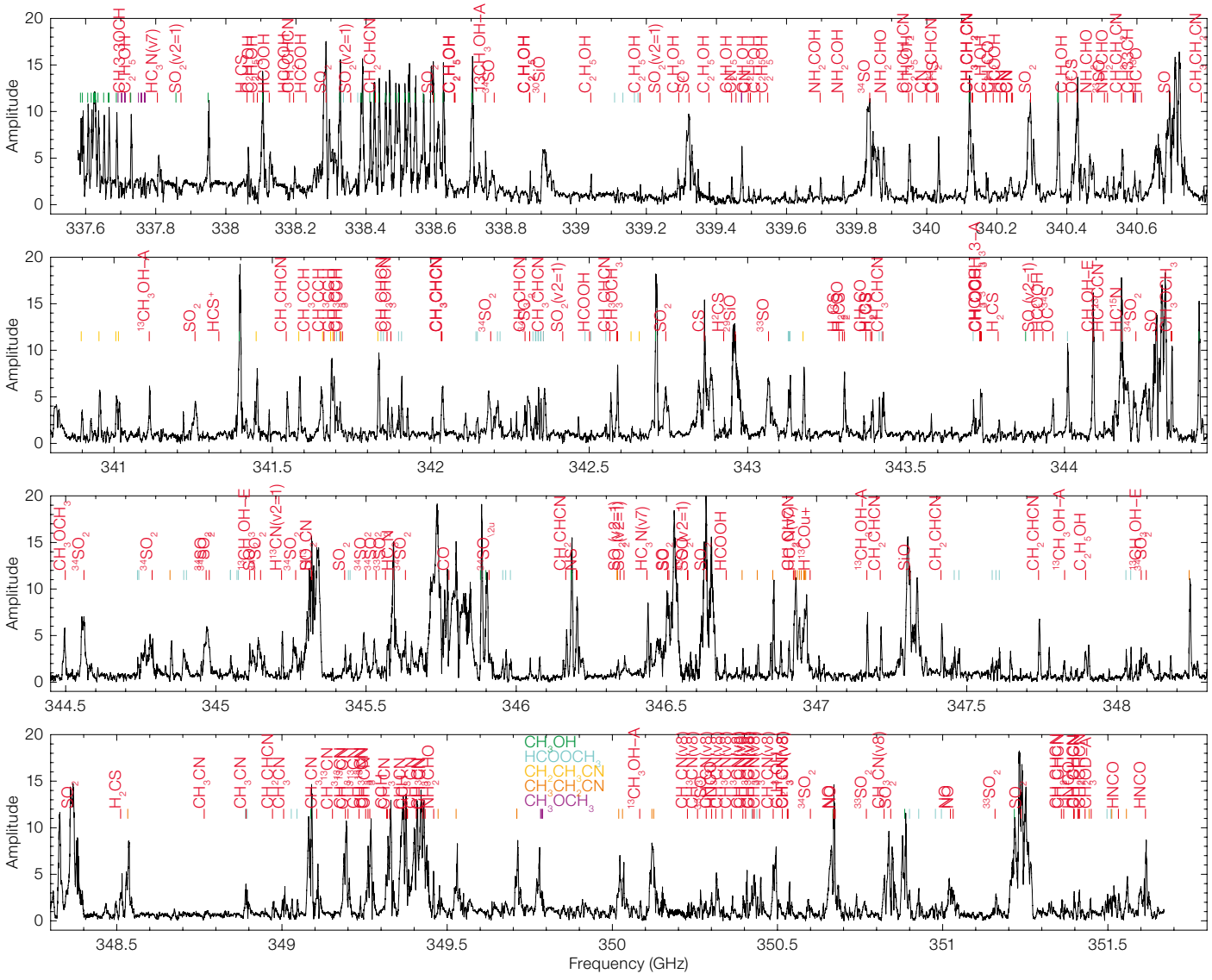

Figure 1. Continuum-subtracted single polarisation *uv*-spectrum of Orion BN-KL. These observations consist of four frequency setups which have been concatenated together. With only five antennas, each frequency setup was observed for 14 minutes, giving a total on source integration time of 56 minutes. The lines identified at the Caltech Submillimeter Observatory by Schilke et al. (1997) are overplotted and labelled in red, except for transitions of CH_3OH (green), $HCOOCH_3$ (cyan), CH_2CH_3CN (yellow), CH_3CH_2CN (orange) and CH_3OCH_3 (magenta).

instrument for exploring the structure and physical properties of the compact sources found in the surveys. Indeed, the talks highlighted that several classes of sources that require such follow-up are already being identified.

Observations conducted during commissioning in 2010 already demonstrate ALMA's potential as a probe of the chemical structure of high-mass star formation regions, thanks to the unprecedented combination of wide instantaneous bandwidth and sensitivity. Figure 1 shows a spectral sweep across part of the band 7 (~345 GHz, 850 μm) window towards the Orion Becklin–Neugebauer Kleinmann–Low (BN-KL) high-mass star formation region. Despite only 14 minutes on-source integration per frequency set-up and only five antennas, ALMA detects a plethora of spectral-line emission features from a wide range of complex molecules towards this hot core. This gives some idea of the complexity of the ALMA datasets that can be expected from more distant and fainter high-mass star forming regions, as the number of ALMA antennas increases from 5 to 16 in Early Science and finally to more than 50 in full operation. Given the expected complexity of ALMA data, the workshop continued with a session discussing the various tools already available and being developed (e.g., XCLASS[14], LIME[15], RADMC-3D[16], MOLLIE[17]) that will be necessary to analyse such datasets. These tools are now maturing to a level that will allow many future ALMA users to perform detailed analysis of the datacubes.

The remainder of the workshop was devoted to the presentation and discussion of science ideas and potential proposal strategies. This began with suggestions on possible ways to organise the community to maximise the science output during ALMA Cycle 0. Some ideas raised were: complementary frequency and line selection; co-ordinated proposals; and the relative merits of surveys and single-object proposals. In the science discussions that followed, several key areas were highlighted which exploit the unique ALMA Early Science capabilities and focus on well-selected samples or unique objects chosen from the large-area surveys. The participants then split into smaller groups to further develop these ideas before reporting back to the full group on the outcome of their discussions. In general there was agreement within the groups on the main science questions to be addressed, the basic observing strategies required to achieve the goals and the future steps needed to develop the ideas. At the close of the workshop, it was decided that each of these groups would plan to continue these discussions in an ongoing build-up to the proposal deadline.

Hans Zinnecker

Figure 2. Group photo of the workshop participants.

Links

1 ALMA Cycle 0 Call for Proposals: http://www.almascience.eso.org/call-for-proposals
2 Workshop website: http://www.eso.org/sci/meetings/2011/alma_es_2011.html
3 CORNISH (COordinated Radio 'N' Infrared Survey for High-mass star formation): http://www.ast.leeds.ac.uk/Cornish/public/index.php
4 BGPS (Bolocam Northern Galactic Plane Survey): http://milkyway.colorado.edu/bgps/
5 ATLASGAL (APEX Telescope Large Area Survey of the Galaxy): http://www.mpifr-bonn.mpg.de/div/atlasgal/
6 Hi-GAL (Herschel Infrared Galactic Plane Survey): https://hi-gal.ifsi-roma.inaf.it/higal/
7 HOBYS (Herschel imaging survey of OB Young Stellar objects): http://www.herschel.fr/cea/hobys/en/
8 MIPSGAL (Spitzer MIPS Galactic Plane survey): http://mipsgal.ipac.caltech.edu/
9 GLIMPSE (Galactic Legacy Infrared Mid-Plane Survey Extraordinaire): http://www.astro.wisc.edu/sirtf/
10 RMS (Red MXS Source survey): http://www.ast.leeds.ac.uk/RMS/
11 UKIDSS (UKIRT Infrared Deep Sky Survey): http://www.ukidss.org/
12 HOPS (H_{MALT90} (O southern Galactic Plane Survey): http://www.jcu.edu.au/school/mathphys/astronomy/awalsh/HOPS/ and Walsh, A. et al, 2008, PASA, 25, 105
13 MALT90 (Millimetre Astronomy Legacy Team 90 GHz Survey): http://malt90.bu.edu/
14 XCLASS: http://www.astro.uni-koeln.de/projects/schilke/XCLASS
15 LIME (LIne Modelling Engine): http://www.strw.leidenuniv.nl/~brinch/website/lime.html
16 RADMC-3D (Radiative transfer Monte Carlo 3D): http://www.ita.uni-heidelberg.de/~dullemond/software/radmc-3d/
17 MOLLIE (MOLecular LIne Explorer): https://www.cfa.harvard.edu/~eketo/

Report on the ESO Workshop

Dynamics of Low-mass Stellar Systems: From Star Clusters to Dwarf Galaxies

held at ESO Vitacura, Santiago, Chile, 4–8 April 2011

Steffen Mieske[1]
Mark Gieles[2]

[1] ESO
[2] Institute of Astronomy, Cambridge, United Kingdom

The dynamics of low-mass stellar systems is not only an interesting subject in its own right, but is also intimately linked to global theories of structure formation, the physics of gravity, and the shape of the stellar initial mass function. Given the wealth of new information gathered very recently in this field, the time was ripe to hold a dedicated meeting on this topic. The workshop brought together a mix of about 100 astronomers who work on both the observation and theory of the dynamics of dwarf galaxies and star clusters, and a total of around 60 oral presentations and about 25 posters were presented.

At the low-mass end of stellar systems, there used to be a well-known dichotomy. On the one hand, there are star clusters with typical sizes of a few parsecs (pc), whose internal dynamics can generally be well described by Newtonian gravity. On the other hand, there are the much more extended dwarf galaxies with sizes of several hundred pc, whose dynamics appear to be dark matter dominated and which are usually related to cosmological substructures (see Figure 1). These classical boundaries have been blurred by the recent discovery of new classes of stellar groupings, such as ultra-faint dwarf spheroidals, ultra-massive super star clusters, ultra-compact dwarf galaxies (UCDs), and dark-matter-poor tidal dwarf galaxies (TDGs).

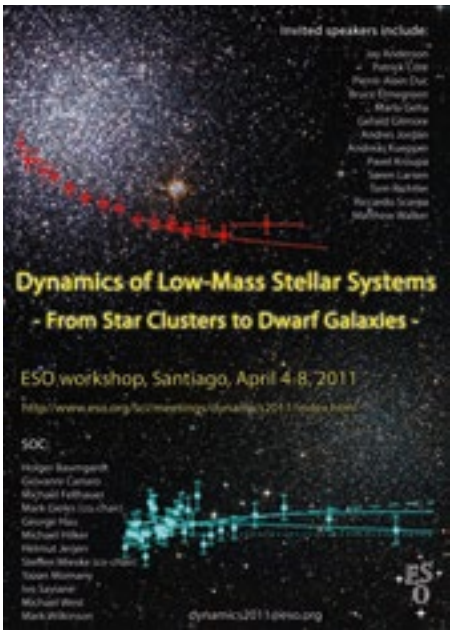

Figure 1. Conference poster, showing ESO images of Omega Centauri at the top left, and the dwarf galaxy Sculptor at the bottom right. The red and blue curves show the radial behaviour of stellar velocity dispersions in these objects (from Scarpa & Fallomo, 2010; Walker et al., 2009). The flat profile for the dwarf galaxy is typically interpreted as indicating the presence of dark matter.

The idea of our workshop, Dynamics of Low-mass Stellar Systems: From Star Clusters to Dwarf Galaxies, was to discuss the internal dynamics of these systems and their use as tracer particles in large-scale potentials. Special emphasis was placed on how the observed dynamics are linked to a more global context of structure formation theories, including a discussion of the concordance cosmological model and possible alternatives. Another focus of this meeting was the transition region between classical star clusters and dwarf galaxies, in particular UCDs.

Internal dynamics of compact stellar systems

The meeting began with a full-day session on the internal dynamics of compact stellar systems. The star cluster mass function and its evolution with time was the main topic of the morning session. Overview talks on this topic were delivered by A. Jordan, B. Elmegreen, S. Larsen and P. Goudfrooij. Clusters in nearby galaxies form with a power-law mass distribution, with indications for a truncation around a few 10^5 solar masses (Larsen). The mass distribution function of old clusters peaks (when using logarithmic mass bins) at around that mass (Jordan, Elmegreen). Despite our long-established understanding of the dynamical evolution of clusters, there is still no consensus on whether the old cluster mass function can be the result of the (dynamical) evolution of a universal power-law distribution, as observed at young ages in the present epoch.

The mass-size relation (or lack thereof) among star clusters was discussed by M. Gieles, a topic that was brought up again several times during the meeting (see also Figure 3). Star cluster sizes seem to be uncorrelated with their masses up to a few million solar masses. Above this, in the realm of UCDs, size increases with mass, joining an extrapolation of the relation for giant galaxies. It was suggested that the lack of a mass-size relation of clusters is the result of dynamical evolution of star clusters away from a primordially existing relation. Subsequently the dynamical evolution of star clusters under the influence of external tides (J. Penarrubia & A.L. Vari) and internal

Figure 2. Conference photo taken in the garden of ESO's Vitacura premises.

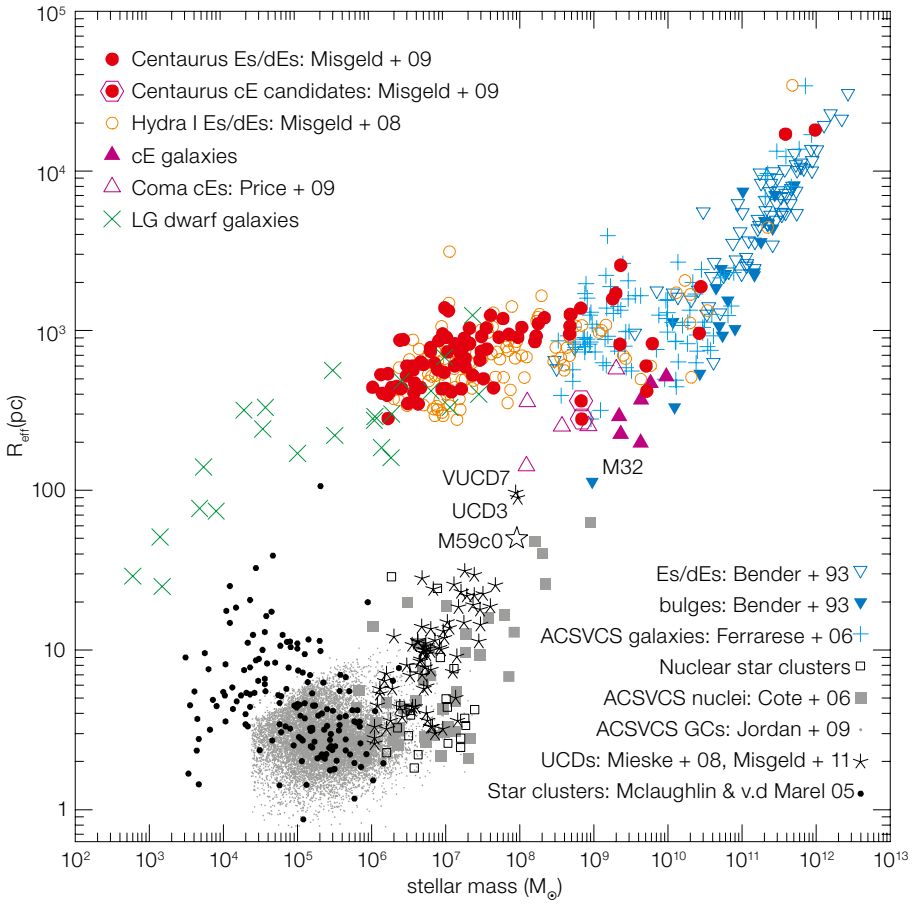

Figure 3. Effective radius plotted *vs.* stellar mass for all pressure-supported stellar systems (from Misgeld & Hilker, 2011). This plot was repeatedly shown during the workshop and the dynamics of systems with masses below ~10^8 solar masses were discussed. Dwarf galaxies are typically larger than 100 pc, while star clusters and UCDs are below that size.

effects (R. Smith & L. Smith) were discussed.

In the afternoon session, several talks on the test of Modified Newtonian Dynamics (MOND) with star cluster dynamics (R. Scarpa, R. Sollima & R. Lane) were presented. Those talks generated a very lively discussion on whether the suggested flattening of the dispersion profile in the outskirts of some clusters is caused by a breakdown of Newtonian gravity, the influence of tidal fields, or contamination. More work, especially in terms of accurate dynamical modelling, will be needed to draw firm conclusions on this matter. The afternoon continued with a review of dynamic evolutionary modelling of globular clusters by D. Heggie, who showed that a proper N-body simulation of a massive globular cluster can(not?) be performed in a human lifetime. The first day wrapped up with talks on the observed internal dynamics of nearby star clusters (A. Stolte & N. Bastian), and we learned that globular clusters (GCs) in Andromeda appear to have dynamical masses that are too low to be possibly explained by pronounced dynamical evolution (J. Strader).

Internal dynamics of dwarf galaxies

The second day of the workshop was dedicated to the dynamics of dwarf galaxies. The scene was set by review presentations on the observed internal dynamics of ultra-faint, classical and tidal dwarf galaxies by M. Geha, M. Walker and P.-A. Duc, respectively. The influence of contaminators and binaries on the derived velocity dispersions was discussed; issues that are of special importance for the faintest dwarf galaxies. It was concluded that most of the Local Group dwarfs have internal dynamics that are consistent with them being dark matter dominated, with some ongoing debate on a few ultra-faint dwarfs. It was furthermore shown that TDGs may require a moderate amount of dark matter (baryonic or non-baryonic) to explain their internal dynamics. Presentations by J. Bullock and M. Bovill drew attention to the problems of the concordance Lambda Cold Dark Matter (ΛCDM) cosmological model in explaining the observed low frequency of bright satellites.

Several presentations then focused on the dynamics of individual Local Group dwarf spheroidals (S. Pasetto, S. Zaggia & E. Lokas) including a comparison between Milky Way and M31 dwarf spheroidals (E. Tollerud). It appears that M31 dwarfs have on average lower mass-to-light (M/L) ratios at comparable luminosities. It was stressed that stochastic fluctuations may be a serious limiting factor in the predictive power of ΛCDM for individual host halos such as the Milky Way or M31. G. Mamon, M. Wilkinson and J. Wolf discussed important aspects of dynamical modelling of dwarf spheroidal galaxies from a theoretical point of view. The afternoon talks were completed by a review by P. Kroupa of the problems of ΛCDM in the Local Group, proposing a scenario where all dwarfs are formed as TDGs without any dark matter. It was shown that galaxy encounters can create counter-rotating tidal debris reminiscent of today's dwarf galaxies (M. Pawlowski). G. Hensler presented the chemo-dynamical aspect of dwarf galaxy evolution in a ΛCDM scenario.

A "hot" discussion session led by M. Wilkinson concluded the second workshop day. The apparent problems of ΛCDM in explaining the properties of Local Group galaxies for a range of masses were debated. This included the missing-satellite problem that extends to higher masses than traditionally reported, and the disc of satellites, the highly anisotropic distribution of Milky Way dwarfs. At the same time, the problems and failures of alternative approaches like MOND to provide a full framework for explaining our observed Universe were highlighted.

Black holes in low-mass stellar systems

The third day focused on black holes in low-mass stellar systems, and whether star clusters extend the well-known mass–sigma (M–σ) relation of giant galaxies to lower masses. J. Anderson showed that, from HST-based proper motion measurements, there is currently no evidence for intermediate-mass black holes in the centres of massive Galactic star clusters. This differed from the results of radial velocity studies via spectroscopy (presentations by N. Luetzgendorf, B. Jahlali & E. Noyola; see Figure 4), which suggest black holes of several tens of thousands of solar masses in a couple of Galactic star clusters. Direct comparison of proper motion and radial velocity data for Omega Centauri showed that the discrepancy can only partially be explained by uncertainties in the adopted cluster centre. H. Baumgardt reviewed the dynamical evolution of star clusters in the presence of black holes. Finally, N. Neumayer showed that several nuclear star clusters contain a comparably massive black hole. Whether or not star clusters follow the extrapolation of the M–σ relation to lower masses is still an open issue, and addressing this problem faces some fundamental limitations due to the finite number of stars that can be used as dynamical tracers in the centres of star clusters. The third workshop day was wrapped up by a dedicated poster session with 20 short presentations.

Star clusters as tracers in large scale potentials

The fourth day of the workshop shifted from the internal dynamics of low-mass stellar systems to their use as tracers in large-scale host galaxy potentials. P. Coté reviewed the link between globular cluster subpopulations and their host galaxy merger histories. This topic was discussed further in presentations by J. Brodie, R. Sanchez-Janssen and A. Huxor. T. Richtler, A. Romanowsky and V. Pota gave an overview of how the kinematics of globular cluster systems can be used to constrain the dark matter halo shape of giant galaxies. The dynamical evolution of star clusters in an external tidal field was discussed in presentations by A. Kuepper, D. Kruijssen, S. Bird and F. Renaud. I. Misgeld then gave an overview of structural and dynamical properties of “hot” stellar systems over ten orders of magnitude in mass (see Figure 3).

The dwarf galaxy – star cluster interface

The earlier presentations then set the scene for the last session of the fourth day which was dedicated to UCDs — the stellar systems at the interface between star clusters and dwarf galaxies. M. Hilker reviewed the general properties of UCDs. M. Frank presented fresh results on the spatially-resolved internal kinematics of the most massive UCD (see Figure 5). He finds that its kinematics are fully consistent with a “normal” star cluster, with no evidence for the presence of dark matter or a black hole. This was considered an important step forward in our understanding of UCDs and their origin. C. Bruens then showed *N*-body simulations, which suggested that UCDs may well be formed by the merging of individual massive star clusters, and M.

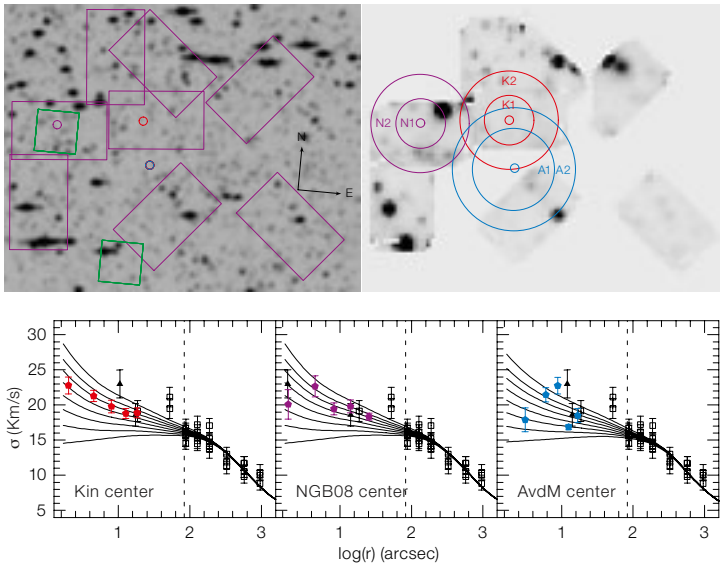

Figure 4. Kinematics of the centre of Omega Centauri measured with the FLAMES–ARGUS spectrograph at the VLT, as presented by E. Noyola at the workshop (Noyola et al., 2010).

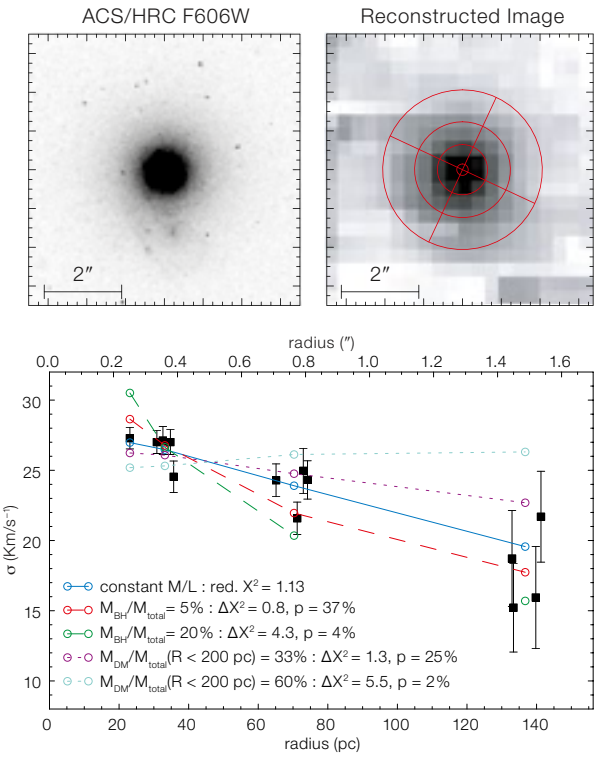

Figure 5. Spatially resolved internal kinematics of Fornax UCD3 measured with the FLAMES–ARGUS spectrograph, as presented by M. Frank at the workshop (Frank et al., 2011).

Norris discussed the ensemble properties of UCDs in a statistical sense.

The fourth day concluded with a discussion session led by S. Mieske. It was noted that the frequency of UCDs is consistent with the hypothesis that they constitute the bright tail of the globular cluster luminosity function. UCDs can be explained as massive star clusters, whose elevated M/L ratios are due to a non-canonical initial mass function. On the other hand, the formation of UCDs via tidal stripping cannot be excluded as an additional channel, given the observational evidence of tidal disruption of dwarf galaxies. Another topic of discussion was whether star clusters would be expected to trace the M–σ relation to a lower value of σ. It was concluded that this would strongly depend on the formation mechanism of putative massive black holes in them.

The last day of the workshop was again dedicated to the interface between star clusters and galaxies. D. Forbes discussed the definition of a galaxy, showing that the presence of multiple stellar populations is considered the most defining feature for a galaxy, according to an online poll amongst astronomers. K. Woodley discussed the star cluster to UCD transition based on an extensive study of the globular cluster system of the nearby elliptical galaxy Centaurus A (NGC 5128). G. da Costa showed new results on the stellar dynamics in the outskirts of Omega Centauri, arguing that possible deviations from a Keplerian velocity dispersion profile are likely due to tidal effects and/or interlopers. P. Assmann and J. Hurley focused in their talks on dwarf galaxy formation via star cluster mergers. The last session was rounded off by presentations on nuclear and bright globular clusters in dwarf galaxies (I. Georgiev) and a discussion of cold halos and extended clusters in M31 (M. Collins).

Conference summary

An inspiring conference summary was delivered by G. Gilmore. He made a general point that the ΛCDM framework provides a very good description of the Universe from the largest scales down to galaxy size scales, and that, in particular, it describes the initial stages of the Universe very well. He also noted, however, that there are considerable problems with ΛCDM predictions at smaller (galaxy) scales. He argued that a possible avenue towards a reconciliation of theory with the observed Universe at small scales may be less massive (= warm) dark matter particles. He also made the point that in comparison with ΛCDM, the concept of MOND does not provide by itself an adequate description of the Universe as a whole, lacking a cosmological framework. He argued that the internal dynamics of Milky Way satellites within the radius of the Magellanic Stream are likely affected by tidal forces, and advocated caution in the interpretation of dynamical data of objects within that radius. He added that objects in the transition region between galaxies and star clusters — such as UCDs — can give fascinating insights into galaxy transformation processes and massive star cluster formation, while constraints on dark matter properties can only be obtained from objects with sizes above ~100 pc, which he considers as galaxies.

Acknowledgements

We warmly thank Maria Eugenia Gomez, Paulina Jiron, the team of ESO IT and General Services, and the entire Local Organising Committee.

References for figures

Frank, M. et al. 2011, MNRAS letters in press, arXiv:1104.2593
Misgeld, I. & Hilker, M. 2011, MNRAS in press, arXiv:1103.1628
Noyola, E. et al. 2010, ApJ, 719L, 60
Scarpa, R. & Fallomo, R. 2010, A&A 523, A43
Walker, M. et al. 2009, ApJ, 704, 1274

Report on the Workshop

The Evolution of Compact Binaries

held at Hotel San Martín, Viña del Mar, Chile, 6–11 March 2011

Linda Schmidtobreick[1]
Matthias R. Schreiber[2]

[1] ESO
[2] Departamento de Física y Astronomía, Universidad de Valparaíso, Chile

The workshop, organised by ESO and the Universidad de Valparaíso, was held with the aim of bringing together people from different communities to concentrate on the specific problem of binary evolution. Compact binaries divide into many classes, but the evolution of all these objects is driven by a common mechanism: angular momentum loss. From the formation of compact binaries over the various phases of contact to their explosive deaths in a supernova Type Ia or gamma-ray burst, the measurement and understanding of the braking mechanisms was the main discussion point of the meeting.

In order to bring astronomers from the different communities to an understanding of the main problems in the evolution of compact binaries, the workshop began with thorough introductory review talks on the main types of compact binaries,

like cataclysmic variables (by Ch. Knigge), low-mass X-ray binaries (P. Charles) and high-mass X-ray binaries (S. Chaty). Further general reviews were given by G. Hussain who thoroughly explained the theory and observations of the magnetic braking mechanism in single stars and binaries, and by M. van der Sluys, who introduced the concept of gravitational radiation and the resultant braking effect.

The sessions themselves were organised following the evolution of compact binaries in chronological order. The full programme of the meeting can be found on the conference web page[1]. We started with close binary formation, which was summarised in a review by K. M. Kratter who gave an overview on the different channels to achieve a close binary configuration and compared the theoretical predictions with observational statistics on multiplicity. The contributed talks in this session concentrated on multiplicity as observed in certain star-forming regions or in certain classes of stars and both theory and observations agree that multiplicity increases strongly towards higher stellar masses.

If the binary components are sufficiently close, the evolving primary will at some point fill its Roche lobe and thus start unstable mass transfer towards the secondary, resulting in a common envelope phase. In her review, N. Ivanova introduced common envelope physics. Due to its short timescale, so far no direct observations exist of this phase. Therefore, the session was naturally dominated by simulations and theoretical discussions on the impact that the common envelope has on the final binary configuration. In particular, the efficiency of the common envelope in bringing stars together, and at the same time expelling the material of the envelope as a planetary nebula, seems to be finally understood, as was demonstrated by M. Zorotovic.

Planetary nebulae also played a major role in the contributions concerned with the post common envelope phase. Together with the hot subdwarfs, planetary nebulae represent the objects that arise directly out of common envelope evolution and no further evolutionary assumptions are needed to link them to this phase. H. Boffin and D. Jones presented good evidence that binarity is responsible for the aspherical morphology of most nebulae and also explained the details of the formation mechanisms. The subsequent discussions concentrated on the statistics of the observed binaries with respect to the expectations from stellar population synthesis, and the strong impact of the Sloan Digital Sky Survey (SDSS) on this field became evident.

Cataclysmic variables, novae, symbiotic stars and X-ray binaries in various flavours were discussed in the session on the contact phase. Since the evolution of any particular binary takes too long to observe, it is important to have homogeneous samples, as was pointed out by several speakers. Surveys like SDSS or selections on X-rays or variability seem to be examples of ways to deal with this problem. The importance of metallicity for binary evolution was stressed by F. Mirabel and F. Valsecchi in their talks about massive binaries and black holes.

"Graveyard or Boom?" was the title of the session about the final stages of binary evolution and both possibilities were introduced in the reviews: F. Röopke gave an overview on supernovae Type 1a and possible progenitors; T. Tauris introduced binary pulsars; and E. Ramirez explained gamma-ray bursts from the evolutionary point of view. Many other contributions dealt with the possible mass increase of white dwarfs in cataclysmic variables, symbiotic stars or double degenerate binaries to thus reach the Chandrasekhar limit and ignite the supernova.

The workshop ended with a short session on telescopes and instruments with talks concerning the latest about the E-ELT, the possibilities of optical interferometry, and the young field of gravitational-wave astronomy.

Intense and lively discussions took place during the whole week of the workshop. The idea of having specialists giving the introductions to the specific physics involved in binary evolution worked excellently. In this format, the experts were also present to answer any specific question that arose from the presentations and during the discussions. This helped to avoid fruitless speculations and to keep the discussions relevant to the subject. On the other hand, since the participants came from different scientific communities, many unorthodox ideas and suggestions came up and gave fresh input to some discussion.

From the feedback that we got during and after the workshop, it seems that everyone had learnt something new, but was also able to contribute to the general level of knowledge. Interaction between the participants was promoted not only by the space given in the individual sessions, but also by the various activities taking place outside the conference room (see the lower figure on the Astronomical News section page, p. 38). The welcome cocktail, a walk through the hills of Valparaíso, a boat trip in the harbour, the conference dinner itself, and the closing lunch helped to get people to talk to each other and thus to found new collaborations and friendships.

The proceedings of this workshop will be published in the Conference Series of the Astronomical Society of the Pacific.

Links

[1] Conference website: http://www.eso.org/sci/meetings/Binary_Evolution2011/

ESO Participates in Germany's Girls' Day Activities

Douglas Pierce-Price[1]

[1] ESO

On 14 April 2011, ESO took part in the Germany-wide Girls' Day activities[1,2], in which technical enterprises, universities and research organisations arranged open days for girls, to give female school students an insight into scientific and technological professions and to encourage more of them to choose such careers in the future.

The ESO Girls' Day event, An Introduction to the Work of the European Southern Observatory, was organised by the Human Resources department, with participation from volunteers across the organisation and support from the education and Public Outreach Department. Spaces were soon fully booked, and about 50 students attended the event at ESO Headquarters in Garching. The girls, aged between 11 and 16, came from schools in Munich and the surrounding area.

In the morning, after being welcomed to ESO, the students were shown a film about the adventure of working at the Very Large Telescope, and could appreciate the unfamiliar landscape of the Atacama Desert and the state-of-the-art facilities on Cerro Paranal. This introduction was followed by presentations on astronomy and the observatory sites, and on careers at ESO.

After lunch, the students split into four groups, to visit different parts of ESO Headquarters. They saw the activities in the optical and electronics laboratories, and the work of the draughtspersons, as well as having another chance to meet some of the astronomers and PhD students at ESO. Throughout the tour they had the opportunity to ask many questions about working at ESO.

Having seen the VLT in the morning's film, the students then had the next best experience to visiting it themselves: a live video-link to both Paranal and the ESO offices in Santiago, where astronomers were available for a question-and-answer session. Seeing the mountaintop at Paranal in real-time, with a giant VLT Unit Telescope moving in the background, was a thrilling experience for the students. The volunteers at the other end of the intercontinental video-link kept the audience informed and entertained in equal measure, thanks to their lively and engaging answers, and it was only limited time that prevented the discussion lasting even longer.

With this "visit" to ESO's flagship site in Chile, the Girls' Day came to an end. Thanks are due to all the staff members who kindly volunteered to speak to the girls and show them around. We hope that the students will remember the experience for a long time, and that it will inspire some of them to pursue careers in science and technology. They may even enter the field of astronomy, in which case perhaps we will have the chance to welcome them back to ESO in the future.

Links

[1] Girls' Day in Germany: http://www.girls-day.de/
[2] English information about Girls' Day in Germany: http://www.girls-day.de/English_Information

Announcement of the ESO Workshop

Ten Years of VLTI: From First Fringes to Core Science

24–27 October 2011, ESO Headquarters, Garching, Germany

The Very Large Telescope Interferometer (VLTI) saw first fringes in 2001 with a very simple but powerful instrument known as VINCI. Since then, the VLTI, with the instruments AMBER and MIDI, has become a major contributor to a number of important research domains in contemporary astrophysics, from the nature of rocky objects in the Solar System, to the nuclear regions of active galaxies, in addition to detailed investigations of stars and their close environment. The VLTI is the first optical interferometer to be implemented as a common user facility. At the VLTI, optical interferometry has evolved from an initial experimental phase, devoted mainly to technology demonstration, to the current phase where astronomers do not need to be "black-belt" interferometrists to use the instruments and extract valuable scientific information about their favourite targets.

There are three themes to the conference. The first is to travel along the road of the VLTI over the last ten years, celebrating its scientific achievements and the successful partnership between ESO and the international interferometric community. Turning the VLTI into a *bona fide* common user facility has required enormous efforts from scientists and engineers at ESO and in the community; the close collaboration between ESO and its user community was essential to this success.

The second theme is to visit the science that the VLTI will be doing in the era of the Atacama Large Millimeter/submillimeter Array (ALMA) and the James Webb

Space Telescope (JWST). The VLTI is evolving, and soon the first generation of instruments will be followed by a new much more powerful suite. The trio of instruments PRIMA, GRAVITY and MATISSE will offer much improved sensitivity and imaging capabilities, characterising planets, stars and black holes at unprecedented levels of detail. These instruments will arrive during a new era in observational astronomy: the Hubble Space Telescope will be nearing the end of its mission; ALMA will have reached its full capability; and JWST will be getting ready to launch. Together, ALMA, JWST and the VLTI will enable unprecedented advances in stellar physics and the nuclei of galaxies.

The third theme of the conference is to project the VLTI beyond the second generation of instruments, at the time when the Extremely Large Telescopes (ELTs) will begin to dominate ground-based optical astronomy. The ELTs will have unprecedented sensitivity while interferometers will have superior spatial resolution. This conference will be an opportunity to preview the science that will be done by the ELTs and interferometers together, and the technical requirements for the VLTI to enable that science.

The Scientific Organising Committee consists of: Olivier Absil (Liège), Roberto Gilmozzi (ESO), Walter Jaffe (Leiden), Fabien Malbet (Grenoble), Alessandro Marconi (Florence), Jorge Melnick (ESO, Chair), Antoine Mérand (ESO), Rafael Millan-Gabet (Caltech), John Monnier (Michigan), Jenny Patience (Exeter), Guy Perrin (Paris Obs.), Didier Queloz (Geneva), Gerd Weigelt (MPIfR Bonn) and Sebastian Wolf (Kiel).

The Local Organising Committee consists of: Francoise Delplancke (Chair), Roberto Gilmozzi, Christian Hummel, Jorge Melnick, Isabelle Percheron, Gerard van Belle and Markus Wittkowski.

The registration deadline is 23 September 2011.

Further details are available at: http://www.eso.org/VLTI_2011/

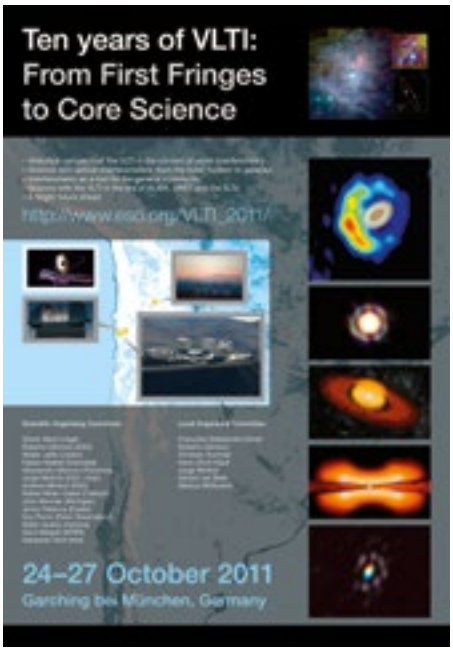

Personnel Movements

Arrivals (1 April–31 June 2011)

Europe	
Martis, Alessandro (IT)	Contract Officer
Vernazza, Pierre (FR)	Fellow
Gonzalez Villalba, Justo Antonio (ES)	ALMA Data Analysis Software Developer
Iribarrem, Alvaro (BR)	Student
Zhao, Fei (CN)	Student

Chile	
Mawet, Dimitri (BE)	Operations Astronomer
Gaytan, Daniel (CL)	Unix and Network Specialist
Riffo, Lidia (CL)	Secretary
Foster-Guanzon, Caroline (CA)	Fellow
Aravena, Manuel (CL)	Fellow
Del Valle, Diego (CL)	Software Engineer

Departures (1 April–31 June 2011)

Europe	
Di Dio, Tommaso (IT)	Accountant
Kerk, Elizabeth (NL)	HR Officer
Swat, Arkadiusz (PL)	Optical Engineer
Pomaroli, Edouard (FR)	Electromechanic
Slijkhuis, Remco (NL)	Archival Data Product Specialist
Bruton, Andrew (GB)	Mechanical Technician
Schleicher, Dominik (DE)	Fellow
Fontani, Francesco (IT)	Fellow
Karovicova, Iva (CZ)	Student
Zabl, Johannes Florian (DE)	Student
Surdej, Isabelle (BE)	Student

Chile	
Camuri, Massimiliano (IT)	Electronic Engineer
Orrego, Oscar (CL)	Guesthouse Supervisor

This striking panoramic photo, taken by ESO Photo Ambassador Yuri Beletsky, shows the sky over Cerro Paranal during the total lunar eclipse of 21 December 2010. The eclipsed moon (red disc) is visible just above the dome of VLT Unit Telescope 2. In the centre (above the VLT Auxilliary Telescope) both the Magellanic Clouds can be seen and to the left (east) the brightest source is the planet Venus, adjacent to the zodiacal light. See Picture of the Week potw1119 for more details.

Fellows at ESO

Ciriaco Goddi

I grew up on a Mediterranean island, the enchanting Sardinia (Italy), a place where the low level of air and light pollution reveals a beautiful, dark, star-filled night sky (almost) all year long. I remember, as a child, being always fascinated (and overwhelmed) by the vastness of the Universe. My passion for scientific subjects and some books read during high school (Weinberg and Hawking were among my favourites) determined my choice: I wanted to be a physicist!

I undertook a path which began with an undergraduate physics degree at the University of Cagliari in Sardinia. My Master's thesis was on astronomy, where I analysed mid-infrared data from planetary nebulae taken with the SWS spectrometer on board the ISO satellite. During my thesis work, I had the invaluable opportunity to visit ESO as a summer student. I had never been in a big institute at that time and I was overall so impressed by the scientific activity on campus, that once back at my home university I decided to enroll in a PhD programme in astronomy. The main goal of my PhD thesis project was to determine 3D gas dynamics in obscured massive star-forming regions. I learned the basics of radio interferometry, in particular very long baseline interferometry, which, despite requiring labour-intensive processing, allows images to be produced with the highest angular resolution in astronomy.

After finishing my PhD in 2005, I spent one year at the INAF–Osservatorio Astrofisico di Arcetri in Florence, just next door to Galileo's villa. There I joined the main research group on star formation in Italy, with whom I still collaborate today.

In the meantime, I was awarded a postdoctoral fellowship at the Harvard-Smithsonian Center for Astrophysics (CfA). I moved to Cambridge (Massachusetts) in 2006 where I lived for three years. The experience was very rewarding, both on a professional and a personal level. At the CfA I met prominent scientists, including authors of books I had studied, and also a Nobel laureate who was sitting just a few offices down from mine! My research there focused on

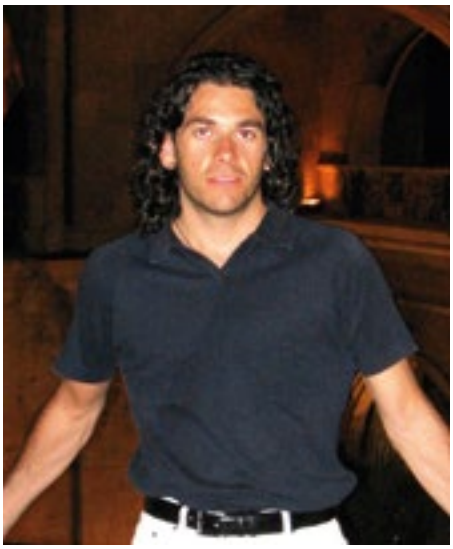

Ciriaco Goddi

the analysis of a large dataset of radio interferometric data aimed at a detailed study of an intriguing, yet enigmatic, region in the Orion Nebula. It is curious that the favorite constellation of my childhood, The Hunter, turned out to be my "pet source" as a professional astronomer. We also developed websites and animations for public outreach, a valuable way, in my view, to spread scientific knowledge among the general public.

I was awarded an ESO fellowship in 2009 and I moved back to Europe. ESO offers an incredibly stimulating scientific atmosphere, with a remarkable diversity of research carried out by excellent astronomers and a rich diet of workshops, seminars, and lively discussions at morning coffee. As a co-organiser of the weekly Informal Discussion, I have had the opportunity to meet and interact with many visiting (and ESO) astronomers and to learn about many aspects of science that I am less familiar with.

One great thing about ESO is the close relationship between the science and the cutting-edge facilities. Soon after joining ESO, I was given the opportunity to go for an observing run at APEX. The experience turned out to be enriching beyond expectations and very exciting for many reasons: the impressive variety of science programmes observed (from Solar System bodies to high-redshift galaxies), the great team (family!) of staff astronomers and engineers/operators, the breathtaking night show of the Milky Way in the southern hemisphere, the majestic mountains and the "martian" landscape of the Atacama desert, and the challenge of working in the rarefied atmosphere at 5000 metres, just one step away from the sky! I ended up spending approximately 80 nights observing in the Atacama desert. APEX is one of the special observatories in the world, and I will miss the real family atmosphere (and the famous *asados*!).

Now, while entering the second half of my fellowship, for my functional work I will join the ALMA commissioning team, the biggest ground-based project in astronomy. I know that probably previous generations of astronomers, at different times, have said this already, but I truly feel we are in a golden age for astronomy. New upcoming facilities like ALMA will revolutionise our knowledge of the Universe and will bring great discoveries... And I feel rather privileged to be part of this revolution!

Petr Kabath

My passion for astronomy started in high school almost two decades ago, leading me to study physics, and especially astronomy, later. Currently, I am an ESO Chile fellow trying to contribute to and unveil some of the most intriguing scientific topics of today, while working at the world-leading Paranal Observatory.

I was born in Brno, Czech Republic, where I officially started my astronomy career at the local public observatory in 1996. Years later, as my interest in astrophysics had steadily increased, I enrolled on a physics course at Masaryk University in Brno. After a year and a half I applied for an Erasmus fellowship, which provides support for one year spent at foreign universities. Tempted by the rumours of the great student life abroad, I chose the Freie Universität (FU) Berlin, and Prof. Baumgärtel's group at the Department of Physical Chemistry, as my temporary home for the academic year 2002–3. Even though I then left astronomy temporarily, since I was investigating the nucleation rates of undercooled liquids at the FU (as part of my

Master's programme), I thoroughly enjoyed my time in Berlin. I was so impressed by the great city and its pulsating life that I decided to stay for six more years and I also met my future wife Martina there.

The year 2006 signified a swift return to astronomy when I landed a PhD position in Prof. Heike Rauer's group at the German Aerospace Centre Berlin (DLR). My astronomy career started over again with long observing runs on transiting exoplanets with the BEST telescope located at the Observatoire de Haute Provence (OHP), France. Subsequently, I exchanged the OHP trips for a significantly more distant destination, Cerro Armazones in Chile, now the chosen site for the future E-ELT. I was very much involved in the building, commissioning and setup of the new transit search telescope BEST II, which started to operate in 2007. Both telescopes were built to support the space mission CoRoT, which is designed to detect transiting exoplanets. So the outcome of my PhD thesis is a fully operational robotic telescope and the first detected candidates for transiting exoplanets.

Since the Chilean Atacama desert is officially the astronomical capital of the world, I was delighted to receive the offer of an ESO Fellowship in 2009. Currently, while performing operational duties at Paranal, I am assigned to the Unit Telescopes 4 and 2. Besides these functional duties, I am working on my own scientific research on exoplanets. My major focus is on the detection and physical characterisation of these distant worlds. Most recently, our team has been attempting to detect and characterise exoplanetary atmospheres with near-infrared instruments, using mostly HAWK-I, ISAAC and SOFI.

Petr Kabath

ESO has given me a great opportunity to conduct my own research and to reinforce and foster collaborations. Even though I am developing my own scientific focus on exoplanetary atmospheres, I am still collaborating with my former colleagues on the BEST II telescope project. Furthermore, a couple of ESO proposals submitted for the current and upcoming observing period are a result of new and productive collaborations with my current colleagues at the ESO offices in Vitacura.

At present, I am mid-way through my four-year contract. I have not yet decided whether I would like to stay in Chile for the final year or go and spend the fourth year somewhere else. Nevertheless, while I am in Chile I am relishing the chance to experience this diverse culture, and appreciating the breathtaking natural beauty of this captivating country while simultaneously being part of ESO. Of course all that would not be possible without the great support from my wife Martina, to whom I am very thankful for her endless patience with me.

Report on the

Garching ESO Fellow Days – 2011

held at ESO Headquarters, Garching, Germany, 4–5 April 2011

Eric Emsellem[1]
Pamela Klaassen[1]
Michael West[1]

[1] ESO

For the first of the newly formatted ESO Fellow Days, a total of 25 fellows, including several ESO COFUND Fellows from Alma Regional Centres in Europe, and one fellow from Chile, gathered. All the fellows briefly introduced themselves and most presented recent research results and perspectives. ESO staff astronomers and students were also invited to these presentations, which beautifully demonstrated the excellence of the science being conducted by ESO Fellows.

The Fellowship Symposia were originally designed to facilitate interactions between fellows spread over the two main ESO sites in Chile and Germany. These symposia took place every two years (the last one in 2009) alternately in Santiago and Garching and gathered together the full set of ESO Fellows. These meetings have been a great opportunity for science discussions, increased exchanges between all ESO staff and have often led to new collaborations or personal science connections. Since ESO Fellow contracts last for three or four years (in Garching and Santiago respectively), this frequency implied that

a few unlucky ESO Fellows would only travel across the Atlantic to visit the other site around the end of their Fellowship.

In order to maximise the timeliness of these meetings, it was decided to change to an annual basis, with two sessions of ESO Fellow Days each year, one at each site, so that "new" fellows could meet with the "old" ones. The more regular meetings are an increased opportunity to advertise in-house the top-level science being done by ESO Fellows. It was thus decided to organise a two-day meeting in Garching, for this, the first 2011 German edition of the new format. The chosen date also provided an opportunity to attend the ALMA Community Days, taking place during same week (see Randall et al. p. 39).

A total of 25 fellows attended the meeting, including seven ESO ALMA–COFUND Fellows from various ALMA Regional Centres across Europe and also one fellow from Chile. Most fellows gave a science presentation on their ongoing and future work. This workshop was designed to allow relatively long (half-hour) talks, giving ample time for the speakers to introduce themselves, present and discuss their field of research and their scientific accomplishments. The presentations covered a wide range of topics including protoplanetary discs, the evolution of debris discs around solar-type stars, high- and low-mass star formation from the formation of the cores to later stages, open clusters, super star clusters, feedback in starburst galaxies, active galactic nuclei, quasars and strong gravitational lensing studies (the full programme is available online[1]).

The talks were of very high quality, and the rather informal atmosphere allowed attendees not too familiar with a field to grasp the essential ingredients and the results emphasised by the speaker. Many interesting discussions took place, often linking the differing areas of expertise of people present in the room.

Long breaks helped to foster scientific and social interactions not only among the fellows themselves, but also with other ESO staff. These breaks were also an opportunity for ESO astronomers to introduce a future instrument or ESO facility, providing a privileged perspective and a chance to seek specific answers to either technical or astrophysical questions. Pamela Klaassen, Joel Vernet, Markus Kasper and Jochen Liske gave presentations on ALMA, MUSE, KMOS, SPHERE and the E-ELT respectively.

A closed session, attended only by the fellows and the head of the Office for Science in Garching, was organised to discuss ways to improve the fellowship programme in general and addressed specific items such as training and the job market. And of course, a social event was organised: a dinner in the centre of Munich was a nice moment for more informal interactions and to reflect on the amazing science and projects being conducted at ESO.

Acknowledgements

This workshop, which we hope will be the first of a long series, would not have been possible without the help of Christina Stoffer and the support from the ESO IT Department. We warmly thank Joel Vernet, Markus Kasper and Jochen Liske for their excellent contributions.

Links

[1] ESO Fellow Days 2011 programme: http://www.eso.org/sci/meetings/2011/fellows_gar_2011/schedule_fellow_days_gar2011.pdf

Colour image of the Sc spiral galaxy NGC 3244 formed from FORS2 images in *B*, *V* and *R* filters. The bright star to the right is a nearby object in the Milky Way. The images were taken during the visit of the President of the Czech Republic Václav Klaus to Paranal. A framed print was presented to President Klaus, as a memento of his visit. Further details of the image can be found in Picture of the Week (potw1120) and of the President's visit to Paranal in the Organisation Release eso1112.

ESO

European Organisation
for Astronomical
Research in the
Southern Hemisphere

ESO Fellowship Programme 2011/2012

The European Organisation for Astronomical Research in the Southern Hemisphere awards several postdoctoral fellowships each year. The goal of these fellowships is to offer young outstanding scientists opportunities and facilities to enhance their research programmes in close contact with the activities and staff at one of the world's foremost observatories.

In Garching, the fellowships start with an initial contract of one year followed by a two-year extension (3 years total). The ESO Headquarters in Garching near Munich, Germany, are situated in one of the most active research areas in Europe and have among the highest concentrations of astronomers. ESO offices are adjacent to the Max-Planck Institutes for Astrophysics and for Extraterrestrial Physics and only a few kilometres away from the Observatory of the Ludwig-Maximilian University. Additionally, ESO participates in the newly formed Excellence Cluster on Astrophysics on the Garching Campus, which brings together nearly 200 scientists to explore the origin and structure of the Universe. Consequently, ESO fellows in Garching have many opportunities to interact and collaborate with astronomers at neighbouring institutes.

In addition to the excellent scientific environment that will allow to develop their scientific skills, as part of the diverse training ESO offers, Garching fellows spend up to 25% of their time in some functional work related to instrumentation, operations support, archive/virtual observatory, VLTI, ALMA, ELT, public affairs, or science operations at the Observatory in Chile.

In Chile, the fellowships are granted for one year initially with an extension of three additional years (4 years total). During the first three years, the fellows are assigned to one of the operations groups on Paranal, ALMA or APEX. Fellows contribute to the operations at a level of 80 nights per year at the Observatory.

Apart from opportunities for scientific interactions within ESO, fellows have the opportunity to collaborate with the rapidly growing Chilean astronomical community as well as with astronomers at other international observatories located in Chile. The addition of a new ALMA building next to ESO's Santiago offices and the arrival of many astronomers and fellows working on the ALMA project has further enhanced the stimulating scientific environment available to ESO Chile fellows.

During the fourth year there is little or no functional work and several options are provided. The fellow may be hosted by a Chilean institution (and will thus have access to all telescopes in Chile via the Chilean observing time). Alternatively, she/he may choose to spend the fourth year either at ESO's astronomy centre in Santiago, or at the ESO Headquarters in Garching, or at any institute of astronomy/astrophysics in an ESO member state.

The programme is open to applicants who will have achieved their PhD in astronomy, physics or related discipline before 1 November, 2012. Young scientists from all astrophysical fields are welcome to apply. For all fellowships, scientific excellence is the prime selection criterion.

We offer an attractive remuneration package including a competitive salary and allowances (tax-free), comprehensive social benefits, and provide financial support for relocating families.

The closing date for applications is 15 October 2011.

Candidates will be notified of the results of the selection process between December 2011 and February 2012. Fellowships begin between April and October of the year in which they are awarded.

Please apply by completing the web application form available at http://jobs.eso.org. Applications must include:
– your Curriculum Vitae with a list of publications (ONLY published papers, NOT papers in preparation);
– your proposed research plan (maximum two pages);
– a brief outline of your technical/observational experience (maximum one page);
In addition three letters of reference from persons familiar with your scientific work should be sent directly to ESO to vacancy@eso.org by the application deadline.

For more information about the fellowship programme and ESO's astronomical research activities please see: http://www.eso.org/sci/activities/FeSt-overview/ESOfellowship.html. For a list of current ESO staff and fellows, and their research interests please see: http://www.eso.org/sci/activities/personnel.html. Details of the Terms of Service for fellows including details of remuneration are available at: http://www.eso.org/public/employment/fellows.html

For further general information about fellowship applications, please see our Frequently Asked Questions – FAQs: http://www.eso.org/sci/activities/FeSt-overview/ESOfellowship-faq.html. Questions not answered by the above FAQ page can be sent to:

For Garching:
Eric Emsellem, Tel. +49 89 320 06-914, e-mail: eemselle@eso.org

For Chile:
Michael West, Tel. +56 2 463 3254, email: mwest@eso.org

ESO, the European Southern Observatory, is the foremost intergovernmental astronomy organisation in Europe. It is supported by 15 countries: Austria, Belgium, Brazil, the Czech Republic, Denmark, France, Finland, Germany, Italy, the Netherlands, Portugal, Spain, Sweden, Switzerland and the United Kingdom. ESO's programme is focused on the design, construction and operation of powerful ground-based observing facilities. ESO operates three observatories in Chile: at La Silla, at Paranal, site of the Very Large Telescope, and at Llano de Chajnantor. ESO is the European partner in the Atacama Large Millimeter/submillimeter Array (ALMA) under construction at Chajnantor. Currently ESO is engaged in the design of the European Extremely Large Telescope.

The Messenger is published, in hardcopy and electronic form, four times a year: in March, June, September and December. ESO produces and distributes a wide variety of media connected to its activities. For further information, including postal subscription to The Messenger, contact the ESO education and Public Outreach Department at the following address:

ESO Headquarters
Karl-Schwarzschild-Straße 2
85748 Garching bei München
Germany
Phone +49 89 320 06-0
information@eso.org

The Messenger:
Editor: Jeremy R. Walsh;
Design: Jutta Boxheimer; Layout, Typesetting: Mafalda Martins;
Graphics: Roberto Duque.
www.eso.org/messenger/

Printed by Mediengruppe UNIVERSAL Grafische Betriebe München GmbH
Kirschstraße 16, 80999 München
Germany

ISSN 0722-6691

Contents

Front cover: The nearby low-mass star-forming region NGC 6729 centred on the variable star R Coronae Australis, is shown in a FORS2 two-colour composite image. Narrow band filter images centred on the emission lines of Hα (red) and [S II] (blue) were combined. Some of the bluest features are shock-excited outflows (Herbig–Haro objects) from very young stars. The nebula NGC 6729 is optically variable and is a complex of gas, dust and embedded young and forming low-mass stars. The data were selected from the ESO archive by Sergey Stepanenko as part of the Hidden Treasures competition and this image was ranked third. See release eso1109 for more details.